



This is a repository copy of *Glucosylpolyphenols as inhibitors of A β -induced Fyn kinase activation and Tau phosphorylation: synthesis, membrane permeability, and exploratory target assessment within the scope of type 2 diabetes and Alzheimer's disease*.

White Rose Research Online URL for this paper:
<https://eprints.whiterose.ac.uk/166108/>

Version: Accepted Version

Article:

de Matos, A.M., Blázquez-Sánchez, M.T., Bento-Oliveira, A. et al. (20 more authors) (2020) Glucosylpolyphenols as inhibitors of A β -induced Fyn kinase activation and Tau phosphorylation: synthesis, membrane permeability, and exploratory target assessment within the scope of type 2 diabetes and Alzheimer's disease. *Journal of Medicinal Chemistry*, 63 (20). pp. 11663-11690. ISSN 0022-2623

<https://doi.org/10.1021/acs.jmedchem.0c00841>

This document is the Accepted Manuscript version of a Published Work that appeared in final form in *Journal of Medicinal Chemistry*, copyright © American Chemical Society after peer review and technical editing by the publisher. To access the final edited and published work see <https://doi.org/10.1021/acs.jmedchem.0c00841>

Reuse

Items deposited in White Rose Research Online are protected by copyright, with all rights reserved unless indicated otherwise. They may be downloaded and/or printed for private study, or other acts as permitted by national copyright laws. The publisher or other rights holders may allow further reproduction and re-use of the full text version. This is indicated by the licence information on the White Rose Research Online record for the item.

Takedown

If you consider content in White Rose Research Online to be in breach of UK law, please notify us by emailing eprints@whiterose.ac.uk including the URL of the record and the reason for the withdrawal request.



eprints@whiterose.ac.uk
<https://eprints.whiterose.ac.uk/>

1
2
3
4
5
6
7
8
9
10
11
12
13
14
15
16
17
18
19
20
21
22
23
24
25
26
27
28
29
30
31
32
33
34
35
36
37
38
39
40
41
42
43
44
45
46
47
48
49
50
51
52
53
54
55
56
57
58
59
60



SCHOLARONE™
Manuscripts

1 2 3 4 5 6 7 8 9 10 11 12 13 14 15 16 17 18 19 20 21 22 23 24 25 26 27 28 29 30 31 32 33 34 35 36 37 38 39 40 41 42 43 44 45 46 47 48 49 50 51 52 53 54 55 56 57 58 59 60

Glucosylpolyphenols as inhibitors of A β -induced Fyn kinase activation and Tau phosphorylation: synthesis, membrane permeability, and exploratory target assessment within the scope of type 2 diabetes and Alzheimer's disease

Ana M. de Matos,^{1,§} M. Teresa Blázquez-Sánchez,^{1,§} Andreia Bento-Oliveira,¹ Rodrigo F. M. de Almeida,¹ Rafael Nunes,^{1,2} Pedro E. M. Lopes,^{1,2} Miguel Machuqueiro,^{1,2} Joana S. Cristóvão,² Cláudio M. Gomes,² Cleide S. Souza,³ Imane G. El Idrissi,⁴ Nicola A. Colabufo,⁴ Ana Diniz,⁵ Filipa Marcelo,⁵ M. Conceição Oliveira,⁶ Óscar López,⁷ José G. Fernandez-Bolaños,⁷ Philipp Dätwyler,⁸ Beat Ernst,⁸ Ke Ning,⁹ Claire Garwood,⁹ Beining Chen,^{3,*} and Amélia P. Rauter^{1,*}

¹Centro de Química Estrutural, Faculdade de Ciências, Universidade de Lisboa, Campo Grande, 1749-016 Lisboa, Portugal; ²Biosystems & Integrative Sciences Institute, Faculdade de Ciências, Universidade de Lisboa, Campo Grande, 1749-016 Lisboa, Portugal; ³Department of Chemistry, The University of Sheffield, Dainton Building, Brook Hill, Sheffield S3 7HF, United Kingdom; ⁴Dipartimento di Farmacia-Scienze del Farmaco, Università degli Studi di Bari "A. Moro", Via Orabona, 4, 70125, Bari, Italy; ⁵UCIBIO, REQUIMTE, Faculdade de Ciências e Tecnologia, Universidade Nova de Lisboa, 2829-516 Caparica, Portugal; ⁶Mass Spectrometry Facility at CQE, Instituto Superior Técnico, Av. Rovisco Pais, 1049-001, Lisboa, Portugal; ⁷Departamento de Química Orgánica, Facultad de Química, Universidad de Sevilla, Apartado 1203, E-41071 Sevilla, Spain; ⁸Department of Pharmaceutical Sciences, University of Basel, Klingelbergstrasse 50, CH-4056 Basel, Switzerland; ⁹Department of Neuroscience, Sheffield Institute for Translational Neuroscience, The University of Sheffield, Sheffield S10 2HQ, United Kingdom.

Abstract

Despite the rapidly increasing number of patients suffering from type 2 diabetes, Alzheimer's disease, and diabetes-induced dementia, there are no disease-modifying therapies able to prevent or block disease progress. In this work, we investigate the potential of nature-inspired glucosylpolyphenols against relevant targets, including islet amyloid polypeptide, glucosidases and cholinesterases. Moreover, with the premise of Fyn kinase as a paradigm-shifting target in Alzheimer's drug discovery, we explore glucosylpolyphenols as blockers of A β -induced Fyn kinase activation, while looking into downstream effects leading to Tau hyperphosphorylation. Several compounds inhibit A β -induced Fyn kinase activation and decrease pTau levels at 10 μ M concentration, particularly the per-*O*-methylated glucosylacetophloroglucinol and the 4-glucosylcatechol dibenzoate, the latter inhibiting also butyrylcholinesterase and β -glucosidase. Both compounds are non-toxic with ideal pharmacokinetic properties for further development. This work ultimately highlights the multitarget nature, fine structural tuning capacity and valuable therapeutic significance of glucosylpolyphenols in the context of these metabolic and neurodegenerative disorders.

Keywords: Glucosylpolyphenols, Fyn kinase, hIAPP, Tau phosphorylation, type 2 diabetes, Alzheimer's disease, diabetes-induced dementia

Introduction

More than 463 million adults are currently suffering from type 2 diabetes (T2D) worldwide,¹ and up to 73% of them are likely to be diagnosed with dementia, including Alzheimer's disease (AD). T2D – the non-insulin dependent type of diabetes – primarily arises from the ingestion of high-fat diets and lack of physical exercise, which leads to hyperinsulinemia, dyslipidemia, insulin resistance and, ultimately, hyperglycemia. In turn, AD is characterized for the presence of extracellular deposits of amyloid beta (A β) in the senile plaques and for intracellular neurofibrillary tangles induced by deposits of hyperphosphorylated Tau protein, accompanied by synaptic dysfunction resulting in neuronal death.² Recent reports indicate that the cellular prion protein (PrP^C) located in the neuronal cell surface works as a high-affinity binding partner of A β oligomers (A β os), leading to the activation of Fyn kinase, which triggers a cell signaling pathway culminating in Tau hyperphosphorylation.³ Indeed, Fyn activity was found to be increased in AD brain by exposure of neurons to A β os via PrP^C.^{4,5} Moreover, genetic deletion of Fyn prevents A β os-induced cell death in hippocampus and Fyn inhibition restores synapse density and memory function in transgenic mice.^{6,7} Interestingly, Fyn inhibition, deficiency, or genetic knockout were found to have increased glucose disposal due to increased insulin sensitivity, improved fatty acid oxidation, with decreased visceral adipose tissue inflammation.⁸⁻¹⁰ Hence, the inhibition of Fyn activity is also a relevant approach in the treatment of diabetes-induced dementia (DID), the so-called “type 3 diabetes”.

Other pathophysiological mechanisms are known to be present in both T2D and AD, namely peripheral and brain insulin resistance and insulin-degrading enzyme (IDE) downregulation leading to increased brain A β levels.² Furthermore, cross-seeding events between the brain-penetrant islet amyloid polypeptide (IAPP) and A β have also been reported, being likely to exacerbate the cognitive decline observed in patients suffering from both conditions.^{11,12} With the lack of therapeutic alternatives able to block disease progression in both cases, we were interested in finding new molecular entities able to tackle several molecular targets common to AD and DID with disease-modifying effects. For this purpose, we turned to nature for inspiration. Polyphenols have been widely reported in the literature for their vast therapeutic potential, with described antidiabetic, anti-inflammatory and neuroprotective effects.^{2,13-16} Polyphenol glucosides (*O*-glucosyl polyphenols) and glucosylpolyphenols¹⁷ (*C*-glucosyl polyphenols, frequently named as polyphenol *C*-glucosides) however, have improved palatability, oral bioavailability due to increased solubility, as well as enhanced biological activity when compared to the corresponding aglycones, including improved amyloid-remodeling effects.^{16,18-21} Importantly, *C*-glycosyl polyphenols are not liable to chemical and enzymatic hydrolysis, as sugar is linked to the polyphenol by a C-C bond, and have been described to show higher antidiabetic effects with

1 improved target selectivity; for instance, the glucosyldihydrochalcone analogue of the glucoside phlorizin is selective
2 towards SGLT-2 vs. SGLT-1 transporters, while phlorizin is not.²²⁻²⁴
3
4

5 For all the above mentioned reasons, we were interested in exploring the potential multitarget bioactivity of
6 glucosylpolyphenols based on the structure of 8- β -D-glucosylgenistein (**1**, Figure 1), a natural glucosylisoflavone
7 previously reported by our group as a new and potent antidiabetic compound with potential against A β ₁₋₄₂-induced
8 neurotoxicity.²⁵ This compound was found to inhibit IAPP aggregation and to interact with A β (1-42) polypeptide
9 through the same binding mode, involving the sugar moiety, H-6 of ring A, and the aromatic protons of ring B. Yet, we
10 did not have information as to whereas one or more phenol moieties were beneficial for activity, or even if the molecular
11 planarity of the aglycone was a crucial feature for the binding epitope and anti-aggregating activity of this compound.
12 Moreover, C-glucosyl polyphenols derived from acetophloroglucinol or hydroquinone have been reported in the
13 literature for having antidiabetic effects.^{26,27} On the basis of this information, we were interested in synthesizing
14 simplified analogues of **1** with a different hydroxylation pattern in ring A, maintaining the sugar β -C linkage found in
15 the original compound (Figure 1). To keep rings A and B linked by a three-bond spacer moiety for mimicking **1**, we
16 planned on inserting benzoate moieties in glucosylhydroquinone (a) and glucosylcatechol derivatives (b), or ketone
17 moieties in glucosylphloroglucinol derivatives (c). Moreover, due to the extremely polar nature of the lead compound,
18 we were also interested in generating more lipophilic analogues of the natural scaffold with higher chances of crossing
19 the blood-brain barrier (BBB), namely by *O*-methyl protection of sugar hydroxy groups. The major goal was to explore
20 the therapeutic potential and physicochemical properties of compound **1**, while comparing them to those of the newly
21 synthesized analogues and elucidating, whenever possible, structural requirements for bioactivity against multiple
22 targets involved in T2D and AD, including IAPP, Fyn kinase activation, Tau hyperphosphorylation, as well as
23 glucosidase and cholinesterase enzymes. Ultimately, we were interested in investigating the therapeutic potential of
24 glucosylpolyphenols against T2D and AD, while identifying new lead molecules for further pharmaceutical
25 development in the context of these pathologies.
26
27
28
29
30
31
32
33
34
35
36
37
38
39
40
41
42
43
44
45
46
47
48
49

50 C-glycosylation is a key and particularly challenging synthetic step in our strategy. Several methods for C-glycosylation
51 are currently known, including nucleophilic attack of aromatic Grignard reagents to glycosyl halides,²⁸ the use of
52 lactones and lithiated compounds,²⁹ catalysis by transition metals or samarium diiodide,^{30,31} intermolecular free radical
53 reactions³² and intramolecular aglycone delivery through the Fries-type rearrangement.³³ The latter approach covers the
54 strategy first developed by Suzuki *et al.*³⁴ and Kometani *et al.*,³⁵ and consists of a Lewis acid-catalyzed rearrangement
55 of a phenol glycoside to a C-glycosyl derivative, known as the Fries-type rearrangement. It has been exploited by various
56 authors up to the present days and successfully applied to the synthesis of flavonoid C-glycosides and of other complex
57
58
59
60

natural products.^{25, 36-38} In this sense, another goal for this work was to explore the feasibility of C-glycosylation by using different glycosyl donors and acceptors, while studying their impact in the efficacy of the Fries-type rearrangement.

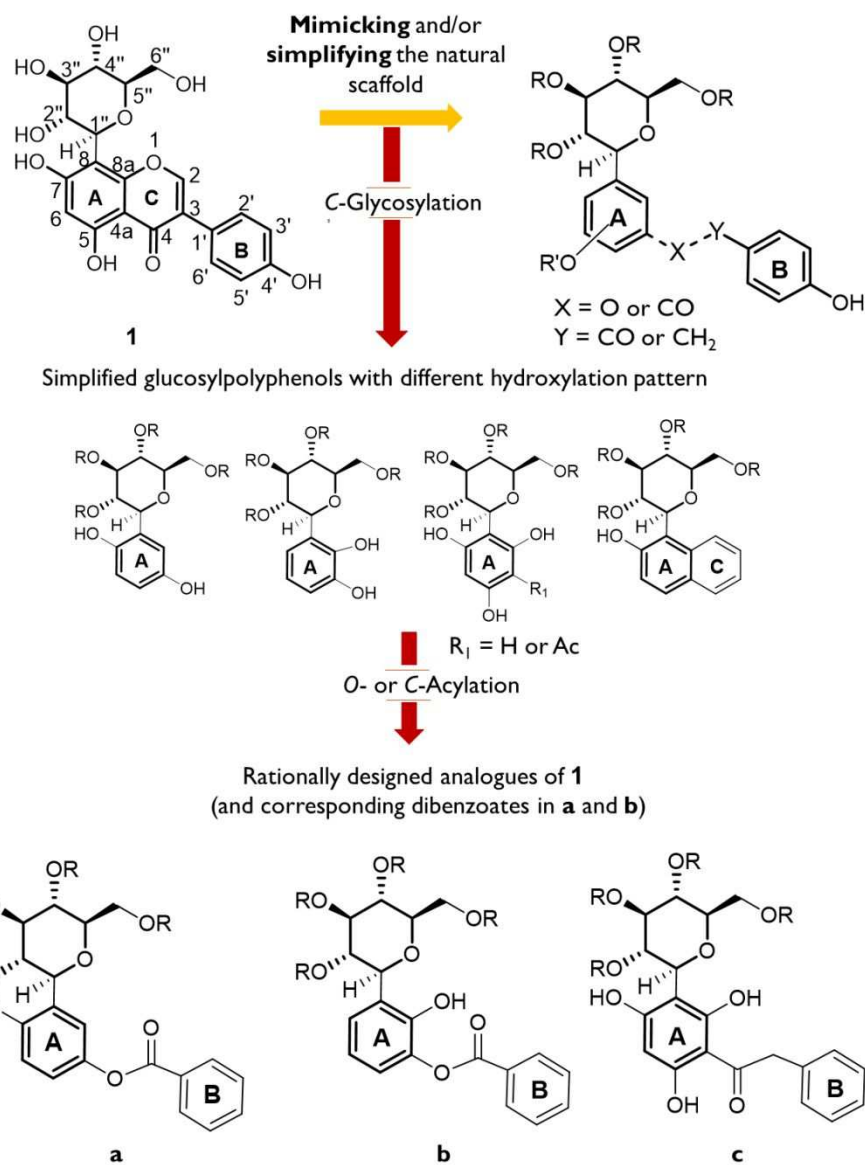


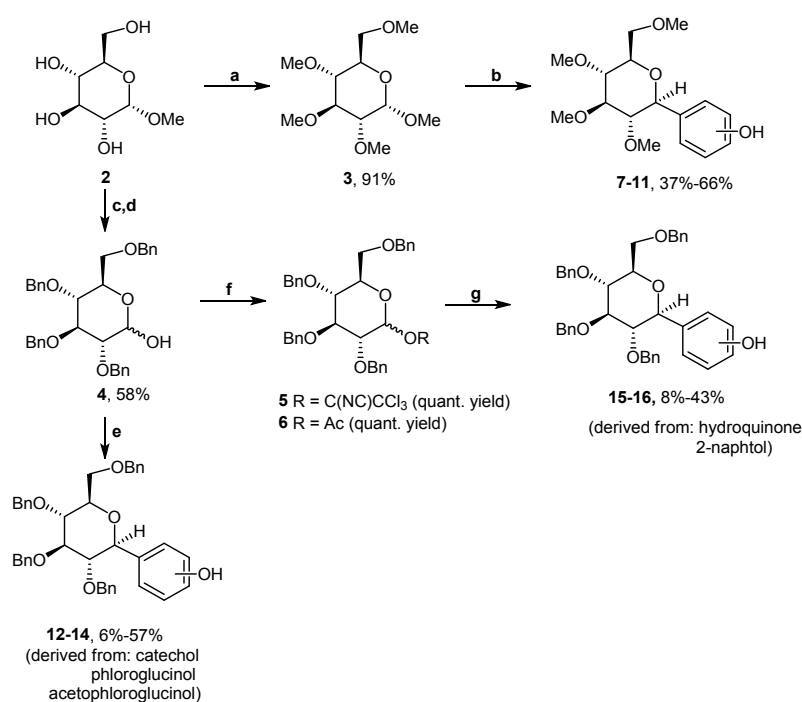
Figure 1. Rationale behind the synthesis of simplified analogues of 8-β-D-glucosylgenistein (**1**). R = H or Me; R' = H or Bz.

Results

Chemistry

A. C-Glucosylation

For the generation of glucosylpolyphenols, we employed either a permethylated glucopyranoside³⁹ (**3**, Scheme 1) or *per*-benzylated glucosyl donors^{25,40} (**4-6**). Polyphenols containing their hydroxy groups in *meta*, *para* and *ortho* orientation were used as acceptors in a series of C-glycosylation reactions, and the differences in their reactivity were attentively explored. 2-Naphthol was also used to generate a C-glucosyl analogue with two fused planar rings, in order to mimic rings A and C in the original structure.

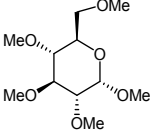
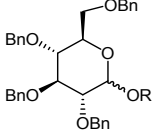
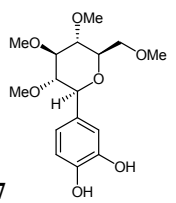
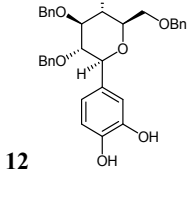
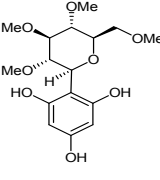
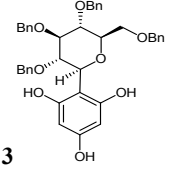
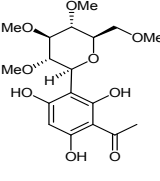
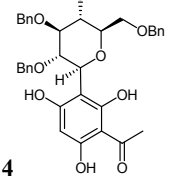
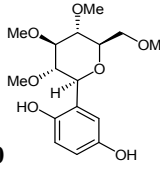
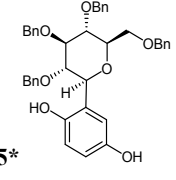
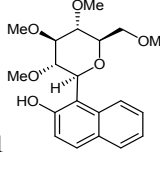
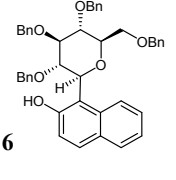


Scheme 1. Preparation of glucosyl donors and protected C-glucosyl phenols. Reagents and conditions: **a**) DMF, NaH, MeI, 0 °C, 3 h; **b**) dry MeCN, polyphenol, drierite, -78 °C → r.t., TMSOTf, 18 h – 48 h; **c**) DMF, NaH, BnBr, 0 °C → r.t., 20 h; **d**) AcOH, H₂SO₄, reflux, 36 h; **e**) dichloromethane/MeCN, drierite, -78 °C → r.t. or 40 °C, TMSOTf, 8 h – 64 h; **f**) for compound **5**: dichloromethane, molecular sieves 3 Å, CCl₃CN, 0 °C, 1 h; for compound **6**: pyridine, DMAP, 0 °C → r.t., Ac₂O, 2.5 h; **g**) for compound **15**: dichloromethane/MeCN, drierite, -78 °C → r.t., BF₃·Et₂O, 40 h; for compound **16**: dichloromethane, molecular sieves 3 Å, 0 °C → r.t., TMSOTf, 20 h.

Precursors and conditions leading to the higher yields are presented in Tables 1 and 2. In the case of catechol and hydroquinone, when using benzyl protected sugar donors, glycosylation yields were drastically lower when compared to reactions either with phloroglucinol or trihydroxyacetophenone as sugar acceptors. In the first two cases, different solvent proportions, anomeric protecting group and promoter equivalents were tried attempting to optimize the reaction

1 efficacy; yet, after much experimentation no significant improvements could be observed. Moreover, no significant
 2 differences were found when trying to improve the efficacy of hydroquinone and catechol C-glycosylation using either
 3 TMSOTf or $\text{BF}_3 \cdot \text{Et}_2\text{O}$. Notwithstanding, for the first time, *per-O*-methyl- β -glucosylated polyphenols have been accessed
 4 in good yields by using TMSOTf as promoter and fully *O*-methylated methyl glucoside as the glycosyl donor. This
 5 methodology constitutes an advantage when compared to other approaches by saving reaction steps in the generation of
 6 donors with good leaving groups.
 7
 8
 9
 10
 11
 12
 13
 14

15 **Table 1.** C-Glycosylation of polyphenols carried out with TMSOTf as promoter

18	19	20	21	22	23	24
Phenol	Glycosyl donor	Isolated Yield (%)	Glycosyl donor	Isolated Yield (%)		
						
26	27	28	29	30	31	32
<i>Catechol</i>		63		6	(R = H)	
<i>ortho</i> -Hydroxylation pattern	7		12			
34	35	36	37	38	39	40
<i>Phloroglucinol</i>		53		42	(R = H)	
<i>meta</i> -Hydroxylation pattern	8		13			
42	43	44	45	46	47	48
<i>Trihydroxyacetophenone</i>		45		57	(R = H)	
<i>meta</i> -Hydroxylation pattern	9		14			
50	51	52	53	54	55	56
<i>Hydroquinone</i>		37		8	(R = Ac)	
<i>para</i> -Hydroxylation pattern	10		15*			
56	57	58	59	60		
<i>2-Naphthol</i>		66		43	(R = CNHCCl ₃)	
	11		16			

*Compound 15 was obtained using $\text{BF}_3 \cdot \text{Et}_2\text{O}$ as promoter

Methyl protected glucosyl donor gave, by reaction with all the acceptors tested, *C*-glucosyl polyphenols as the major products (**7-11**, Table 1). Interestingly, with benzyl protected glucosyl donors only glucosylphloroglucinol **13**, 3-glucosyl-2,4,6-trihydroxyacetophenone **14** and 1-glucosylnaphthalen-2-ol **16** were formed in moderate yields as the electron-donating effects of their aglycones was strong enough to promote *C*-glucosylation. On the other hand, catechol and hydroquinone gave *C*-glucosyl derivatives in very low yield (Table 1), even after increasing reaction time, changing solvent proportion, promoter and/or polyphenol molar proportion, and temperature (Table 2).

Table 2. Comparison of experimental conditions used in the *C*-glucosylation of hydroquinone and catechol with benzyl protected sugar donors.

Compound Nr.	Sugar Donor Nr.	Polyphenol	Solvent	Promotor	Temperature	Time	Isolated Yield
12	4	Catechol 150 mol %	DCM/MeCN (5:1)	TMSOTf 100 mol %	- 78 °C → 40 °C	64 h	6%
12	6	Catechol 150 mmol %	DCM/MeCN (5:1)	BF ₃ ·Et ₂ O 100 mol%	- 78 °C → 40 °C	60 h	2%
15	5	Hydroquinone 200 mol%	DCM/MeCN (1:1)	TMSOTf 50 mol %	- 78 °C → 40 °C	21 h	6%
15	5	Hydroquinone 150 mol%	DCM/MeCN (1:1)	TMSOTf 50 mol %	- 78 °C → rt	40 h	2%
15	5	Hydroquinone 150 mol%	DCM/MeCN (5:1)	TMSOTf 50 mol %	- 78 °C → 40 °C	40 h	6%
15	5	Hydroquinone 150 mol%	DCM/MeCN (2:1)	TMSOTf 50 mol %	- 78 °C → 40 °C	24 h	6%
15	5	Hydroquinone 200 mol%	MeCN	TMSOTf 100 mol %	- 78 °C → 82 °C	72 h	1%
15	4	Hydroquinone 150 mol%	DCM/MeCN (5:1)	BF ₃ ·Et ₂ O 100 mol%	- 78 °C → 40 °C	96 h	7%
15	6	Hydroquinone 150 mol%	DCM/MeCN (5:1)	BF ₃ ·Et ₂ O 100 mol%	- 78 °C → 40 °C	40 h	8%

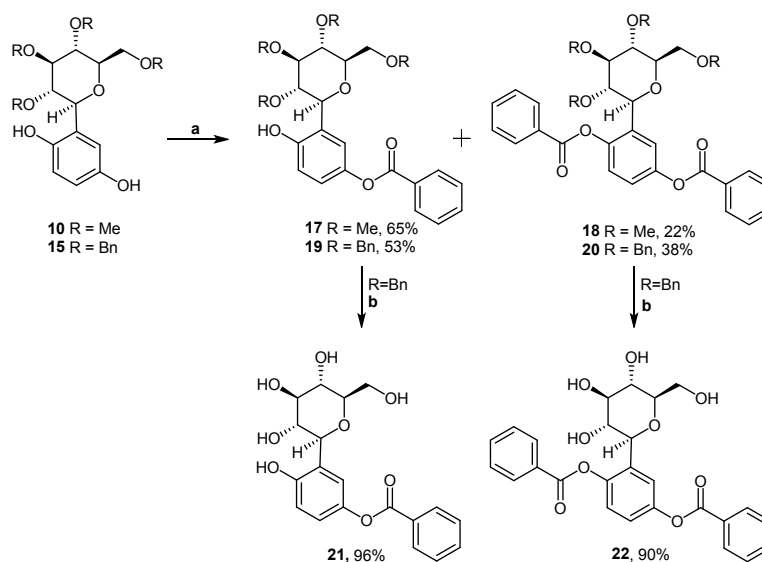
DCM – dichloromethane

Notably, after careful analysis of the NMR spectra we observed that the *para*-isomers are formed in the synthesis of catechol *C*-glucosides **7** and **12**, thus indicating that the Lewis acid-promoted Friedel–Crafts-type *C*-glycosylation is the favored reaction mechanism, prevalent over the Fries-type rearrangement described for unprotected phenols. While the synthesis of D-rhamnosyl⁴¹ and D-glucosyl^{42,43} aromatic derivatives has been previously described with protected

phenols, to the best of our knowledge, this is the first report of exceptions to the Fries-type rearrangement in the *C*-glycosylation of unprotected phenols.

B. *O*-Acylation

A benzoyl group was regioselectively introduced in glucosylhydroquinone derivatives **10** and **15** to afford analogues of **1** on the basis of a *para* hydroxylation pattern (a, Figure 1). Using imidazole, DMAP and benzoyl chloride, the desired ester derivatives **17** and **19** were obtained as the major products in good yield, together with their dibenzoate analogues **18** and **20** (Scheme 2). Further deprotection of benzyl protected derivatives through catalytic hydrogenation gave the corresponding deprotected compounds **21** and **22**. For comparison purposes, compounds **14** and **16** were also debenzylated to afford compounds **23** and **24**, respectively (*vd.* experimental section).

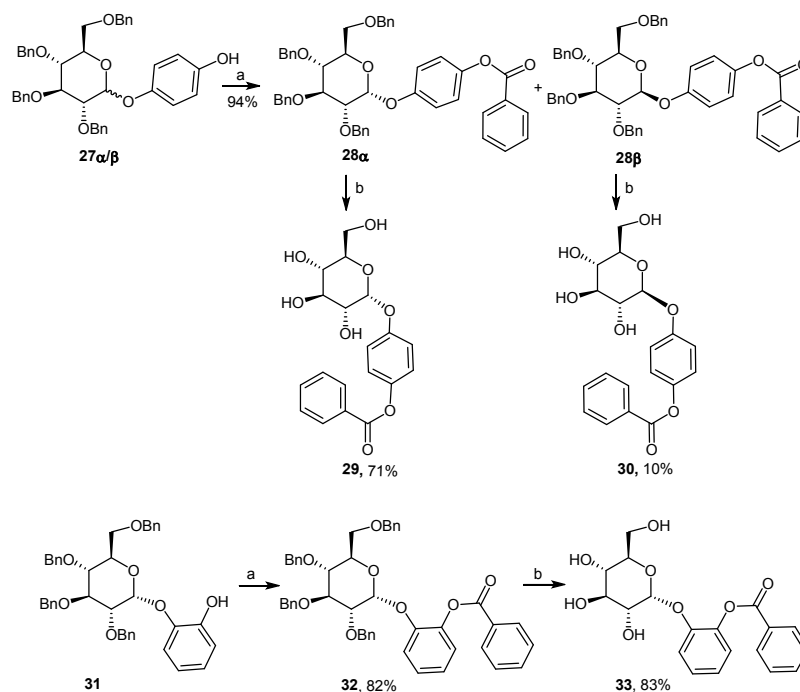


Scheme 2. Preparation of glucosylhydroquinone benzoates. Reagents and conditions: a) Dichloromethane, imidazole, DMAP, BzCl, 0 °C → r.t., 60 h – 120 h, b) EtOAc, Pd/C, H₂, r.t., 16 h – 22 h (R=Bn).

The observed regioselectivity of these *O*-acylation reactions may be related with stereochemical hindrance and eventual hydrogen bonding between the free hydroxy group and the sugar, thus enhancing the relative reactivity of the remaining phenol hydroxy group towards esterification. Accordingly, regioselective esterification was not observed with glucosylcatechol derivatives **7** and **12** (structure type b, Figure 1, Table 2). Instead, by applying the same experimental procedure, an inseparable mixture of mono-benzoylated compounds was obtained, which supports this hypothesis. For

comparison of bioactivity, the dibenzoate catechol analogues of compounds **18** and **22** were also synthesized (*vide* experimental section, compounds **25** and **26**, respectively).

Moreover, the hydroquinone and catechol *per-O*-benzyl glycosides **27 α,β** and **31** (Scheme 3), obtained as major products under the *C*-glucosylation reaction conditions (Table 2), were also benzoated and deprotected to afford the corresponding α -glycosides **29** and **33** as major products in excellent overall yield.

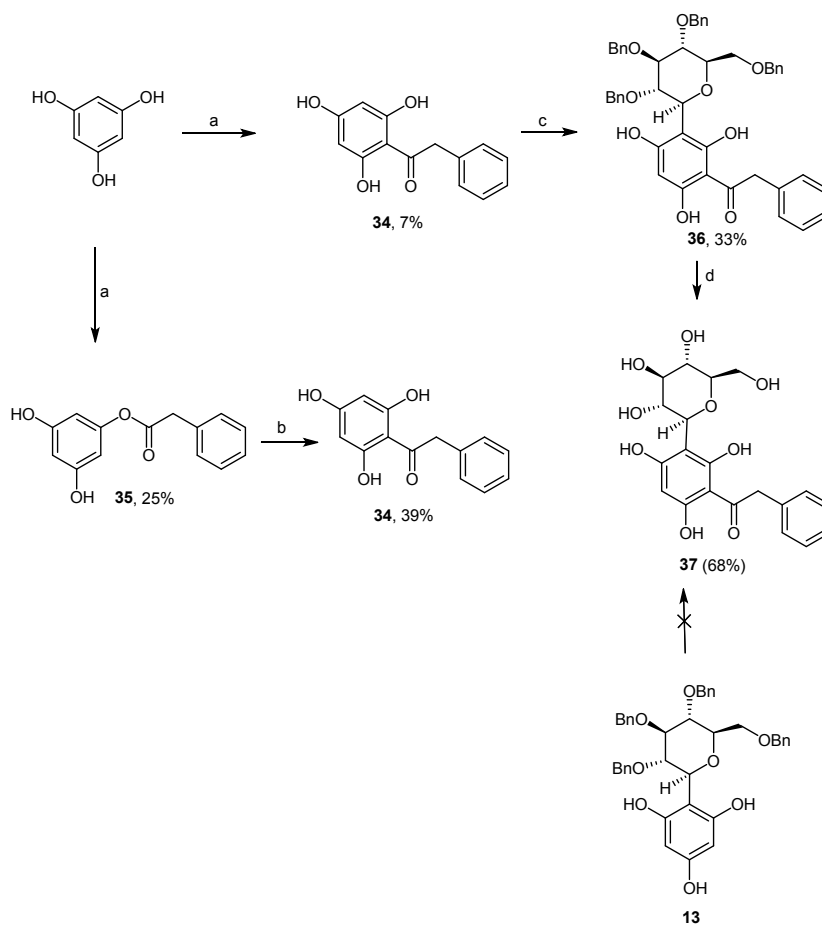


Scheme 3. Preparation of *O*-glucosyl hydroquinone and *O*-glucosyl catechol benzoates. Reagents and conditions: a) Dichloromethane, imidazole, DMAP, BzCl, 0 °C → r.t., 60 h – 120 h, b) EtOAc, Pd/C, H₂, r.t., 16 h – 22 h.

C. *C*-Acylation

The glucosylphloroglucinol **13** was originally chosen as the precursor of the planned analogue of compound **1** with the *meta* hydroxylation pattern (c, Figure 1). Provided that this trihydroxybenzene is an extremely electron-rich aromatic system, we were expecting a very straightforward Friedel-Crafts-type acylation to occur with phenylacetyl chloride in the presence of a Lewis acid. After much experimentation employing a number of Lewis acids (e.g. BF₃·Et₂O, TMSOTf, FeCl₃, TfOH) and several different conditions without any success, we hypothesized that the sugar moiety could be reducing the reactivity of the aromatic ring or even being degraded in the course of these reactions. The initial *C*-acylation of the phenol residue followed by *C*-glycosylation turned out to be the best option to address this issue. Due

activated nucleophilic carbons, the control of *O*-/*C*-acylation was not an easy task. While an equimolecular amount or an excess of TfOH in absence of solvent generated the di-*C*-acylated product, the use of TfOH 2% in MeCN rendered a mixture of the *O*-/*C*-acylated products in a ratio of ca. 1/0.3 (Scheme 4). Then, using an excess of TfOH, which acted both as the solvent and catalyst, compound **35**, obtained in 25% yield from trihydroxybenzene, was rearranged into the *C*-acylated analogue **34** in 39% yield, which was subsequently *C*-glycosylated to afford compound **36** in 33% yield. After catalytic hydrogenation the final analogue **37** was isolated in 68% isolated yield.



Scheme 4. Preparation of compound **37**. Reagents and conditions: a) phenylacetyl chloride, 2% TfOH/MeCN, 0°C → r.t., overnight, **34**, 7%; **35**, 25% b) TfOH, 100 °C, 2 h, 39%; c) TMSOTf, dichloromethane/MeCN, compound **4**, drierite, - 40 °C → r.t., overnight, 33%; d) MeOH/EtOAc, Pd/C, H₂, r.t., 3 h, 68%.

Computational Studies, Epitope Mapping, and Bioactivity Assays

1
2
3
4
5
6
7
8
9
10
11
12
13
14
15
16
17
18
19
20
21
22
23
24
25
26
27
28
29
30
31
32
33
34
35
36
37
38
39
40
41
42
43
44
45
46
47
48
49
50
51
52
53
54
55
56
57
58
59
60

A. DFT calculations and molecular interactions of rationally designed analogues with hIAPP by STD-NMR

IAPP is co-secreted with insulin by pancreatic β -cells. In prediabetes, insulin resistance leads to a compensatory hypersecretion of insulin and IAPP, leading to its aggregation and deposition in the pancreas in the form of cytotoxic amyloid oligomers and fibrils. Along with disease progression, this accumulation will lead to the loss and dysfunction of β -cells, which justifies why patients with advanced T2D are no longer able to produce insulin, despite being insulin resistant.² Hence, IAPP is an important therapeutic target in T2D, particularly in the prevention of pancreatic dysfunction arising from aberrant insulin secretion. In this context the interaction of **1** against hIAPP was previously unveiled by saturation-transfer difference (STD) NMR techniques, being also shown, by Atomic Force Microscopy, the ability of this compound to inhibit hIAPP aggregation into amyloid oligomers and fibrils.²³ Based on these findings, we were interested in assessing if the rationally designed analogues **21** and **37** (aimed at mimicking the original scaffold) would exhibit the same level of interaction with hIAPP and if the binding epitope would be maintained in the absence of the central fused ring system. Being more easily accessed in fewer synthetic steps, both **21** and **37** have increased molecular flexibility when compared to the lead compound **1**. DFT calculations [PBE0/6-311G** (H₂O)] show that low-energy conformations of compounds **21** and **37** are superimposable with compound **1** (Figure 2), namely with its *anti*-conformer (defined by an antigeometry for the H1"-C1"-C8-C7 torsion angle), which is the preferentially adopted conformation of **1** in the presence of A β (1-42) oligomers,²⁵ suggesting that these molecules are able to mimic the original spatial orientation of the sugar moiety relatively to rings A and B (see Figures S1-S2 and further details in the Supporting Information).

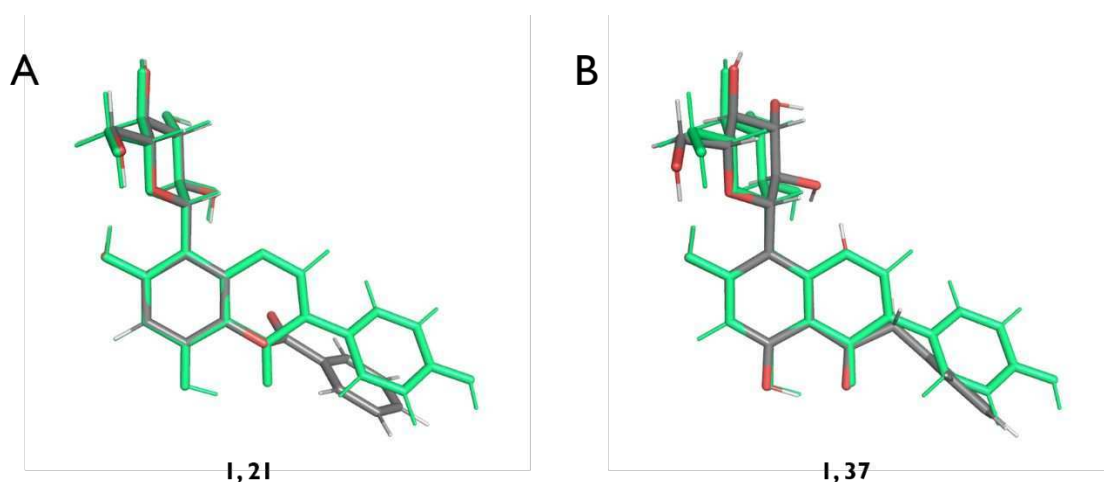


Figure 2. DFT-calculated structure of *anti*-**1** (in green), which is the preferentially adopted conformation in the presence of A β (1-42) oligomers,²⁵ superimposed to the lowest energy conformations identified at the PBE0/6-311G** (H₂O) level of theory for compounds (A) **21** and (B) **37** (in grey, red and white), obtained by root mean square (RMS)-fitting using all ring A carbon atoms of each compound.

The STD-derived binding epitope obtained for compounds **1**, **21** and **37** against hIAPP by STD-NMR (Figure 3 and Figures S3-S4) suggests that molecular planarity is not a structural requirement for binding and the absence of the central fused ring system in compounds **21** and **37** does not disrupt the interaction of these compounds with hIAPP. As in the case of compound **1**, the highest STD intensities correspond to the protons of the aromatic core of compounds **21** and **37** (% STD > 80%), when compared to those detected for the glucosyl group (% STD < 40%).

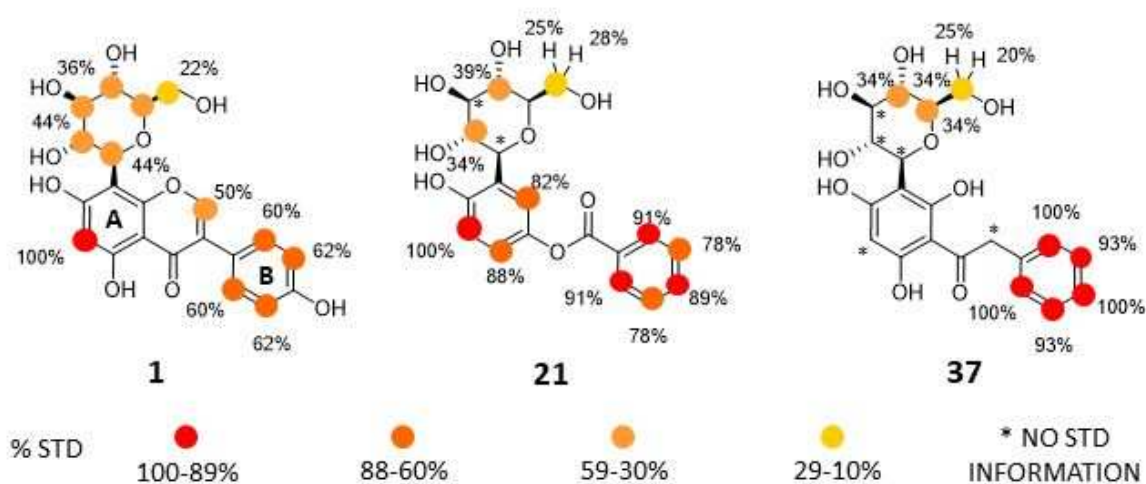


Figure 3. STD-derived epitope mapping obtained for compounds **1**,²⁵ **21** and **37** with hIAPP oligomers.

These experiments show that the binding affinity of the antidiabetic lead **1** is not related to the molecular planarity of the isoflavone core. Being accessed in only 5 synthetic steps (instead of the 9 needed for the synthesis of the lead molecule **1**), compounds **21** and **37** exhibit a clear binding against hIAPP. Given the reported anti-amyloidogenic properties of **1** against hIAPP,²⁵ these results encourage further studies of these two simpler analogues to evaluate their potential for the prevention of IAPP-induced pancreatic failure.

B. Inhibition of PrPC-A β oligomers interaction

1 In the last few years, the failure of several clinical trials targeting soluble and fibrillar A β by monoclonal antibodies
2 have motivated the scientific community to work in the diversification of therapeutic targets for AD. One possible
3 strategy is to focus on the downstream effects of A β rather than on its accumulation and aggregation.⁴⁴ Soluble A β os
4 were shown to bind to PrP^C on the neuronal cell surface initiating a cascade through activation of Fyn kinase. Indeed, it
5 is possible to monitor the activation of Src family kinases (SFKs) such as Fyn kinase by measuring the expression of
6 phosphospecific epitopes, as previously reported.³

7 Furthermore, it is commonly assumed that formation of A β fibrils and plaque deposits is a crucial event in the
8 pathogenesis of AD.⁴⁵ However, there is accumulating evidence that soluble oligomers are the most cytotoxic form of
9 A β although it is still unclear which size and morphology of the aggregates exert neurotoxicity. As with most of the
10 identified A β receptors, PrP^C was found to bind A β os with much higher affinity than monomeric A β (mA β). In this
11 work, Natural A β os, a kind gift from Sheffield Institute for Translational Neuroscience – SITraN (UK), were used.
12 These were derived from Chinese Hamster Ovary cells (7PA2 cells) stably transfected with cDNA encoding APP751,
13 an amyloid precursor protein that contains the Val717Phe familial Alzheimer's disease mutation, as previously
14 described.⁴⁶ The A β os solution contains between 12,000–14,000 pg/mL of total A β os as measured by ELISA. This
15 concentration is comparable to that of A β peptides detected in human cerebrospinal fluid. The A β os prepared represent
16 a heterogeneous population of monomers, dimers, trimers, tetramers, higher state soluble oligomers and other cellular
17 proteins as previously reported by Western blotting⁴⁴ without further purification. The A β os preparation using the same
18 protocol has been applied in the same way by other groups.⁴⁶ The same batch of the recombinant soluble A β os was used
19 for all experiments described in the manuscript to minimize impact of experimental variations caused by the
20 heterogeneous preparation of the A β os. 1,000 pg/mL of natural A β os were used to treat HEK 293 cells,
21 immunocytochemistry (ICC) was performed to detect cellular prion protein, then the slides were imaged with Confocal
22 Microscope Leica TCS SP5 II objective 63X oil form Leica Microsystems (Figure 4, A). In order to validate the observed
23 binding between PrP^C and A β os we performed a PRNP knockdown by using the commercially available kit ON-
24 TARGETplus Human PRNP (5621) siRNA – SMARTpool. Because only the PrP^C on the cell surface fraction is
25 involved in the interaction with A β os, the knockdown was combined with acute cleavage promoted by phospholipase
26 C (PLC). A live cell staining and imaging was performed, and cells were analyzed by Flow Cytometry: Fluorescence-
27 Activated Cell Sorting (FACS). As controls were used untreated cells and cells treated with ON-TARGETplus Non-
28 targeting siRNA Pool (scrambled siRNA). The result was a protein expression reduction by more than 80% (Figure 4,
29 B). It is also interesting to note that phospholipase C (PLC) can cleave PrP^C on the surface and improve the effects of
30 knockdown further, i.e. further reduces the PrP^C on the cell surface.

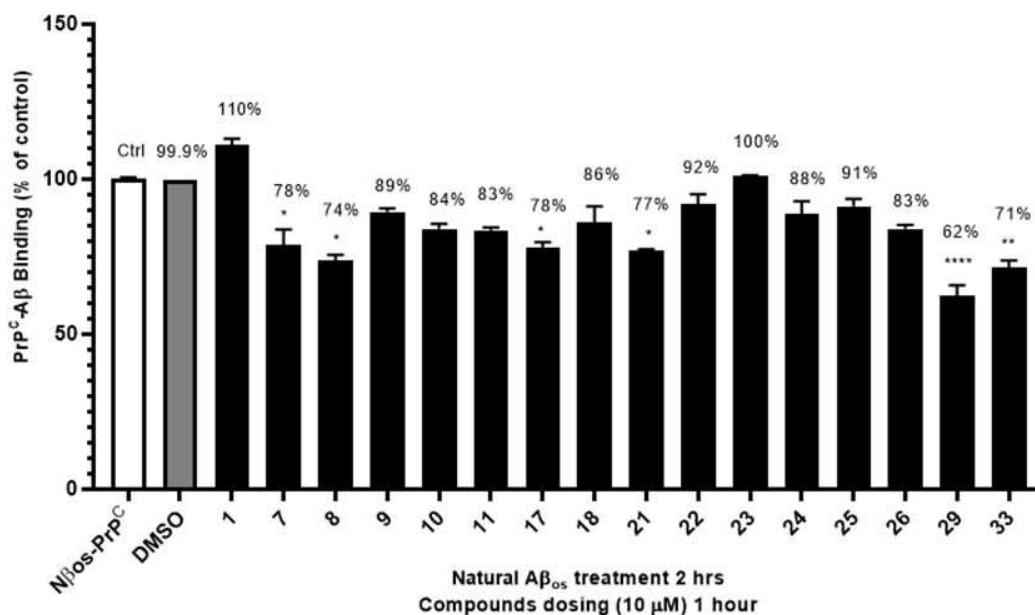


Figure 5. Screening for compounds able to induce a PrP^C-NAβ_{os} binding inhibition. All compounds were tested at 10 μM as final concentration. Results are expressed as the mean ± standard error mean (SEM); n = 3. Significant differences between control are indicated with **** $p \leq 0.0001$. The PrP^C-NAβ₁₋₄₂ binding (%) after treatment with the compounds is also indicated.

C. Inhibition of Aβ-induced Fyn activation

The Opera[®] High Content Screening System was used in this section, as it is applied to test drugs capable of reversing the altered phenotype observed in AD such as Fyn activation.

Figure 6 shows that the level of Fyn activation of hiPSC derived neural progenitor cells from healthy donors increased upon treatment with Aβ, i.e. pFyn production is increased. However, we observed that the level of Aβ-induced Fyn activation was reduced back to normal control values in the presence of the commercial Fyn kinase inhibitor PP1, an inhibitor of Src family tyrosine kinases Lck, Fyn, Hck, and Src. Moreover, it shows that compounds **8** and **9** (simple *per-O*-methylglucosylphenols), **18** (*per-O*-methylglucosylhydroquinone dibenzoate), **21** (rationally designed glucosylhydroquinone monobenzoate), **25** and **26** (both glucosylcatechol dibenzoate derivatives), **23** and **24** (fully unprotected glucosylacetophloroglucinol and glucosyl-naphthalene-2-ol) were able to significantly reduce Aβ-induced Fyn activation at 10 μM. Moreover, these C-glucosyl polyphenols are indeed more active than aglycone genistein.

Fyn kinase plays an important role in the physiology of neuronal cells by regulating cell proliferation and differentiation during the development of the CNS. This enzyme is also involved in signalling transduction pathways that regulate survival, metabolism and neuronal migration.⁴⁷ Considering that Fyn inhibition below the physiological levels (basal levels) could be deleterious for the homeostasis of the cells, we decided to investigate the effects of the compounds

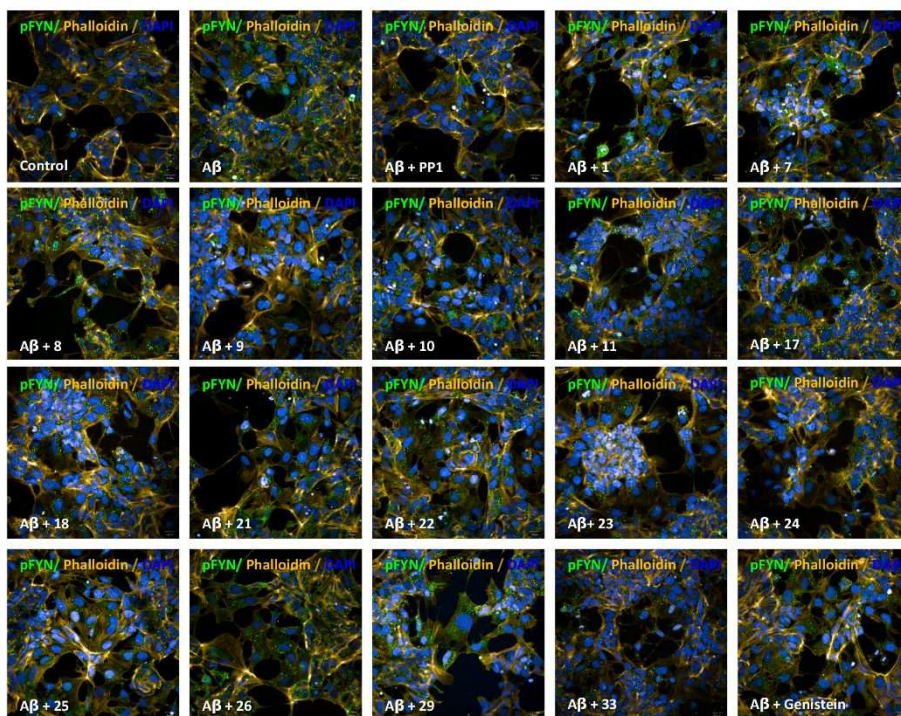
1 on the basal levels of pFyn. Thus, neuronal progenitor cells were treated with the compounds without addition of A β to
2 determine whether the effects observed are independent of A β treatment, and it was confirmed that tested compounds
3 and PP1 alone do not reduce the basal levels of pFyn (Figure 6 C).
4

5
6
7 A rather diverse selection of compounds was able to produce the desired effects, ranging from per-*O*-methyl and
8 polyhydroxy forms. Curiously, the natural compound that served as the inspiration for this study (**1**) was only able to
9 cause a non-significant reduction in A β -induced Fyn activation. Yet, the rationally designed and more flexible
10 hydroquinone monobenzoate (**21**) exhibited significant differences when compared to A β alone. In fact, chemical
11 modifications made in the original scaffold towards simpler versions of compound **1** without ring B (*e.g.* in compounds
12 **8**, **9**, and **23**) were generally more beneficial for the desired activity. On the other hand, no conclusions could be drawn
13 regarding the advantages or disadvantages of sugars decorated with per-*O*-methyl groups, as no correlation between
14 structure and activity could be found regarding this matter. A good example is the presence and absence of these groups
15 in the two most complex hits found in this assay, compounds **25** and **26**, respectively.
16
17

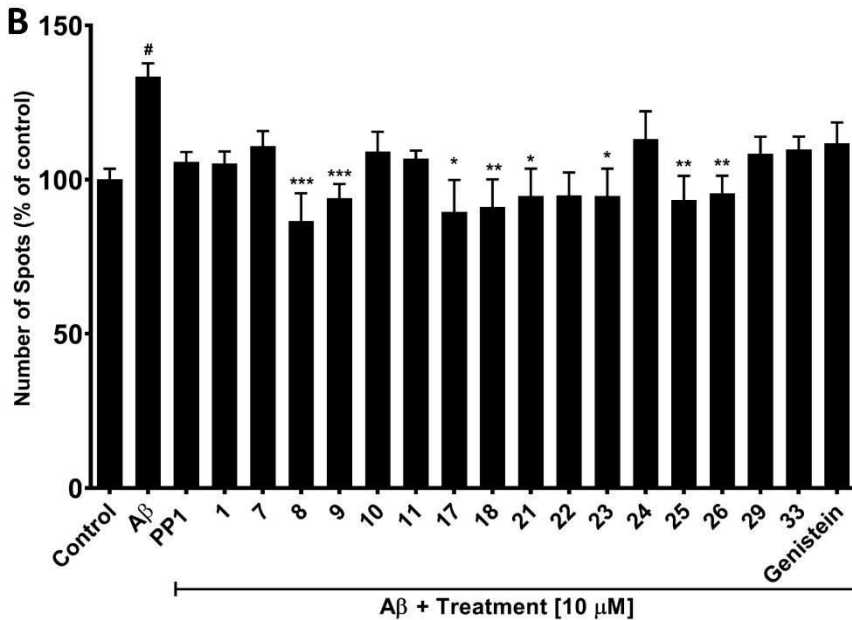
18
19
20 We also evaluated the activity of Fyn kinase in the presence of some compounds by ADP-Glo™ kinase assay, a
21 luminescent ADP detection assay (Figure 7). This assay provides a homogeneous and high-throughput screening method
22 to measure kinase activity by quantifying the amount of ADP produced during a kinase reaction.
23
24

25
26
27 As presented in Figure 7, PP1 was able to reduce the Fyn kinase activity at different concentrations from 1 to 50 μ M,
28 as expected. Furthermore, from the evaluated compounds, only **8** and **10** were able to act as Fyn kinase inhibitors,
29 denoting that they may have an added therapeutic value against DID given the recognized role of Fyn kinase activity in
30 insulin sensitivity and lipid utilization.⁸⁻¹⁰ The fact that compounds **8** and **10**, but not **9**, were able to inhibit Fyn activity
31 indicates that in per-*O*-methyl sugar-containing structures, the acetyl moiety is detrimental for activity, and the *para*-
32 and *ortho*-hydroxylation pattern of the polyphenol is not relevant.
33
34
35
36
37
38
39
40
41
42
43
44
45
46
47
48
49
50
51
52
53
54
55
56
57
58
59
60

A



B



C

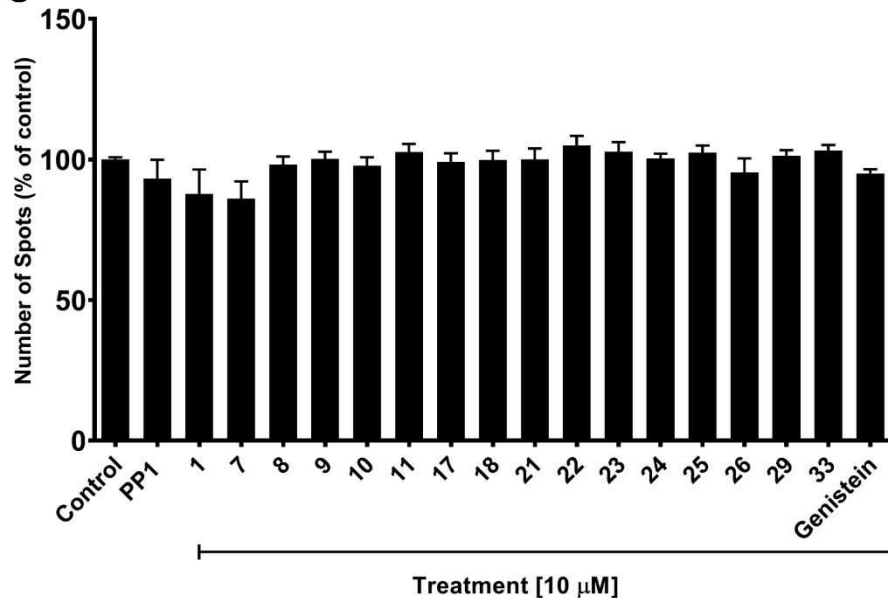


Figure 6. Effect of glucosylphenols in A β -induced Fyn activation (A, B); effect of glucosylphenols on the basal levels of pFyn, in the absence of A β (C). The indirect activation of Fyn kinase was measured by immunofluorescence using Opera[®] High Content Screening System (A). Cells were exposed to 10 μ M of compounds in association with A β . The results were normalized against the control group, which was considered as 100%. (B and C) Percentage of number of pFyn + spots in each treatment group. Results are expressed as the mean \pm standard error mean (SEM); n = 3. Significant differences between control are indicated with # ($p \leq 0.05$) and * ($p < 0.05$) when compared to A β treatment (* $p < 0.05$) or ** ($p < 0.01$) or *** ($p < 0.001$).

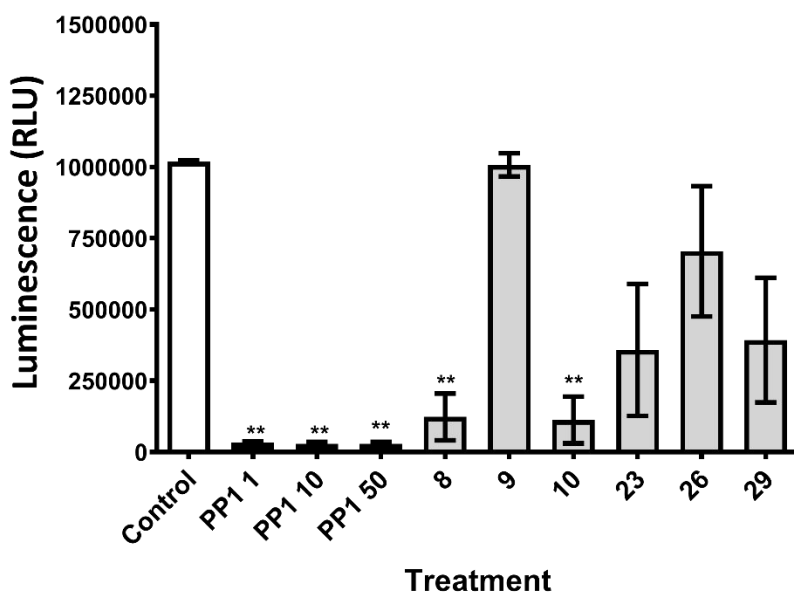


Figure 7. Effect of glucosylpolyphenols and the polyphenol glucoside **29** in the inhibition of Fyn kinase activity measured by the ADP-Glo[™] kinase assay. Results are expressed as the mean \pm SEM; n = 3. Significant differences between control are indicated with * ($p < 0.05$) or ** ($p < 0.01$) when compared with A β treatment.

It is also important to note that, as tested by a thioflavin-T (ThT) fluorescence assay with A β (1-42) (see Figure S5 in Supporting Information), compounds of this series do not significantly inhibit A β (1-42) aggregation *per se*, which suggests that the inhibition of A β -induced Fyn kinase activation is unlikely to occur exclusively via direct interaction with A β . Most importantly, these results indicate that these compounds are not PAINS acting *via* autoxidation of catechol/hydroquinone and subsequent covalent binding to proteins, contrarily to quercetin, a well-known PAIN compound⁴⁸ used as positive control in this assay.

To estimate eventual behavior of compounds **9**, **23**, and **26** as pan-assay interference compounds (PAINS), in particular as membrane PAINS, we have evaluated their potential using a computational protocol. The potential of mean force

(PMF) for translocating a hydrophobic probe across a POPC bilayer loaded with compounds **9**, **23**, and **26** (10% mol/mol) and their calculated membrane permeabilities, are shown in Figure S6 and Table S1 in Supporting Information. Membrane PAINS, even mild ones such as resveratrol,⁷⁸ make the membrane significantly more permeable to hydrophobic compounds. In contrast, none of our compounds led to a significant increase in membrane permeability, thus indicating that they do not act as membrane PAINS. In addition, we submitted their structure to the badapple online service,⁷⁹ and the resulting promiscuity indicators also confirm that these compounds will unlikely act as PAINS.

D. Aggregation Studies

With the formation of aggregates, the concentration of free monomers in solution decreases, while the number and/or size of particles in suspension increase, and, consequently, so does light scattering. On the other hand, aggregate formation might also induce changes in vibrational progression and the appearance of exciton bands, which are readily detected in the electronic absorption spectra through changes in the spectral envelope, such as emergence of new bands, band broadening and variation of the absorbance at λ_{max} , which, if there is no aggregation and other interferences, should have a linear relation with the concentration of the molecule.⁵¹

Aggregating and non-aggregating compounds have been successfully identified using static light scattering and/or electronic absorption spectroscopy to detect such alterations caused by aggregation. For instance, quercetin⁵² and miconazole^{50,53} were found to aggregate, while fluconazole and ketoconazole are non-aggregating molecules.⁵⁰

Taking these findings into consideration, static light scattering, and electronic absorption spectroscopy were used to assess compound aggregation behavior. Only compounds with interesting bioactivity were selected for these experiments, namely compounds **8**, **9**, **10**, **18**, **21**, **23**, **24**, **25**, **26** and **33**. The compounds under study were compared with ketoconazole, a known non-aggregating molecule acting as the negative control, and with quercetin, a promiscuous aggregator, used as the positive control.

Light scattering intensity for compounds **8**, **9**, **10**, **23**, **24** and **33** (Figure 8A and B), **21** and **26** (Figure 8C and D) was similar or weaker than for ketoconazole, for concentrations ranging from 10 μM up to 100 μM . Moreover, the values for those compounds were significantly lower than the light scattering intensity measured for quercetin. These results indicate that those eight compounds do not aggregate in this concentration range. Moreover, by comparing the normalized absorption spectra for each compound at different concentrations (Supporting Information, Figures S7 and S8), no alterations were observed in the absorption spectra of those eight-compounds, both in terms of energy, vibrational progression or number of bands, also pointing to the absence of aggregation for these compounds. On the other hand, at

1 high concentrations the absorption spectra of the positive control, quercetin, suffers drastic changes (Figure S7 -
2 quercetin). First, the typical band of the monomeric species, with maximum at ca. 385 nm,⁵⁴ suffers a blue shift to
3 330 nm and becomes broader. This is caused by the loss of the double bond character due to rotation of the 2-1' bond
4 out of plane, and consequently the loss of the planar conformation.⁵⁴ Also, new bands are visible at ca. 375 nm that
5 indicate the presence of extended conjugation, through catechol-catechol bonds. A new band is also visible for the
6 highest concentration of 100 μ M between 245 and 270 nm, which, when compared with the absorption spectra of the
7 different ionization states of the molecule^{55,56} may indicate an increase of the non-protonated quercetin species.⁵⁷ All
8 these changes are related to the aggregation of the compound. In fact, the pKa of a compound in an aggregate (e.g.,
9 micellar) environment is different from the one of the monomeric species in solution, shifting the ionization
10 equilibrium.⁵⁸ If any of the compounds tested were aggregating, changes in the absorption spectra would be readily
11 detected, which was not the case.

12 For compounds **18** and **25**, solutions with only 1.25% and 2.5% DMSO were visibly turbid, especially for 100 μ M,
13 which is an indication of the low aqueous solubility of these compounds that might be due to their high lipophilicity.
14 With a value as high as 5% of DMSO, the solutions with higher compound concentrations (50 μ M and 100 μ M) were
15 still turbid. However, this was not the case at 10 μ M and, as can be observed in Figure 8 for this concentration (at which
16 the cellular studies were conducted), the light scattering intensity is lower than for the non-aggregator ketoconazole.
17 This indicates that at this concentration these two compounds are not aggregating.

18 Finally, a linear relationship was confirmed between the concentration and the peak absorbance for the lower energy
19 band of each compound and for the non-aggregating ketoconazole (Figures S9 and S10), while for the promiscuous
20 quercetin such relation does not follow a linear behavior (Figure S9 - Quercetin).

21 In summary, compounds **8**, **9**, **10**, **21**, **23**, **24**, **26** and **33** are not promiscuous aggregators in the concentration range
22 tested, which encompasses all the concentrations used for the other assays. Our results for compounds **18** and **25** show
23 that at the concentration of 10 μ M no aggregation was detected but at high concentrations, the herein presented inhibition
24 constants should be considered only as estimates and interpreted with caution.

25 The aggregation studies confirm that bioactivities herein reported are not due to non-specific effects resulting from the
26 formation of compound aggregates and are thus the result of bona fide specific compound activity.

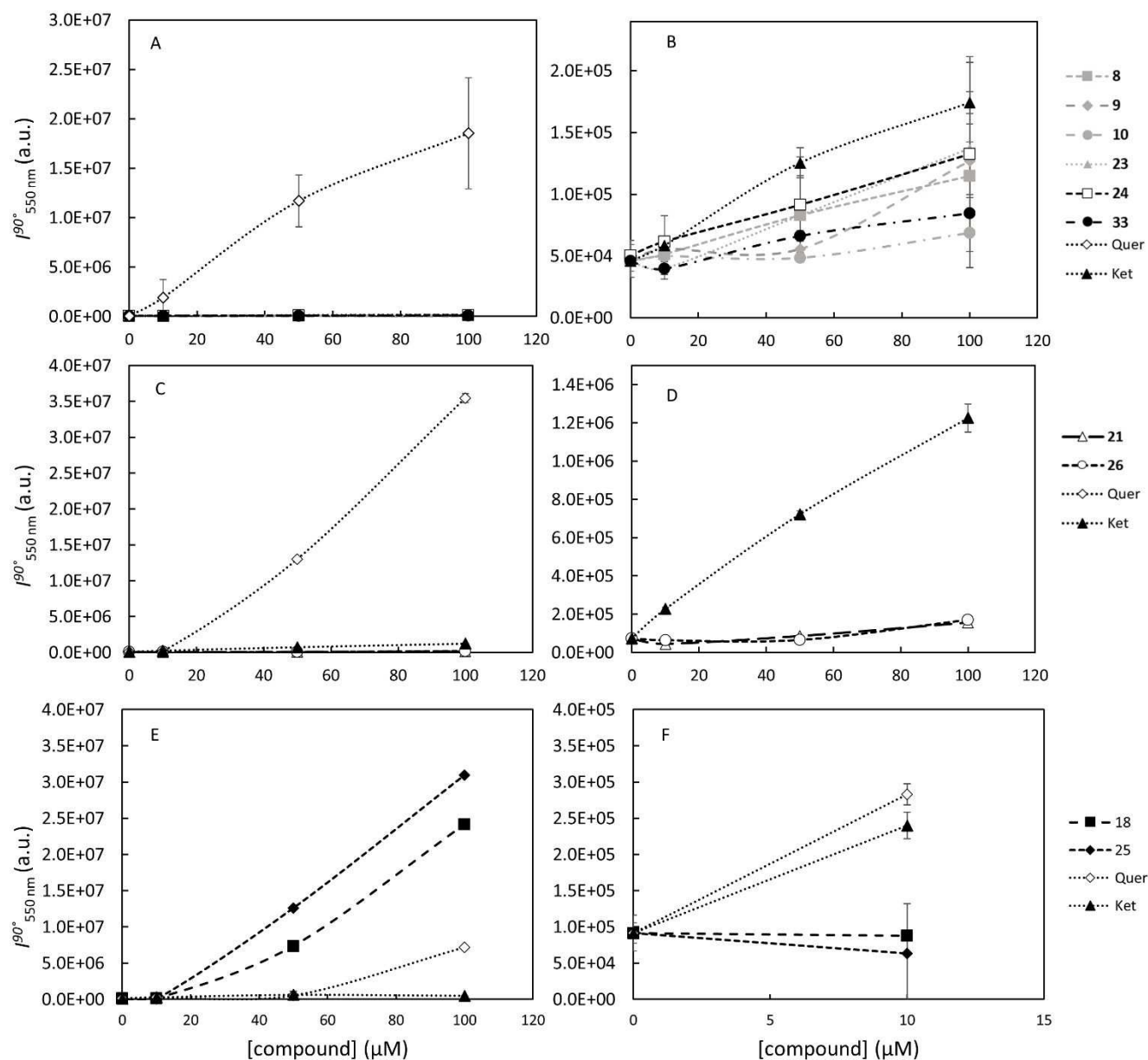


Figure 8. Static light scattering intensity at 550 nm and 90°, for compounds 8, 9, 10, 23, 24, 33 (A and B), 21, 26 (C and D), 18 and 25 (E and F), and the respective controls: Ketoconazole (Ket) and Quercetin (Quer) at 10, 50 and 100 μM. Samples were dissolved in 10 mM PBS (with 100 mM NaCl, pH 7.4) and 1.25% (A and B), 2.5% (C and D) or 5% (E and F) DMSO. The values are the mean ± S.D. of at least two independent experiments. The graphics without Quer (B and D) are for a better depiction of the behavior of low scattering compounds. Graphic F is a zoom-in of E for a better observation of what is happening for the lowest concentration of the compounds. The lines are merely to guide the eye.

E. Inhibition of A β -induced Tau phosphorylation

Intraneuronal Neurofibrillary tangles (NFTs) of paired helical filaments (PHF)s are a histopathological hallmark of Alzheimer's disease (AD). These NFTs are formed of hyperphosphorylated Tau. Tau is hyperphosphorylated in AD brain at multiple sites including at residues Thr181.⁵⁹⁻⁶² In order to assess if the compounds are indeed able to accomplish the desired downstream effects by reducing A β -induced Tau pathology, we performed a high-content image screening (HCS) for phosphorylated Tau (pTau), at Thr181 as recognized by the antibody AT270, using

compounds that previously revealed to inhibit A β -induced Fyn activation. Our data (Figure 9) revealed that cortical neurons exposed to A β have increased pTau levels when compared to DMSO controls. On the other hand, neurons treated with A β in addition to 10 μ M of compounds **9**, **10**, **18**, **23**, **25**, **26**, **29**, and genistein significantly reduced the levels of pTau when compared to the A β controls. Even though there was a reduction of pTau in cells treated with compounds **8** and **33**, this reduction was found not to be statistically significant. From all tested compounds, **9**, **18**, **23**, **25** and **26** were able to reduce A β -induced Fyn activation, with concomitant decrease in A β -induced pTau.

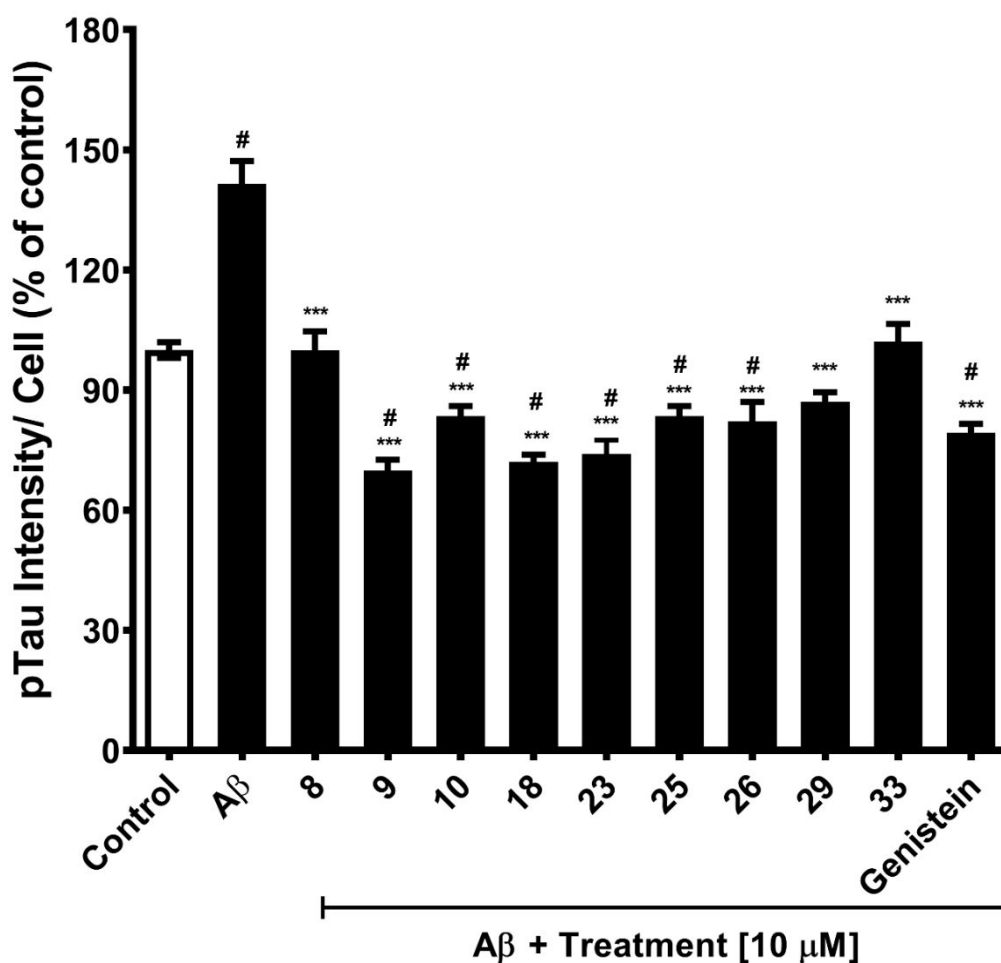


Figure 9. Effect of compounds against hyperphosphorylation of Tau induced by A β . Neurons treated with A β oligomers were evaluated against pTau (AT270). Tau hyperphosphorylation was measured by immunofluorescence using Opera[®] High Content Screening System. Cells were exposed to 10 μ M of each compound in association with A β for 4 days. Results were normalized against the control group considered as 100%. The values are expressed as the mean \pm SEM; n = 3. Significant differences between control are indicated with # ($p \leq 0.05$) and * ($p < 0.05$), ** ($p < 0.01$) or *** ($p < 0.001$) when compared with A β treatment.

F. Cytotoxicity in neuronal cells derived from hiPSCs

In order to confirm that the synthesized compounds are not cytotoxic at relevant concentrations, we have differentiated hiPSC cells derived from health control MIFF1⁶³ into neural cells. We observed that, after 20 days of differentiation, these cells express specific neural progenitor markers such as Nestin. NPC cells were treated with each compound for 24 hours, and none presented any signs of cytotoxicity at 10 μ M (Figure 10). Furthermore, compounds **23**, **26**, and **29** were not cytotoxic in concentrations up to 100 μ M, while **9** is safe to administer up to a 50 μ M concentration (data not shown).

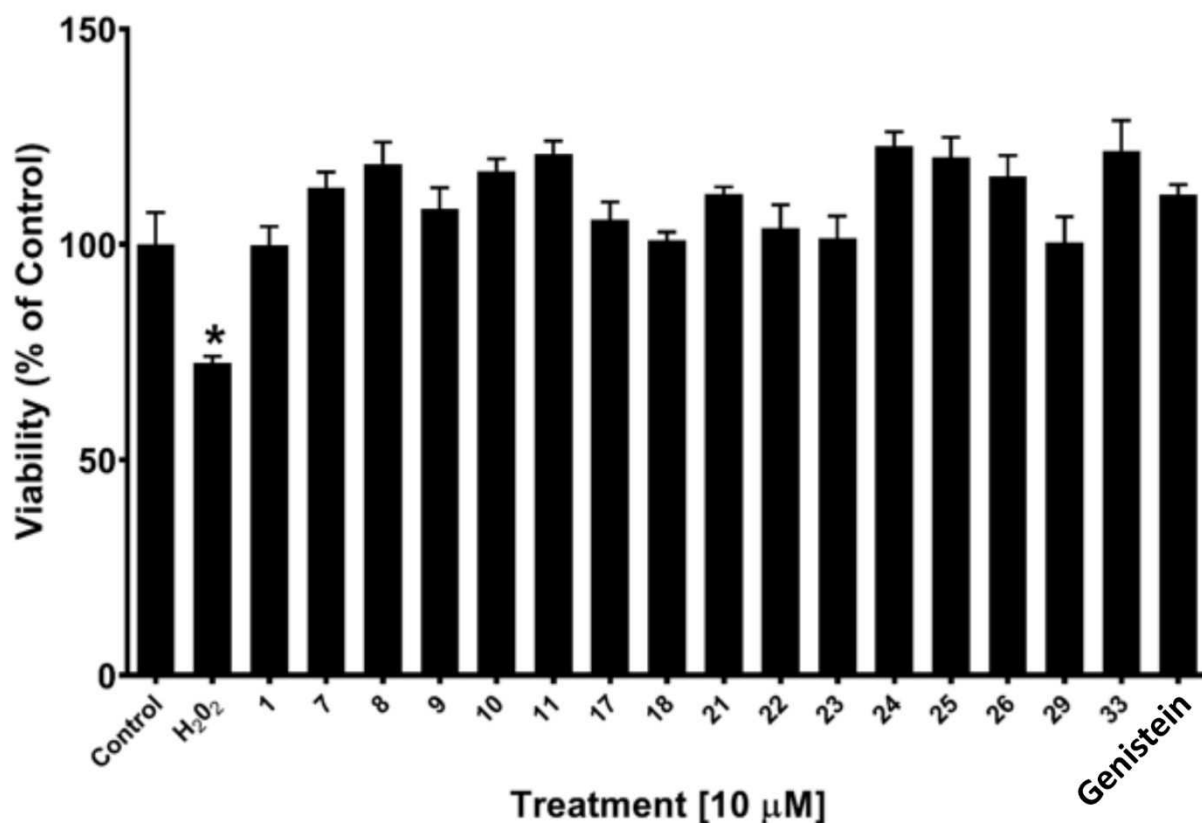


Figure 10. Cytotoxicity of *C*-glucosyl phenols and glucosides **29**, **33** in neuronal cells derived from hiPSCs. Cell viability was measured in an MTT assay. Cells were exposed to 10 μ M of each compound for 24 h. Results were normalized relative to a control group considered as 100%. The values are expressed as the mean \pm SEM; n = 3. Significant differences between control are indicated with * ($p < 0.05$).

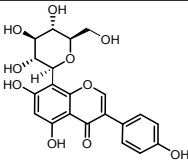
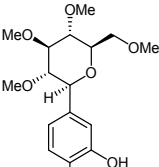
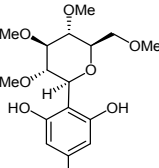
G. Glycosidase and cholinesterase inhibitory activity screening

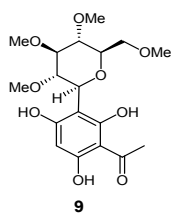
Postprandial glycemia control is key in managing T2D clinical manifestations. This control can be achieved through the inhibition of intestinal glucosidases, in particular α -glucosidase.⁶⁴ These enzymes catalyze the hydrolysis of complex carbohydrates present in the gut into simple sugars able to be absorbed into the blood stream and thus contribute to the increase of glycemia levels.⁶⁵ Since we had previously elucidated the powerful α -glucosidase inhibitory activity of the ethyl acetate extract of *Genista tenera* where compound **1** is the major component (97.6% for the extract vs. 82.2% for

the commercial drug acarbose), we were interested in finding out if it was due to the presence of the lead *C*-glucosyl isoflavone.⁶⁶ However, **1** was found to have only modest activity, with 14% inhibition at 100 μ M (Table 3). This compound was a slightly better β -glucosidase inhibitor, being able to decrease its activity in 23% at the same concentration. Notably, these activities are cumulative with the antihyperglycemic effects of **1** observed in Wistar rats, since treatment was administered i.p.

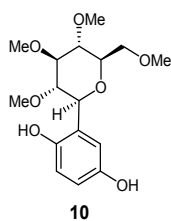
Genistein, on the other hand, is a powerful α -glucosidase uncompetitive inhibitor (84% inhibition at 100 μ M; $K_{ib} = 12 \pm 2 \mu$ M) and a moderate β -glucosidase competitive inhibitor (44% inhibition at 100 μ M; $K_{ia} = 66 \pm 13 \mu$ M), indicating that the presence of the C-C linked sugar moiety at C-8 is, in this case, detrimental to activity. Remarkably, the catechol glucoside **33** was found to be the best glucosidase inhibitor amongst the synthesized analogues, with an excellent α -glucosidase competitive inhibitor activity (74% inhibition at 100 μ M; $K_{ia} = 39 \pm 4 \mu$ M), and a modest β -glucosidase inhibitor activity (13% inhibition at 100 μ M). Apart from this compound, only three others were able to concomitantly inhibit both glucosidases: the hydroquinone derivatives **17** and **29**, and the naphthalen-2-ol derivative **24**.

Table 3. Glycosidase and cholinesterase (AChE and BuChE) inhibitory efficacy of compound **1** and analogues at 100 μ M.

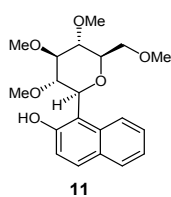
Compound	α -Glucosidase Inhibition	β -Glucosidase Inhibition	AChE Inhibition	BuChE Inhibition
 1	14%	23%	26%	n.i.
 7	n.i.	14%	15%	16%
 8	n.i.	15%	n.i.	10%



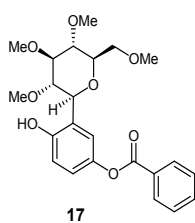
n.i. n.i. n.i. **16%**



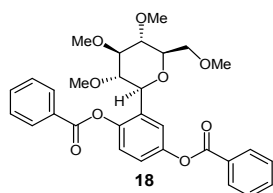
n.i. n.i. n.i. **21%**



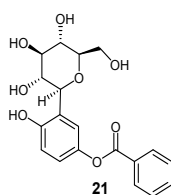
n.i. **16%** n.i. **23%**



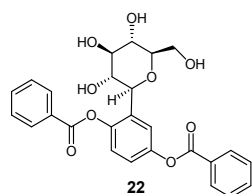
11% **24%** **14%** **12%**



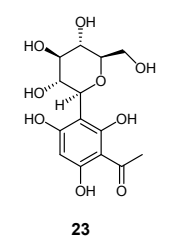
n.i. **18%** **19%** **16%**



n.i. **17%** n.i. n.i.

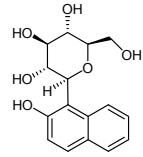
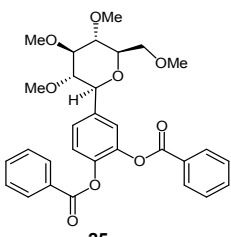
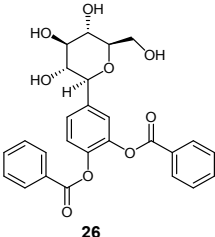
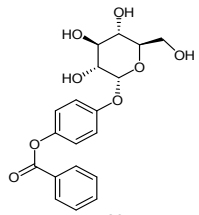
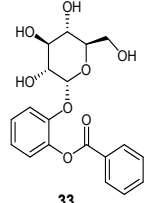
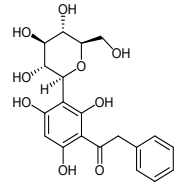
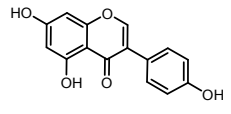


n.i. **18%** n.i. **21%**



n.i. **24%** n.i. **15%**

1
2
3
4
5
6
7
8
9
10
11
12
13
14
15
16
17
18
19
20
21
22
23
24
25
26
27
28
29
30
31
32
33
34
35
36
37
38
39
40
41
42
43
44
45
46
47
48
49
50
51
52
53
54
55
56
57
58
59
60

	12%	23%	n.i.	10%
24				
	n.i.	27%	n.i.	12%
25				
	n.i.	17%	n.i.	39%
26				
	18%	19%	n.i.	10%
29				
	74% Competitive inhibition $K_{ia} = 39 \pm 4 \mu\text{M}$	13%	10%	17%
33				
	n.i.	n.i.	n.i.	17%
37				
	84% Uncompetitive inhibition $K_{ib} = 12 \pm 2 \mu\text{M}$	44% Competitive inhibition $K_{ia} = 66 \pm 13 \mu\text{M}$	12%	41%
Genistein				

K_{ia} - inhibition constant of the inhibitor binding the free enzyme; K_{ib} - inhibition constant of the inhibitor binding the enzyme-substrate

Complex; n.i. = no inhibition; n.d. = not determined.

1 Acetylcholinesterase (AChE) and butyrylcholinesterase (BuChE) are two well-characterized therapeutic targets in AD
2 owing to their ability to catalyse the hydrolysis of the neurotransmitter acetylcholine, which is responsible for the
3 cognitive functionality, and whose level is particularly low in AD patients. Three of the so far four FDA-approved drugs
4 for AD consist of selective or dual cholinesterase inhibitors, including donepezil, galantamine and rivastigmine.² The
5 inhibition of AChE and BuChE correlate with lower A β levels, decreased A β aggregation, improved learning and
6 memory.⁶⁷⁻⁷⁰ BuChE is considered to play a minor role in the regulation in acetylcholine levels in healthy brains;
7 however, the levels of this enzyme progressively increase in AD, whereas those of AChE decline or remain unchanged.⁷¹
8 Not so well studied and divulged is the role of butyrylcholinesterase in the etiology of T2D. However, elevated AChE,
9 but especially serum BuChE activity have been correlated with insulin resistance, increased adiposity and abnormal
10 serum lipid profile, being regarded as a risk factor for T2D.⁷²⁻⁷⁵ Thus, these two enzymes may be regarded as additional
11 therapeutic targets for DID.

12 Similar to what was described for α -glucosidase, the ethyl acetate extract of *Genista tenera* was capable of inhibiting
13 this enzyme (77.0% at 130 μ g/mL).⁶⁶ Hence, we were interested in assessing whether the anticholinergic activity of the
14 extract was due to the presence of **1** as a major component. This compound was however able to inhibit AChE only by
15 26% at 100 μ M (43 μ g/mL) and, in this assay, genistein presented merely half of the inhibitory capacity of **1** (Table 3).
16 On the contrary, genistein was a much stronger BuChE inhibitor than **1**, displaying 41% inhibition at 100 μ M. From the
17 synthesized analogues of **1**, only compounds **7**, **17**, **18** and **33** were active against AChE, while roughly all presented a
18 BuChE inhibition capacity of, at least, 10%. Compounds **10**, **11**, **22** and **26** were able to inhibit BuChE in over 20% at
19 100 μ M, from which compound **26** stands out with 39% inhibition.

20 H. Membrane permeability assays

21 Compounds were tested in a parallel artificial membrane permeability assay (PAMPA) in order to measure and
22 rationalize their potential to cross membrane barriers. Testosterone was used as the positive control in this assay. It is
23 important to note that this assay merely looks into the ability of compounds to passively diffuse through cell membranes.
24 Being glycosides, it is possible that the sugar moiety acts as a shuttle for their passage into the brain through GLUT-1
25 transporters highly expressed in the blood-brain barrier (BBB), as previously reported for similar molecules.⁷⁶

26 To complete our analysis, the partition coefficient at physiological pH ($\log D_{7.4}$) was also determined for most
27 compounds. Ideally, $\log D$ values should be located between 1 and 4 for a good compromise between solubility and

membrane permeability allowing oral availability, good cell permeation and low metabolic susceptibility.⁷⁷ Results are presented in Table 4.

Table 4. Calculated partition coefficient ($c \log P$), effective permeability ($\log P_e$) and partition coefficient at pH 7.4 ($\log D_{7.4}$) of the synthesized compounds and genistein

Compound Nr.	$c \log P^{a,b}$	$\log P_e$	$\log D_{7.4}$
1	-0.17	- 4.63 ± 0.15	-0.1 ± 0.1
7	0.74	- 5.33 ± 0.08	1.1 ± 0.1
8	0.58	- 5.24 ± 0.17	1.6 ± 0.2
9	1.06	- 4.74 ± 0.02	2.3 ± 0.3
10	0.75	- 5.52 ± 0.07	n.d.
11	1.96	- 4.39 ± 0.04	2.7 ± 0.2
17	2.70	Membrane retention over 80%	3.2 ± 0.1
18	3.95	Equilibrated	> 2.5
21	0.60	- 6.35 ± 0.12	< 0.5
22	1.93	- 5.18 ± 0.61	2.0 ± 0.2
23	-1.23	Below detection limit	n.d.
24	-0.44	- 6.41 ± 0.24	n.d.
25	3.81	Partial membrane retention	> 2.5
26	1.95	- 5.06 ± 0.08	n.d.
29	0.59	Below detection limit	1.0 ± 0.1
33	0.58	- 5.85 ± 0.54	0.1 ± 0.3
37	0.13	n.d.	n.d.
Genistein	2.45	- 4.49 ± 0.04	3.3 ± 0.2
Testosterone	2.99	- 4.42 ± 0.09	---

n.d. = not determined; n.d. - not determined; ^aCalculated using ALOGPS 2.1. ^bBased on $c \log P$ values, **1**, **23** and **24**

are classified as hydrophilic compounds ($c \log P < 0$); **7**, **8**, **10**, **21**, **29**, **33** and **37** are classified as moderately lipophilic ($c \log P 0-1$); **9**, **11**, **17**, **18**, **22**, **25**, **26** and genistein are classified as lipophilic compounds ($c \log P > 1$) (Table 5, Experimental Section).

The optimal effective permeability of compound **1** ($\log P_e > -5.7$) indicates that it can cross membrane barriers, which is consistent with the therapeutic use of the plant *Genista tenera* in traditional medicine in the form of an antidiabetic tea infusion. Moreover, our results for compounds **7-11** suggest that the transformation of the sugar hydroxy groups into methyl ether moieties succeeded at enhancing membrane permeability (see fully unprotected compounds **23** and **24**). Among these compounds is **9**, the *per*-methylglucosyl derivative of acetophloroglucinol, which was found to decrease A β -induced Fyn activation with consequent downstream effects in the reduction of Tau hyperphosphorylation. This compound presented an effective permeability ($\log P_e = -4.74 \pm 0.02$) and determined $\log D$ values (2.3 ± 0.3) that are compatible with the desired pharmacokinetic profile and thus contrasting with its bioactive polyhydroxy analogue **23**. When applied to compounds with more than one aromatic ring, this sugar *per*-methylation approach resulted in extremely lipophilic compounds with a tendency to equilibrate or to get retained in biological membranes (compounds **17**, **18** and **25**). In contrast, with three aromatic rings but without the sugar *O*-methyl groups, compound **26**, another promising hit in our bioactivity experiments, presents an acceptable effective permeability ($\log P_e = -5.06 \pm 0.08$).

Discussion and Conclusions

In the present work we have developed a library of glucosylpolyphenols inspired in the natural product with therapeutic potential **1** and explored their activity against multiple AD and T2D targets, namely Fyn kinase, Tau hyperphosphorylation, hIAPP, glucosidase and cholinesterase enzymes. On the path towards their synthesis, we disclosed the feasibility and effectiveness of *C*-glucosylation of polyphenols with different hydroxylation pattern and rationalized the importance of sugar protecting groups in these reactions. Moreover, we present an exception to the Fries-type rearrangement leading to the *C*-glycosylation of unprotected polyphenols, which afforded compounds **7** and **12** – two important precursors in the synthesis of novel bioactive molecular entities against our targets of interest. Being structurally less complex and synthesized in only 5 steps (*vs.* 9 steps required for the generation of the natural isoflavone **1**), the rationally designed analogue **21** is here presented as a new alternative for tackling hIAPP detrimental effects in T2D and DID. STD-NMR experiments show that compound **21** clearly binds to hIAPP and in general with a similar binding epitope to that of compound **1**, which highlights that the absence of the central fused ring system of

1 isoflavone core does not disrupt the binding towards hIAPP. This result opens the door to further exploit this compound
2 as a molecular probe against IAPP-induced pancreatic failure and IAPP-promoted cross-seeding events with A β . Even
3 though it is not the right option when it comes to glucosidase or cholinesterase inhibition, our investigation revealed
4 that compound **21** is effective in the prevention of A β -induced Fyn activation. Yet, we herein disclose that much simpler
5 C-glucosyl polyphenols embody the right scaffold to tackle the chain of processes culminating in Tau
6 hyperphosphorylation. One of these compounds is **9**, embodying a *per-O*-methylglucosyl C-C linked to 2,4,6-
7 trihydroxyacetophenone. It was found to inhibit A β -induced Fyn kinase activation, and to consequently reduce the levels
8 of hyperphosphorylated Tau. Moreover, it has the right balance between effective permeability and lipophilicity to be
9 orally available and brain penetrant, as revealed in PAMPA and log $D_{7,4}$ determination assays. With the additional
10 advantage of being efficiently synthesized in only 2 steps, our results indicate that **9** should indeed be regarded as a new
11 promising scaffold for further development against A β -induced Tau pathology in AD.
12
13
14
15
16
17
18
19
20
21
22
23

24 Another promising compound discovered in this study was **26**, with the free glucosyl group C-C linked to catechol
25 dibenzoate. Indeed, it stood out in the PAMPA assay for being one of the polyhydroxy sugar derivatives with potential
26 to cross biological membranes with the desired activity when it comes to A β -induced Fyn kinase activation and
27 consequent Tau hyperphosphorylation levels. Furthermore, it was found to be a BuChE inhibitor (39% inhibition at 100
28 μ M). Curiously, when it comes to therapeutic potential through glucosidase inhibition, its *O*-glucosyl catechol
29 monobenzoate analogue **33** was the best within this series. It was able to inhibit α -glucosidase in 74% at 100 μ M, as
30 well as β -glucosidase, AChE and BuChE, but only to a lower extent (10%-17% at 100 μ M). These results illustrate the
31 impact of C-glycosylation vs. *O*-glycosylation in the fine tuning of bioactivity of analogue structures, and present both
32 the C-glucosyl catechol **26** and *O*-glucosyl catechol **33** as new lead compounds against DID.
33
34
35
36
37
38
39
40
41
42
43

44 Ultimately, this study strongly evidences the potential of glucosylpolyphenols as therapeutic agents against AD and
45 T2D and offers several lead structures with different hydroxylation pattern and adequate physicochemical profiles for
46 further development against relevant therapeutic targets for both diseases. Very importantly, it shows, for the first time,
47 that C-glucosyl polyphenols are promising scaffolds able to tackle A β -induced Fyn kinase activation with enough
48 efficacy to reduce Tau phosphorylation, thus having the potential to change the paradigm of drug discovery against AD
49 and DID.
50
51
52
53
54
55
56
57
58

59 Experimental Section

HPLC grade solvents and reagents were obtained from commercial suppliers and were used without further purification. Genistein was purchased from Sigma Aldrich while compound **1** was synthesized according to the previously described methodology.²⁵ Thin layer chromatography (TLC) was carried out on aluminum sheets (20 × 20 cm) coated with silica gel 60 F-254, 0.2 mm thick (Merck) with detection by charring with 10% H₂SO₄ in ethanol. Column chromatography (CC) was performed using silica gel 230–400 mesh (Merck). Melting points were obtained with a SMP3 Melting Point Apparatus, Stuart Scientific, Bibby. Optical rotations were measured with a Perkin–Elmer 343. Nuclear Magnetic Resonance (NMR) experiments were recorded on a Bruker Avance 400 spectrometer at 298 K, operating at 100.62 MHz for ¹³C and at 400.13 MHz for ¹H for solutions in CDCl₃, CO(CH₃)₂ or CD₃OD (Sigma-Aldrich). Chemical shifts are expressed in δ (ppm) and the proton coupling constants *J* in Hertz (Hz), and spectra were assigned using appropriate COSY, DEPT, HMQC, and HMBC spectra (representative examples are provided in the supporting information appendix). High resolution mass spectra of new compounds were acquired on a Bruker Daltonics HR QqTOF Impact II mass spectrometer (Billerica, MA, USA). The nebulizer gas (N₂) pressure was set to 1.4 bar, and the drying gas (N₂) flow rate was set to 4.0 L/minute at a temperature of 200 °C. The capillary voltage was set to 4500 V and the charging voltage was set to 2000 V. The purity of the final compounds tested was above 95% as confirmed by HPLC-DAD and/or HPLC-DAD-MS.

General methodology for the synthesis of 2,3,4,6-tetra-O-methyl-β-D-glucopyranosylpolyphenols 7-10 and 2-hydroxy-1-(2,3,4,6-tetra-O-methyl-β-D-glucopyranosyl)naphthalene (11). Methyl 2,3,4,6-tetra-O-methyl-α-D-glucopyranoside³⁹ (1.0 g, 4.0 mmol) and the polyphenol/2-hydroxyhaphthalene (8.0 mmol, 2 eq.) were dissolved in dry MeCN (18 mL). The mixture was stirred in the presence of 0.2 g of drierite, under N₂ atmosphere, for 10 min at room temperature. Then, TMSOTf (0.73 mL, 4.0 mmol, 1 eq.) was added dropwise at -78 °C. The temperature was kept at -78 °C in the first 30 min and then allowed to increase to room temperature. The mixture was stirred for 18-48 h, after which the reaction was quenched by adding a few drops of triethylamine. The mixture was washed with brine and extracted with EtOAc (3 x 20 mL), the organic layers were combined, dried over MgSO₄ and concentrated under reduced pressure.

1,2-Dihydroxy-4-(2,3,4,6-tetra-O-methyl-β-D-glucopyranosyl)benzene (7). The reaction crude was purified by column chromatography (dichloromethane/MeOH 1:0 → 50:1) to give **7** as a yellowish solid in 63% yield. R_f (dichloromethane/MeOH 20:1) = 0.31; m.p. = 117.5 – 118.4 °C; [α]_D²⁰ = - 2 ° (c 0.7, CHCl₃); ¹H NMR [(CD₃)₂CO] δ 6.96 (s, 1H, H-3), 6.84 (d, 1H, *J*_{ortho} = 8.07 Hz, H-6), 6.78 (br d, 1H, *J*_{ortho} = 8.07 Hz, H-5), 3.98 (d, 1H, *J*_{1-2'} = 9.47 Hz, H-1'), 3.65 (s, 3H, OCH₃), 3.61-3.51 (m, 5H, H-6'a and H-6'b, OCH₃), 3.43-3.39 (m, 1H, H-5'), 3.37 (s, 3H, OCH₃), 3.29-3.24 (m, 2H, H-3', H-4'), 3.06-3.02 (m, 4H, H-2', OCH₃). ¹³C NMR [(CD₃)₂CO] δ 144.8 (C-1)*, 144.6 (C-2)*,

131.5 (C-4), 119.31 (C-5), 114.7 (C-6), 114.6 (C-3), 88.34 (C-3'), 85.9 (C-2'), 81.0 (C-1'), 79.8 (C-4'), 78.8 (C-5'), 71.7 (C-6'), 60.0, 59.6, 59.4, 58.5 (OCH₃). *Permutable signals. HRMS-ESI (*m/z*): [M+H]⁺ calcd for C₁₆H₂₅O₇ 329.1595, found 329.1597; [M+Na]⁺ calcd for C₁₆H₂₄NaO₇ 351.1414, found 351.1411.

1,3,5-Trihydroxy-2-(2,3,4,6-tetra-O-methyl-β-D-glucopyranosyl)benzene (8). The reaction crude was purified by column chromatography (dichloromethane/MeOH 1:0 → 40:1) followed by recrystallization in diethyl ether, affording **8** as a white solid in 53% yield. R_f (dichloromethane /MeOH 20:1) = 0.35; m.p. = 181.5 – 182.1 °C; [α]_D²⁰ = + 25 ° (*c* 0.4, CHCl₃); ¹H NMR [(CD₃)₂CO] δ 8.17 (br s, 1H, OH-5), 7.94 (br s, 2H, OH-1, OH-3), 5.93 (s, 2H, H-4, H-6), 4.77 (d, 1H, J_{1'-2'} = 9.53 Hz, H-1'), 3.62-3.54 (m, 5H, H-6'a and H-6'b, OCH₃), 3.52 (s, 3H, OCH₃), 3.41 (br d, J_{4'-5'} = 9.14 Hz, 1H, H-5'), 3.34 (s, 3H, OCH₃), 3.31-3.19 (m, 3H, H-2', H-3', H-4'), 3.10 (s, 3H, OCH₃). ¹³C NMR [(CD₃)₂CO] δ 159.6 (C-5), 158.3 (C-1, C-3), 104.0 (C-2), 96.5 (C-4, C-6), 88.7 (C-3'), 84.7 (C-2'), 80.0 (C-4'), 79.5 (C-5'), 75.3 (C-1'), 71.7 (C-6'), 60.9, 60.6, 60.2, 59.3 (OCH₃). [M+H]⁺ calcd for C₁₆H₂₅O₈ 344.1544, found 344.1545; [M+Na]⁺ calcd for C₁₆H₂₄NaO₈ 367.1363, found 367.1369.

1-[2,4,6-Trihydroxy-3-(2,3,4,6-tetra-O-methyl-β-D-glucopyranosyl)phenyl]ethan-1-one (9). The reaction crude was purified by column chromatography (dichloromethane /MeOH 1:0 → 50:1) to give **9** as a colourless oil in 46% yield. R_f (dichloromethane /MeOH 20:1) = 0.38 [α]_D²⁰ = + 91 ° (*c* 0.4, CHCl₃); ¹H NMR (CDCl₃) δ 8.11 (br s, 1H, OH), 5.91 (br s, 1H, H-5), 4.73 (d, 1H, J_{1'-2'} = 9.80 Hz, H-1'), 3.68-3.64 (m, 5H, H-6'a and H-6'b, OCH₃), 3.58 (s, 3H, OCH₃), 3.48-3.44 (m, 4H, H-5', OCH₃), 3.35-3.26 (m, 6H, H-2', H-3', H-4', OCH₃), 2.66 (CH₃-Ac); ¹³C NMR (CDCl₃) δ 203.9 (C=O), 164.4 (C-2), 161.8 (C-4)*, 160.1 (C-6)*, 106.0 (C-1), 102.3 (C-5), 97.2 (C-3), 87.7 (C-3'), 84.9 (C-2'), 79.0 (C-5'), 78.8 (C-4'), 75.1 (C-1'), 71.0 (C-6'), 61.1, 61.0, 60.7, 59.2 (OCH₃). *Permutable signals. HRMS-ESI (*m/z*): [M+H]⁺ calcd for C₁₈H₂₇O₉ 387.1660, found 387.1600; [M+Na]⁺ calcd for C₁₈H₂₆NaO₉ 409.1469, found 409.1473.

1,4-Dihydroxy-2-(2,3,4,6-tetra-O-methyl-β-D-glucopyranosyl)benzene (10). The reaction crude was purified by column chromatography (dichloromethane /MeOH 1:0 → 40:1), followed by recrystallization in diethyl ether to afford **10** as a white solid in 37% yield. R_f (dichloromethane /MeOH 20:1) = 0.34; m.p. = 124.5 – 125.0 °C; [α]_D²⁰ = + 18 ° (*c* 0.5, CHCl₃); ¹H NMR [(CD₃)₂CO] δ 7.77 (s, 1H, OH-1), 7.36 (s, 1H, OH-4), 6.74 (s, 1H, H-3), 6.69-6.64 (m, 2H, H-5, H-6), 4.38 (d, 1H, J_{1'-2'} = 9.59 Hz, H-1'), 3.66 - 3.56 (m, 5H, OCH₃, H-6'a and H-6'b), 3.52 (s, 3H, OCH₃), 3.41 (br d, 1H, J_{5'-4'} = 8.11 Hz, H-5'), 3.34 (s, 3H, OCH₃), 3.29-3.21 (m, 2H, H-3', H-4'), 3.14 (t, 1H, J_{2'-1'-2'-3'} = 9.72 Hz, H-2'), 3.09 (s, 3H, OCH₃). ¹³C NMR [(CD₃)₂CO] δ 150.9 (C-4), 148.7 (C-1), 126.4 (C-2), 117.5 (C-6)*, 116.0 (C-5)*, 115.3 (C-3), 88.7 (C-3'), 85.4 (C-2'), 80.0 (C-4'), 79.2 (C-5'), 78.0 (C-1'), 71.0 (C-6'), 60.5, 60.2, 60.1, 58.9 (OCH₃). *Permutable

signals. HRMS-ESI (m/z): $[M+H]^+$ calcd for $C_{16}H_{25}O_7$ 329.1595, found 329.1582; $[M+Na]^+$ calcd for $C_{16}H_{24}NaO_7$ 351.1414, found 351.1395.

2-Hydroxy-1-(2,3,4,6-tetra-*O*-methyl- β -D-glucopyranosyl)naphthalene (11). The reaction crude was purified by column chromatography (Hex/ dichloromethane 1:1 \rightarrow dichloromethane/MeOH 100:1) to give **11** as a yellow oil in 66% yield. R_f (Hex/EtOAc) = 0.58; $[\alpha]_D^{20} = +89^\circ$ (c 1.0, $CHCl_3$); 1H NMR ($CDCl_3$) δ (ppm) 8.54 (s, 1H, OH-2), 7.97 (d, 1H, $J_{ortho} = 7.46$ Hz, H-8), 7.72-7.68 (m, 2H, H-4, H-5), 7.43 (t, 1H, $J_{ortho} = 7.64$ Hz, H-7), 7.28 (t, 1H, $J_{ortho} = 7.39$ Hz, H-6), 7.14 (d, 1H, $J_{ortho} = 8.83$ Hz, H-3), 5.24 (d, 1H, $J_{1'-2'} = 9.65$ Hz, H-1'), 3.67-3.58 (m, 8H, 2 x OCH_3 , H-6'a and H-6'b), 3.51-3.45 (m, 3H, H-2', H-4', H-5'), 3.43-3.27 (m, 4H, H-3', OCH_3), 2.70 (s, 3H, OCH_3). ^{13}C NMR ($CDCl_3$) δ (ppm) 154.5 (C-2), 132.6 (C-8a), 130.3 (C-4), 128.7 (C-4a), 128.3 (C-5), 126.4 (C-7), 123.0 (C-6), 122.6 (C-8), 119.7 (C-3), 114.7 (C-1), 87.8 (C-3'), 84.2 (C-2'), 78.7 (C-4'), 78.6 (C-5'), 76.7 (C-1'), 70.5 (C-6'), 61.0, 60.7, 60.2, 59.3 (OCH_3). $[M+H]^+$ calcd for $C_{20}H_{27}O_6$ 363.1802, found 363.1796; $[M+Na]^+$ calcd for $C_{20}H_{26}NaO_6$ 385.1622, found 385.1624.

1,2-Dihydroxy-4-(2,3,4,6-tetra-*O*-benzyl- β -D-glucopyranosyl)benzene (12) and 2-hydroxy-1-(2,3,4,6-tetra-*O*-benzyl- α -D-glucopyranosyloxy)benzene (31). To a solution of 2,3,4,6-tetra-*O*-benzyl- α -/ β -D-glucopyranose (**4**, 2 g, 3.70 mmol) in dry dichloromethane (50 mL), catechol (0.81 g, 7.40 mmol, 2 eq.) in dry MeCN (10 mL) was added, together with drierite (0.25 g), under N_2 atmosphere. The mixture was stirred for 5 minutes at room temperature, which was then lowered to $-78^\circ C$. TMSOTf (0.68 mL, 3.70 mmol, 1 eq.) was added in a dropwise manner. After stirring for 30 minutes, the mixture was stirred for 64 h at $40^\circ C$. The reaction was stopped by adding a few drops of triethylamine; then, the mixture was filtered through a pad of celite, washed with dichloromethane and concentrated under vacuum. The residue was purified by column chromatography (1:0 \rightarrow 15:1 Cyclohexane/AcOEt), affording compound **12** in 6% yield as a colorless oil and compound **18** as a white solid in 35% yield.

1,2-Dihydroxy-4-(2,3,4,6-tetra-*O*-benzyl- β -D-glucopyranosyl)benzene (12): R_f (Hexane/AcOEt 4:1) = 0.14; $[\alpha]_D^{20} = -2^\circ$ (c 0.1, $CHCl_3$); 1H NMR ($CDCl_3$) δ (ppm) 7.37-7.16 (m, 18H, benzyl aromatics), 6.99-6.97 (m, 2H, benzyl aromatics), 6.85-6.82 (m, 2H, H-3, H-6), 6.79-6.76 (m, 1H, H-5), 5.00, 4.96 (part A_1 of A_1B_1 system, 1H, $J_{A_1-B_1} = 11.23$ Hz, Ph- CH_2), 4.90 (m, 2H, part B_1 of A_1B_1 system, part A_2 of A_2B_2 system, Ph- CH_2), 4.64-4.55 (m, 3H, part B_2 of A_2B_2 system, Ph- CH_2 and Ph- CH_2), 4.40, 4.36 (part A_3 of A_3B_3 system, 1H, $J_{A_3-B_3} = 10.28$ Hz, Ph- CH_2), 4.12 (d, 1H, $J_{1'-2'} = 9.63$ Hz, H-1'), 3.92, 3.88 (part B_3 of A_3B_3 system, 1H, $J_{A_3-B_3} = 10.27$ Hz, Ph- CH_2), 3.81-3.72 (m, 4H, H-3', H-4', H-6'a and H-6'b), 3.65-3.61 (m, 1H, H-5'), 3.51 (t, 1H, $J_{2'-3'-2'-1'} = 9.15$ Hz, H-2'). ^{13}C NMR ($CDCl_3$) δ (ppm) 144.7 (C-2), 143.2 (C-1), 138.6, 138.1, 137.8, 137.7 (benzyl C_q -aromatics), 131.3 (C-4), 128.4-127.6 (benzyl CH-aromatics), 120.7 (C-5),

115.2 (C-6), 114.9 (C-3), 86.7 (C-3'), 83.9 (C-2'), 81.7 (C-1'), 79.0 (C-5'), 78.4 (C-4'), 75.7, 75.1, 74.8, 73.5 (CH₂-Ph), 69.2 (C-6'). HRMS-ESI (*m/z*): [M+H]⁺ calcd for C₄₀H₄₁O₇ 633.2847, found 633.2853; [M+Na]⁺ calcd for C₄₀H₄₀NaO₇ 655.2666, found 655.2667.

2-Hydroxy-1-(2,3,4,6-tetra-O-benzyl- α -D-glucopyranosyloxy)benzene (31): R_f (Hex/AcOEt 4:1) = 0.58; m.p. = 104.2-106.0 °C; [α]_D²⁰ = + 68 ° (*c* 1.0, CHCl₃); **¹H NMR** (CDCl₃) δ (ppm) 7.37-7.22 (m, 17H, benzyl aromatics), 7.18-7.15 (m, 3H, benzyl aromatics), 7.09 (d, 1H, *J*_{ortho} = 8.06 Hz, H-3), 7.02-6.95 (m, 2H, H-4, H-6), 6.75 (dt, 1H, *J*_{ortho} = 7.68 Hz, *J*_{meta} = 1.58 Hz, H-5), 4.99-4.90 (m, 3H, H-1', Ph-CH₂), 4.87-4.81 (m, 2H, part A₁ of A₁B₁ system, part A₂ of A₂B₂ system, Ph-CH₂), 4.72, 4.68 (part A₂ of A₂B₂ system, 1H, *J*_{A₂-B₂} = 11.96 Hz, Ph-CH₂), 4.64, 4.60 (part A₃ of A₃B₃ system, 1H, *J*_{A₃-B₃} = 12.08 Hz, Ph-CH₂), 4.55, 4.51 (part B₁ of A₁B₁ system, 1H, *J*_{A₁-B₁} = 11.04 Hz, Ph-CH₂), 4.50, 4.46 (part B₃ of A₃B₃ system, 1H, *J*_{A₃-B₃} = 11.93 Hz, Ph-CH₂), 4.21-4.14 (m, 2H, H-3', H-4'), 3.81-3.69 (m, 3H, H-6'a and H-6'b, H-5'), 3.67 (dd, 1H, *J*_{1'-2'} = 3.53 Hz, *J*_{2'-3'} = 9.65 Hz, H-2'). **¹³C NMR** (CDCl₃) δ (ppm) 148.6 (C-2), 145.2 (C-1), 138.4, 138.1, 137.8, 137.0 (benzyl C_q-aromatics), 128.5-127.7 (benzyl CH-aromatics), 125.2 (C-4), 120.3 (C-5)*, 119.9 (C-3)*, 115.8 (C-6), 101.1 (C-1'), 81.9 (C-3'), 79.0 (C-2'), 77.5 (C-5'), 75.6, 75.0, 74.2, 73.5 (CH₂-Ph), 71.5 (C-4'), 68.3 (C-6'). *Permutable signals. HRMS-ESI (*m/z*): [M+H]⁺ calcd for C₄₀H₄₁O₇ 633.2847, found 633.2853; [M+Na]⁺ calcd for C₄₀H₄₀NaO₇ 655.2666, found 655.2667.

1,3,5-Trihydroxy-2-(2,3,4,6-tetra-O-benzyl- β -D-glucopyranosyl)benzene (13). To a solution of 2,3,4,6-tetra-O-benzyl- α - β -D-glucopyranose (2 g, 3.70 mmol) in dry dichloromethane (50 mL), 2,4,6-trihydroxyacetophenone (0.93 g, 7.40 mmol, 2 eq.) in dry MeCN (50 mL) was added, together with drierite (0.25 g), under N₂ atmosphere. The mixture was stirred for 5 minutes at room temperature, which was then lowered to -78 °C. TMSOTf (0.68 mL, 3.70 mmol, 1 eq.) was added in a dropwise manner. After stirring for 30 minutes, the mixture was left at room temperature under stirring overnight. The reaction was stopped by adding a few drops of triethylamine; then, dichloromethane was evaporated and the mixture was washed with brine and extracted with ethyl acetate (3 x 50 mL). The organic layers were combined, dried over MgSO₄, filtered and concentrated under vacuum. The residue was purified by column chromatography (10:1 → 5:1 Cyclohexane/Acetone), affording compound **13** in 42% yield as a colorless oil. R_f (Cyclohexane/Acetone 3:2) = 0.41; [α]_D²⁰ = + 12 ° (*c* 0.2, CHCl₃); **¹H NMR** (CDCl₃) δ (ppm) 7.35-7.19 (m, 16H, benzyl aromatics), 7.16-7.12 (m, 2H, benzyl aromatics), 7.08-7.04 (m, 2H, benzyl aromatics), 6.02 (s, 2H, H-4, H-6), 4.93 (A₁B₁ system, 2H, Ph-CH₂), 4.83-4.79 (m, 2H, H-1', part A₂ of A₂B₂ system, Ph-CH₂), 4.65, 4.63 (part A₃ of A₃B₃ system, 1H, *J*_{A₃-B₃} = 10.21 Hz, Ph-CH₂), 4.59, 4.55 (part A₄ of A₄B₄ system, 1H, *J*_{A₄-B₄} = 12.05 Hz, 1H, Ph-CH₂), 4.54, 4.50 (part B₃ of A₃B₃ system, 1H, *J*_{A₃-B₃} = 10.91 Hz, Ph-CH₂), 4.45, 4.41 (part B₄ of A₄B₄ system, 1H, *J*_{A₄-B₄} = 12.05 Hz, Ph-CH₂), 3.88 (t, 1H, *J*_{4'-3'-4'-5'} = 8.80 Hz, H-4'), 3.79-3.65 (m, 4H, H-2', H-3', H-6'a and H-6'b), 3.56 (br d, 1H, *J*_{5'-4'} = 9.71 Hz, H-5'). **¹³C NMR** (CDCl₃) δ

(ppm) 157.3 (C-1, C-3), 156.3 (C-5), 138.4, 138.9, 137.6, 136.4 (benzyl C_q-aromatics), 128.8-127.5 (benzyl CH-aromatics), 104.1 (C-2), 97.8 (C-4, C-6), 86.2 (C-3'), 82.7 (C-2'), 78.7 (C-5'), 77.2 (C-4'), 76.2 (C-1'), 75.6, 75.5, 75.2, 73.4 (CH₂-Ph), 67.6 (C-6'). HRMS-ESI (*m/z*): [M+H]⁺ calcd for C₄₀H₄₁O₈ 649.2796, found 649.2806; [M+Na]⁺ calcd for C₄₀H₄₀NaO₈ 671.2615, found 671.2621.

1-[2,4,6-Trihydroxy-3-(2,3,4,6-tetra-*O*-benzyl-β-D-glucopyranosyl)phenyl]ethan-1-one (14). Synthesis and characterization as described in the literature.²⁵

1,4-Dihydroxy-2-(2,3,4,6-tetra-*O*-benzyl-β-D-glucopyranosyl)benzene (15) and 4-hydroxy-1-(2,3,4,6-tetra-*O*-benzyl-α-/β-D-glucopyranosyloxy)benzene (27α,β). To a solution of 1-*O*-acetyl-2,3,4,6-tetra-*O*-benzyl-α-/β-D-glucopyranose (**6**, 2.16 g, 3.70 mmol) in dry dichloromethane (50 mL), hydroquinone (0.61 g, 5.55 mmol, 1.5 eq.) in dry MeCN (10 mL) was added, together with drierite (0.25 g), under N₂ atmosphere. The mixture was stirred for 5 minutes at room temperature, which was then lowered to 0 °C. BF₃·Et₂O (1.1 mL, 3.70 mmol, 1 eq.) was added in a dropwise manner. After stirring for 30 minutes, the temperature was raised to 40 °C and the mixture stirred for 44 h. The reaction was stopped by adding a few drops of triethylamine; then, the mixture was filtered through a pad of celite, washed with dichloromethane and concentrated under vacuum. The residue was purified by column chromatography (50:1 → 30:1 Toluene/Acetone) followed by recrystallization in diethyl ether to afford compound **15** in 8% yield as a white solid and **27α,β** isolated as a white solid with α/β ratio = 4:1 in 36% yield.

1,4-Dihydroxy-2-(2,3,4,6-tetra-*O*-benzyl-β-D-glucopyranosyl)benzene (15). R_f (Toluene/Acetone 10:1) = 0.43; m.p. = 107.2-109.1 °C; [α]_D²⁰ = + 16 ° (*c* 0.3, CHCl₃); ¹H NMR [CO(CD₃)₂] δ (ppm) 7.40-7.19 (m, 18H, benzyl aromatics), 7.10-7.07 (m, 2H, benzyl aromatics), 6.86 (d, 1H, *J*_{meta} = 2.15 Hz, H-3), 6.75-6.69 (m, 2H, H-5, H-6), 4.97, 4.93 (part A₁ of A₁B₁ system, 1H, *J*_{A₁-B₁} = 11.24 Hz, Ph-CH₂), 4.89-4.87 (m, part B₁ of A₁B₁ system, part A₂ of A₂B₂ system, 2H, Ph-CH₂), 4.67-4.53 (m, 4H, part B₂ of A₂B₂ system, Ph-CH₂, H-1'), 4.46, 4.42 (A₃ of A₃B₃ system, 1H, *J*_{A₃-B₃} = 10.41 Hz, Ph-CH₂), 4.01, 3.97 (B₃ of A₃B₃ system, 1H, *J*_{A₃-B₃} = 10.45 Hz, Ph-CH₂), 3.84-3.75 (m, 4H, H-3', H-4', H-6'a and H-6'b), 3.68-3.64 (m, 2H, H-2', H-5'). ¹³C NMR [CO(CD₃)₂] δ (ppm) 151.2 (C-1), 149.2 (C-4), 140.0, 139.5, 139.4, 139.0 (benzyl C_q-aromatics), 129.0-128.0 (benzyl CH-aromatics), 126.3 (C-2), 117.8 (C-6), 116.4 (C-5), 116.1 (C-3), 87.0 (C-3'), 83.5 (C-2'), 79.6 (C-5'), 78.8 (C-1'), 78.7 (C-4'), 75.8, 75.3, 75.2, 73.7 (CH₂-Ph), 69.5 (C-6'). HRMS-ESI (*m/z*): [M+H]⁺ calcd for C₄₀H₄₁O₇ 633.2851, found 633.2853; [M+Na]⁺ calcd for C₄₀H₄₀NaO₇ 655.2666, found 655.2671.

4-Hydroxy-1-(2,3,4,6-tetra-*O*-benzyl-α-/β-D-glucopyranosyloxy)benzene (27α,β). R_f (Toluene/Acetone 10:1) = 0.50; m.p. = 138.4 – 141.2 °C; [α]_D²⁰ = + 53 ° (*c* 0.4, CHCl₃); ¹H NMR (CDCl₃) δ 7.38-7.24 (m, 95H, CH-Ph), 3.18-3.12

(m, 5H, *CH*-Ph), 6.92-6.88 (m, 10H, H-3_α, H-3_β, H-5_α, H-5_β), 6.62 (d, 10H, $J_{ortho} = 8.73$ Hz, H-2_α, H-2_β, H-6_α, H-6_β), 5.32 (d, 4H, $J_{1'-2'} = 3.33$ Hz, H-1'_α), 5.06, 5.02 (part A₁ of A₁B₁ system, 5H, $J_{A_1-B_1} = 10.81$ Hz, *CH*₂-Ph), 4.97, 4.93 (part A₂ of A₂B₂ system, 1H, $J_{A_2-B_2} = 10.90$ Hz, *CH*₂-Ph), 4.89-4.76 (m, 16H, H-1'_β, part B₁ of A₁B₁ system, part B₂ of A₂B₂ system, *CH*₂-Ph), 4.69, 4.65 (part A₃ of A₃B₃ system, 4H, $J_{A_3-B_3} = 11.98$ Hz, *CH*₂-Ph), 4.59-4.47 (m, 11H, *CH*₂-Ph), 4.40, 4.36 (part B₃ of A₃B₃ system, 4H, $J_{A_3-B_3} = 11.99$ Hz, *CH*₂-Ph), 4.20 (t, 4H, $J_{3'-2'} = J_{3'-4'} = 9.28$ Hz, H-3'_α), 3.93 (br d, 4H, $J_{5'-4'} = 9.59$ Hz, H-5'_α), 3.78-3.63 (m, 17H, H-2'_α, H-4'_α, H-2'_β, H-3'_β, H-4'_β, H-5'_β, H-6'a_α, H-6'a_β), 3.57 (br d, 5H, $J_{6'a-6'b} = 9.94$ Hz, H-6'b_α, H-6'b_β). ¹³C NMR (CDCl₃) δ 151.6 (C-4_β), 151.3 (C-1_β), 151.2 (C-4_α), 150.5 (C-1_α), 138.7, 138.5, 138.2, 137.9, 137.9, 137.7 (C_q-Ph), 128.6-127.8 (*CH*-Ph), 118.5 (C-3_β, C-5_β), 118.3 (C-3_α, C-5_α), 116.1 (C-2_β, C-6_β), 116.1 (C-2_α, C-6_α), 102.8 (C-1'_β), 96.4 (C-1'_α), 84.6 (C-2'_β), 82.1 (C-3'_β), 82.0 (C-3'_α), 79.8 (C-2'_α), 77.8 (C-4'_β), 77.5 (C-4'_α), 75.9, 75.2, 75.2 (*CH*₂-Ph), 73.5, 73.5, 73.4 (*CH*₂-Ph), 70.7 (C-5'_α), 70.2 (C-5'_β), 68.9 (C-6'_β), 68.3 (C-6'_α). HRMS-ESI (*m/z*): [M+H]⁺ calcd for C₄₀H₄₁O₇ 633.2847, found 633.2847; [M+Na]⁺ calcd for C₄₀H₄₀NaO₇ 655.2666, found 655.2669.

2-Hydroxy-1-(2,3,4,6-tetra-*O*-benzyl-β-D-glucopyranosyl)naphthalene (16). To a solution of 2,3,4,6-tetra-*O*-benzyl-α-D-glucopyranosyl trichloroacetimidate (**5**, 1.27 g, 1.85 mmol) in dry dichloromethane (10 mL), 2-naphthol (0.222 g, 0.83 eq.) was added in the presence of activated molecular sieves (3Å), at 0 °C, under N₂ atmosphere. TMSOTf (0.33 mL, 1.85 mmol, 1 eq.) was then added in a dropwise manner and the mixture stirred for 20 hours at room temperature. The reaction was stopped by adding a few drops of triethylamine; then, the mixture was filtered through a pad of celite, washed with dichloromethane and concentrated under vacuum. The residue was purified by column chromatography (P. Ether/EtOAc 1:0 → 15:1), affording compound **16** as a colourless oil in 43% yield. R_f (Hexane/EtOAc 5:1) = 0.47; $[\alpha]_D^{20} = +3^\circ$ (*c* 0.3, CHCl₃); ¹H NMR (CDCl₃) δ (ppm) 8.73 (br s, 1H, OH-2), 8.07 (d, 1H, $J_{ortho} = 7.75$ Hz, H-8), 7.87-7.79 (m, 2H, H-4, H-5), 7.48-6.95 (m, 22H, benzyl aromatics, H-6, H-7), 6.33 (d, 1H, $J_{ortho} = 7.13$ Hz, H-3), 5.47 (d, 1H, $J_{1'-2'} = 9.68$ Hz, H-1'), 5.06-5.46 (m, 6H, Ph-CH₂), 4.25-3.41 (m, 8H, H-2', H-3', H-4', H-5', H-6'a and H-6'b, Ph-CH₂). ¹³C NMR (CDCl₃) δ (ppm) 154.8 (C-2), 138.7, 138.1, 137.8, 136.8, (benzyl C_q-aromatics), 132.7 (C-8a), 130.5 (C-4), 128.7-127.5 (benzyl CH-aromatics, C-4a, C-5), 126.7 (C-7), 123.2 (C-6), 122.9 (C-8), 119.8 (C-3), 114.6 (C-1), 86.2 (C-3'), 81.9 (C-2'), 78.7 (C-4'), 77.8 (C-5'), 77.1 (*CH*₂-Ph), 76.9 (C-1'), 75.7, 75.4, 73.4 (*CH*₂-Ph), 67.8 (C-6'). HRMS-ESI (*m/z*): [M+H]⁺ calcd for C₄₄H₄₃O₆ 667.3054, found 667.3047; [M+Na]⁺ calcd for C₄₄H₄₂NaO₆ 689.2874, found 689.2874.

4-Hydroxy-3-(2,3,4,6-tetra-*O*-methyl-β-D-glucopyranosyl)benzen-1-yl benzoate (17) and 3-(2,3,4,6-Tetra-*O*-methyl-β-D-glucopyranosyl)benzen-1,4-diyl dibenzoate (18). Compound **10** (0.50 g, 1.55 mmol, 1 eq.) was dissolved in dry dichloromethane (21 mL) together with imidazole (0.12 g, 1.71 mmol, 1.1 eq.) and DMAP (cat.). After stirring

for 10 min at 0 °C, benzoyl chloride (0.2 mL, 1.71 mmol, 1.1 eq.) was added dropwise. The reaction mixture was stirred at room temperature for 66 h, after which it was washed with brine and extracted with dichloromethane (2 x 20 mL). The organic layers were combined, dried over MgSO₄ and concentrated under reduced pressure. The residue was purified by column chromatography (P. Ether/EtOAc 1:0 → 2:1), affording compound **17** as a colourless oil in 65% yield and compound **18** as a white solid in 22% yield.

4-Hydroxy-3-(2,3,4,6-tetra-O-methyl-β-D-glucopyranosyl)benzen-1-yl benzoate (17). R_f (P. Ether/EtOAc 2:1) = 0.31; [α]_D²⁰ = + 16 ° (c 0.7, MeOH); ¹H NMR (CDCl₃) δ 8.18 (d, 2H, J_{ortho} = 7.38 Hz, H-2', H-6'), 7.75 (s, 1H, OH-4), 7.62 (t, 1H, J_{ortho} = 7.38 Hz, H-4'), 7.50 (t, 2H, J_{ortho} = 7.61 Hz, H-3', H-5'), 7.08-7.04 (m, 2H, H-2, H-6), 6.95 (d, 1H, J_{ortho} = 6.95 Hz, H-5), 4.32 (d, 1H, J_{1"-2"} = 9.60 Hz, H-1"), 3.67 (s, 3H, OCH₃), 3.64-3.62 (m, 2H, H-6"a and b), 3.58 (s, 3H, OCH₃), 3.43-3.40 (m, 4H, H-5", OCH₃), 3.36-3.28 (m, 2H, H-3", H-4"), 3.24 (s, 3H, OCH₃), 3.21-3.19 (m, 1H, H-2"). ¹³C NMR (CDCl₃) δ 165.6 (C=O), 152.7 (C-4), 144.0 (C-1), 133.6 (C-4'), 130.2 (C-2', C-6'), 129.8 (C-1'), 128.6 (C-3', C-5'), 125.0 (C-3), 122.4 (C-6), 121.3 (C-2), 118.1 (C-5), 88.2 (C-3"), 84.8 (C-2"), 79.2 (C-4"), 79.1 (C-1"), 78.8 (C-5"), 70.9 (C-6"), 61.0, 60.7, 59.4 (OCH₃). HRMS-ESI (m/z): [M+H]⁺ calcd for C₂₃H₂₉O₈ 433.1857, found 433.1861; [M+Na]⁺ calcd for C₂₃H₂₈NaO₈ 455.1676, found 455.1678.

3-(2,3,4,6-Tetra-O-methyl-β-D-glucopyranosyl)benzene-1,4-diyl dibenzoate (18). R_f (P. Ether/EtOAc 2:1) = 0.47; m.p. = 102.6 – 103.8 °C; [α]_D²⁰ = + 5 ° (c 0.7, CHCl₃); ¹H NMR (CDCl₃) δ 8.24-8.20 (m, 4H, H-2', H-6'), 7.65 (t, 2H, J_{ortho} = 6.99 Hz, H-4'), 7.56-7.51 (m, 4H, H-3', H-5'), 7.40 (d, 1H, J_{meta} = 2.22 Hz, H-3), 7.32-7.24 (m, 2H, H-5, H-6), 4.43 (d, 1H, J_{1"-2"} = 8.77 Hz, H-1"), 3.58 (s, 3H, OCH₃), 3.56 (br s, 1H, H-6"a), 3.51 (s, 3H, OCH₃), 3.48-3.44 (m, 1H, H-6"b), 3.39-3.33 (m, 4H, OCH₃, H-5"), 3.23-3.12 (m, 6H, OCH₃, H-2", H-3", H-4"). ¹³C NMR (CDCl₃) δ 165.1 (C=O), 164.7 (C=O), 148.5 (C-1), 146.3 (C-4), 133.8, 133.6 (C-4'), 132.8 (C-3), 130.4, 130.3 (C-2', C-6'), 129.8, 129.5 (C-1'), 128.7 (C-3', C-5'), 124.0 (C-5), 122.1 (C-6), 121.9 (C-2), 88.5 (C-3"), 85.5 (C-2"), 80.0 (C-4"), 79.4 (C-5"), 76.2 (C-1"), 71.8 (C-6"), 60.9, 60.7, 60.6, 59.5 (OCH₃). HRMS-ESI (m/z): [M+H]⁺ calcd for C₃₀H₃₃O₉ 537.2119, found 537.2108; [M+Na]⁺ calcd for C₃₀H₃₂NaO₉ 559.1939, found 559.1900.

4-Hydroxy-3-(2,3,4,6-tetra-O-benzyl-β-D-glucopyranosyl)benzen-1-yl benzoate (19) and 3-(2,3,4,6-tetra-O-benzyl-β-D-glucopyranosyl)benzene-1,4-diyl dibenzoate (20). Compound **15** (0.48 g, 0.77 mmol) was dissolved in dry dichloromethane (50 mL) together with imidazole (0.081 g, 1.18 mmol, 1.5 eq.) and DMAP (cat.). After stirring for 10 min at 0 °C, benzoyl chloride (1.4 mL, 1.18 mmol, 1.5 eq.) was added dropwise. The reaction mixture was stirred at room temperature for 72 h, after which it was washed with brine and extracted with dichloromethane (2 x 20 mL). The

organic layers were combined, dried over MgSO_4 and concentrated under reduced pressure. The residue was purified by column chromatography (Hexane/Acetone 1:0 \rightarrow 10:1), affording compound **19** as a colourless oil in 53% yield and compound **20** as a white solid in 38% yield.

4-Hydroxy-3-(2,3,4,6-tetra-O-benzyl- β -D-glucopyranosyl)benzen-1-yl benzoate (19). R_f (Hexane/Acetone 3:1) = 0.22; $[\alpha]_D^{20} = +25^\circ$ (c 0.1, CHCl_3); $^1\text{H NMR}$ (CDCl_3) δ (ppm) 8.18 (d, 2H, $J_{\text{ortho}} = 7.46$ Hz, H-2', H-6'), 7.64 (t, 1H, $J_{\text{ortho}} = 7.20$ Hz, H-4'), 7.51 (t, 2H, $J_{\text{ortho}} = 7.83$ Hz, H-3', H-5'), 7.35-7.07 (m, 22H, benzyl aromatics, H-2, H-6), 6.98 (d, 1H, $J_{\text{ortho}} = 7.73$ Hz, H-5), 4.98-4.89 (m, A_1B_1 system, 2H, Ph-CH_2), 4.87, 4.83 (part A_2 of A_2B_2 system, 1H, $J_{A_2-B_2} = 10.85$ Hz, Ph-CH_2), 4.63-4.47 (m, 4H, part B_2 of A_2B_2 system, part A_3 of A_3B_3 system, Ph-CH_2), 4.44 (d, 1H, $J_{1''-2''} = 9.18$ Hz, H-1''), 4.03, 3.99 (part A_3 of A_3B_3 system, 1H, $J_{A_3-B_3} = 10.15$ Hz, Ph-CH_2), 3.89 (t, 1H, $J_{4'''-3'''-4'''-5'''} = 9.04$ Hz, H-4''), 3.80-6.69 (m, 4H, H-2'', H-3'', H-6''a and H-6''b), 3.59 (br d, 1H, $J_{5''-4''} = 9.72$ Hz, H-5''). $^{13}\text{C NMR}$ (CDCl_3) δ (ppm) 165.3 (C=O), 153.0 (C-4), 143.7 (C-1), 138.5, 137.9, 137.8, 137.0 (benzyl C_q -aromatics), 133.5 (C-4'), 130.1 (C-2', C-6'), 129.6 (C-1'), 128.8-127.6 (C-3', C-5', benzyl CH-aromatics), 124.1 (C-3), 122.6 (C-6), 121.9 (C-2), 118.3 (C-5), 86.1 (C-3''), 81.7 (C-2''), 80.5 (C-5''), 78.6 (C-1''), 77.3 (C-4''), 75.6, 75.6, 75.2, 73.4 (Ph-CH_2), 67.8 (C-6''). HRMS-ESI (m/z): $[\text{M}+\text{H}]^+$ calcd for $\text{C}_{47}\text{H}_{45}\text{O}_8$ 737.3109, found 737.3116; $[\text{M}+\text{Na}]^+$ calcd for $\text{C}_{47}\text{H}_{44}\text{NaO}_8$ 759.2928, found 759.2936.

3-(2,3,4,6-tetra-O-benzyl- β -D-glucopyranosyl)benzen-1,4-diyl dibenzoate (20). R_f (Hexane/Acetone 3:1) = 0.34; $[\alpha]_D^{20} = +11^\circ$ (c 0.2, CHCl_3); $^1\text{H NMR}$ (CDCl_3) δ (ppm) 8.21, 8.16 (d, 4H, $J_{\text{ortho}} = 7.48$ Hz, H-2', H-6'), 7.64, 7.59 (t, 2H, $J_{\text{ortho}} = 7.31$ Hz, H-4'), 7.52, 7.45 (t, 4H, $J_{\text{ortho}} = 7.69$ Hz, H-3', H-5'), 7.35-7.05 (m, 23H, benzyl aromatics, H-2, H-5, H-6), 4.91-4.82 (A_1B_1 system, 2H, $J_{A_1-B_1} = 10.82$ Hz, Ph-CH_2), 4.81, 4.87 (part A_2 of A_2B_2 system, 1H, $J_{A_2-B_2} = 10.73$ Hz, Ph-CH_2), 4.55-4.46 (m, 5H, H-1'', part B_2 of A_2B_2 system, part A_3 of A_3B_3 system, Ph-CH_2), 4.22, 4.18 (part B_3 of A_3B_3 system, 1H, $J_{A_3-B_3} = 10.75$ Hz, Ph-CH_2), 3.77-3.52 (m, 6H, H-2'', H-3'', H-4'', H-5'', H-6''a and H-6''b). $^{13}\text{C NMR}$ (CDCl_3) δ (ppm) 164.9, 164.7 (C=O), 148.5 (C-1), 146.4 (C-4), 138.6, 138.2, 138.1, 137.8 (benzyl C_q -aromatics), 133.7, 133.6 (C-4'), 132.6 (C-3), 130.4 (C-2', C-6'), 129.5, 129.4 (C-1'), 128.7-127.6 (C-3', C-5', benzyl CH-aromatics), 124.0 (C-5), 122.4 (C-2), * 122.3 (C-6), * 86.8 (C-3''), 82.8 (C-2''), 79.5 (C-5''), 78.2 (C-4''), 77.3 (C-1''), 75.6, 75.1, 74.9, 74.3 (Ph-CH_2), 69.0 (C-6''); *Permutable signals. HRMS-ESI (m/z): $[\text{M}+\text{H}]^+$ calcd for $\text{C}_{54}\text{H}_{49}\text{O}_9$ 841.3371, found 841.3381.

3-(β -D-Glucopyranosyl)-4-hydroxybenzen-1-yl benzoate (21) To a solution of compound **19** (0.215 mg, 0.29 mmol) in ethyl acetate (15 mL), Pd/C (10%, 50 mg) was added. The mixture was stirred under H_2 atmosphere for 26 hours at room temperature. After reaching completion, the reaction was stopped by filtering Pd/C through a pad of celite and the solvent evaporated under reduced pressure. The residue was purified by column chromatography (30:1 \rightarrow 10:1 dichloromethane/MeOH) to afford compound **21** as a yellowish oil in 96% yield. R_f (dichloromethane/MeOH 7:1) =

0.44; $[\alpha]_D^{20} = +50^\circ$ (*c* 0.2, MeOH); $^1\text{H NMR}$ $[\text{CO}(\text{CD}_3)_2]$ δ (ppm) 8.17 (d, 2H, $J_{\text{ortho}} = 7.38$ Hz, H-2', H-6'), 7.72 (t, 2H, $J_{\text{ortho}} = 7.45$ Hz, H-3', H-5'), 7.59 (t, 1H, $J_{\text{ortho}} = 7.67$ Hz, H-4'), 7.26 (d, 1H, $J_{\text{meta}} = 2.35$ Hz, H-2), 7.06 (dd, 1H, $J_{\text{ortho}} = 8.74$ Hz, $J_{\text{meta}} = 2.58$ Hz, H-6), 6.89 (d, 1H, $J_{\text{ortho}} = 8.69$ Hz, H-5), 4.60 (d, 1H, $J_{1''-2''} = 9.34$ Hz, H-1''), 3.87 (d, 1H, $J_{6''\text{a}-6''\text{b}} = 10.59$ Hz, H-6''a), 3.76 (dd, 1H, $J_{6''\text{b}-6''\text{a}} = 10.99$ Hz, $J_{6''\text{b}-5''} = 4.28$ Hz, H-6''b), 3.63-3.47 (m, 4H, H-2'', H-3'', H-4'', H-5''). $^{13}\text{C NMR}$ $[\text{CO}(\text{CD}_3)_2]$ δ (ppm) 165.9 (C=O), 153.7 (C-4), 144.8 (C-1), 134.5 (C-4'), 130.8 (C-1'), 130.7 (C-2', C-6'), 129.6 (C-3', C-5'), 128.5 (C-3), 122.6 (C-2), 121.7 (C-6), 117.9 (C-5), 81.9 (C-5''), 79.7 (C-3''), 77.7 (C-1''), 76.6 (C-2''), 71.3 (C-4''), 62.6 (C-6''). HRMS-ESI (*m/z*): $[\text{M}+\text{H}]^+$ calcd for $\text{C}_{19}\text{H}_{21}\text{O}_8$ 377.1231, found 377.1226; $[\text{M}+\text{Na}]^+$ calcd for $\text{C}_{19}\text{H}_{20}\text{NaO}_8$ 399.1050, found 399.1045.

3-(β -D-Glucopyranosyl)benzene-1,4-diyl dibenzoate (22) To a solution of compound **20** (0.273 g, 0.32 mmol) was dissolved in ethyl acetate (15 mL), Pd/C (10%, 64 mg) was added. The mixture stirred under H_2 atmosphere for 22 hours at room temperature. After reaching completion, the reaction was stopped by filtering Pd/C through a pad of celite and the solvent evaporated under reduced pressure. The residue was purified by column chromatography (EtOAc) to afford compound **22** as a white solid in 90% yield. R_f (EtOAc) = 0.48; m.p. = 99.7-102.5 $^\circ\text{C}$; $[\alpha]_D^{20} = +11^\circ$ (*c* 0.8, MeOH); $^1\text{H NMR}$ $[\text{CO}(\text{CD}_3)_2]$ δ (ppm) 8.25, 8.21 (d, 2H, $J_{\text{ortho}} = 7.46$ Hz, H-2', H-6'), 7.77-7.72 (m, 2H, H-4'), 7.64-7.60 (m, 4H, H-3', H-5'), 7.50 (d, 1H, $J_{\text{meta}} = 2.11$ Hz, H-2), 7.40 (d, 1H, $J_{\text{ortho}} = 8.76$ Hz, H-5), 7.35 (dd, 1H, $J_{\text{ortho}} = 8.78$ Hz, $J_{\text{meta}} = 2.55$ Hz, H-6), 4.59 (d, 1H, $J_{1''-2''} = 9.41$ Hz, H-1''), 3.73 (d, 1H, $J_{6''\text{a}-6''\text{b}} = \text{Hz}$, H-6''a), 3.59-3.37 (m, 5H, H-2'', H-3'', H-4'', H-5'', H-6''b). $^{13}\text{C NMR}$ $[\text{CO}(\text{CD}_3)_2]$ δ (ppm) 165.5 (C=O), 165.2 (C=O), 149.3 (C-1), 147.6 (C-4), 134.6 (C-3), 134.4 (C-4'), 130.8, 130.7 (C-2', C-6'), 130.6, 130.3 (C-1'), 129.6, 129.6 (C-3', C-5'), 124.6 (C-5), 122.7 (C-6), 122.6 (C-2), 81.8 (C-3''), 79.6 (C-2''), 77.3 (C-1''), 75.4 (C-4''), 71.6 (C-5''), 63.0 (C-6''). HRMS-ESI (*m/z*): $[\text{M}+\text{H}]^+$ calcd for $\text{C}_{26}\text{H}_{25}\text{O}_9$ 481.1493, found 481.1499; $[\text{M}+\text{Na}]^+$ calcd for $\text{C}_{26}\text{H}_{24}\text{NaO}_9$ 503.1313, found 503.1308.

4-(2,3,4,6-Tetra-O-methyl- β -D-glucopyranosyl)benzene-1,2-diyl dibenzoate (25) Compound **7** (0.650 g, 1.98 mmol) was dissolved in dichloromethane (43 mL) and imidazole (0.447 g, 6.57 mmol, 3.3 eq.) was added at 0 $^\circ\text{C}$. After stirring for 10 min at 0 $^\circ\text{C}$, benzoyl chloride (0.78 mL, 6.67 mmol, 3.3 eq.) was added dropwise. The reaction mixture was stirred at room temperature for 24 h, after which it was washed with brine and extracted with dichloromethane (2 x 20 mL). The organic layers were combined, dried over MgSO_4 and concentrated under reduced pressure. The residue was purified by column chromatography (Hexane/Acetone 10:0 \rightarrow 5:1), affording compound **25** as a colourless oil in 88% yield. R_f (Hexane/EtOAc 2:1) = 0.38; $[\alpha]_D^{20} = -18^\circ$ (*c* 0.1, CHCl_3); $^1\text{H NMR}$ (CDCl_3) δ 8.05 (br d, 4H, $J_{\text{ortho}} = 7.49$ Hz, H-2', H-6'), 7.53 (t, 2H, $J_{\text{ortho}} = 6.71$ Hz, H-4'), 7.46 (br s, 1H, H-3), 7.42-7.34 (m, 6H, H-3', H-5', H-5, H-6), 4.16 (d, 1H, $J_{1''-2''} = 9.45$ Hz, H-1''), 3.69 (s, 3H, OCH_3), 3.66-3.65 (m, 2H, H-6''a and H-6''b), 3.59 (s, 3H, OCH_3), 3.47-3.42 (m, 4H, H-5'', OCH_3), 3.37-3.25 (m, 2H, H-3'', H-4''), 3.16 (s, 3H, OCH_3), 3.07 (t, 1H, $J_{2''-1''-2''-3''} = 9.13$ Hz, H-2''). $^{13}\text{C NMR}$

(CDCl₃) δ 164.3 (C-O), 142.4 (C-2), 142.3 (C-1), 138.2 (C-4), 133.7 (C-4'), 130.2 (C-2', C-6'), 128.9, 128.9 (C-1'), 128.6 (C-3', C-5'), 125.6 (C-5), 123.2 (C-6), 122.6 (C-3), 88.5 (C-3''), 86.2 (C-2''), 80.5 (C-1''), 79.8 (C-4''), 79.2 (C-5''), 71.8 (C-6''), 61.0, 60.7, 60.6, 59.6 (OCH₃). HRMS-ESI (*m/z*): [M+H]⁺ calcd for C₃₀H₃₃O₉ 537.2119, found 537.2102; [M+Na]⁺ calcd for C₃₀H₃₂NaO₉ 559.1939, found 559.1914.

4-(β-D-Glucopyranosyl)benzene-1,2-diyl dibenzoate (26) To a solution of compound **25** (0.810 g, 1.51 mmol) in dry dichloroethane (90 mL), BBr₃·SMe₂ (11.5 g, 37.12 mmol, 25 eq.) were slowly added and the reaction stirred under reflux for 17 hours. The mixture was allowed to reach room temperature, washed with sodium bicarbonate and extracted with dichloromethane (3 x 100 mL). The organic layers were combined, dried over MgSO₄, filtered and concentrated under vacuum. The residue was purified by column chromatography (40:1 → 30:1 EtOAc/MeOH), affording compound **26** in 8% yield as a brownish solid. R_f(dichloromethane/MeOH 6:1) = 0.60; m.p. = 77.3 – 78.1 °C; [α]_D²⁰ = -11 ° (*c* 0.3, CHCl₃); ¹H NMR [CO(CD₃)₂] δ (ppm) 8.05 (t, 4H, *J*_{ortho} = 7.23 Hz, H-2', H-6'), 7.67-7.62 (m, 2H, H-4'), 7.55 (br s, 1H, H-3), 7.51-7.44 (m, 6H, H-3', H-5', H-5, H-6), 4.38 (br s, 1H, OH), 4.31 (d, 1H, *J*_{1"-2"} = 9.41 Hz, H-1''), 3.90 (br d, 1H, *J*_{6"a-6"b} = 10.75 Hz, H-6"a), 3.80 (br s, 1H, OH), 3.74 (dd, 1H, *J*_{6"b-6"a} = 10.89 Hz, *J*_{6"b-5"} = 4.37 Hz, H-6"b), 3.61-3.47 (m, 3H, H-3'', H-4'', H-5''), 3.42 (t, 1H, *J*_{2"-1"-2"-3"} = 8.83 Hz, H-2''). ¹³C NMR [CO(CD₃)₂] δ (ppm) 164.7 (C=O), 143.1 (C-2), 142.8 (C-1), 140.4 (C-4), 134.7 (C-4'), 130.7 (C-2', C-6'), 129.8 (C-1'), 129.6 (C-3', C-5'), 126.9 (C-5), 123.6 (C-6), 123.4 (C-3), 81.8 (C-1''), 81.7 (C-5''), 79.8 (C-3''), 76.3 (C-2''), 71.7 (C-4''), 63.1 (C-6''). HRMS-ESI (*m/z*): [M+Na]⁺ calcd for C₂₆H₂₄NaO₉ 503.1313, found 503.1326.

4-(2,3,4,6-Tetra-O-benzyl-α-/β-D-glucopyranosyloxy)benzen-1-yl benzoate (28α,β) Compound **27α,β** (*α/β* ratio = 4:1, 0.570 g, 0.90 mmol) was dissolved in dry dichloromethane (20 mL) together with imidazole (0.135 g, 1.98 mmol, 2.2 eq.) and DMAP (cat). After stirring for 10 min at 0 °C, benzoyl chloride (0.230 mL, 1.98 mmol, 2.2 eq.) was added dropwise. The reaction mixture was stirred at room temperature for 24 h, after which it was washed with brine and extracted with dichloromethane (2 x 20 mL). The organic layers were combined, dried over MgSO₄ and concentrated under reduced pressure. The residue was purified by column chromatography (Hexane/EtOAc 10:1 → 5:1), affording **28α,β** as a mixture in *α/β* ratio = 10:1 as a colourless oil isolated in 94 % yield; R_f(Hexane/EtOAc 10:1) = 0.23; [α]_D²⁰ = -4 ° (*c* 0.2, CHCl₃); ¹H NMR (CDCl₃) δ (ppm) 8.20 (d, 20H, *J*_{ortho} = 7.65 Hz, H-2'_α, H-6'_α), 8.10 (d, 2H, *J*_{ortho} = 7.65 Hz, H-2'_β, H-6'_β), 7.66-7.58 (m, 11H, H-4'_α, H-4'_β), 7.54-7.45 (m, 22H, H-3'_α, H-5'_α, H-3'_β, H-5'_β), 7.40-7.10 (m, 264H, benzyl aromatics, H-2_α, H-3_α, H-5_α, H-6_α, H-2_β, H-3_β, H-5_β, H-6_β), 5.44 (d, 10H, *J*_{1"-2"} = 2.84 Hz, H-1''_α), 5.08-4.80 (m, 38H, H-1''_β, Ph-CH₂), 4.71-4.40 (m, 51H, Ph-CH₂), 4.20 (t, 10H, *J*_{3"α-2"α-3"α-4"α} = 9.17 Hz, H-3''_α), 3.90-3.57 (m, 57H, H-2''_α, H-4''_α, H-5''_α, H-6''_α, H-6''_β, H-2''_β, H-3''_β, H-4''_β, H-5''_β, H-6''_{αβ}, H-6''_β). ¹³C NMR (CDCl₃) δ (ppm) 165.4 (C=O_α), 165.4 (C=O_β), 155.1 (C-4_β), 154.4 (C-4_α), 146.0 (C-1_β), 145.6 (C-1_α), 138.7, 138.5, 138.1, 138.0, 139.0, 137.7 (benzyl C_q-

1 aromatics), 133.6 (C-4'_{α/β}), 130.2 (C-2'_α, C-6'_α), 129.9 (C-2'_β, C-6'_β), 128.6-127.6 (benzyl CH-aromatics, C-3'_α, C-5'_α, C-
2 3'_β, C-5'_β), 122.6 (C-2_β, C-6_β), 122.5 (C-2_α, C-6_α), 117.9 (C-3_β, C-5_β), 117.5 (C-3_α, C-5_α), 102.1 (C-1''_β), 95.9 (C-1''_α),
3 82.0 (C-3''_β), 81.9 (C-3''_α), 79.6 (C-5''_{α/β}), 77.6 (C-4''_β), 77.2 (C-4''_α), 75.8, 75.2, 75.1, 73.5, 73.4 (Ph-CH₂), 70.9 (C-2''_β),
4 70.8 (C-2''_α), 68.1 (C-6''_{α/β}). HRMS-ESI (*m/z*): [M+H]⁺ calcd for C₄₇H₄₅O₈ 737.3109, found 737.3117; [M+Na]⁺ calcd
5 6 7 for C₄₇H₄₄NaO₈ 759.2928, found 759.2938.

10 **4-(α-D-Glucopyranosyloxy)benzen-1-yl benzoate (29)** To a solution of the mixture **28**_{α,β} (α/β ratio = 10:1) (0.350 g,
11 0.47 mmol) in ethyl acetate (20 mL), Pd/C (10%, 50 mg) was added. The mixture stirred under H₂ atmosphere for 18
12 hours at room temperature. After reaching completion, the reaction was stopped by filtering Pd/C through a pad of celite
13 and the solvent evaporated under reduced pressure. The residue was purified by column chromatography (100:1 → 5:1
14 AcOEt/MeOH) to afford compound **29** as a white powder in 71% yield. R_f (dichloromethane/MeOH 9:1) = 0.35; m.p.
15 = 161.7 – 162.6 °C; [α]_D²⁰ = + 74 ° (*c* 0.1, CHCl₃); ¹H NMR (MeOD) δ (ppm) 8.16 (d, 2H, *J*_{ortho} = 7.72 Hz, H-2', H-6'),
16 7.68 (t, 1H, *J*_{ortho} = 7.56 Hz, H-4'), 7.55 (t, 2H, *J*_{ortho} = 7.66 Hz, H-3', H-5'), 7.26 (d, 2H, *J*_{ortho} = 8.91 Hz, H-2, H-6), 7.15
17 (d, 2H, *J*_{ortho} = 8.95 Hz, H-3, H-5), 5.49 (d, 1H, *J*_{1"-2"} = 3.36 Hz, H-1''), 3.99 (t, 1H, *J*_{3"-2"-3"-4"} = 9.11 Hz, H-3''), 3.81-3.68
18 (m, 3H, H-5'', H-6''_a and H-6''_b), 3.50 (dd, 1H, *J*_{2"-1"} = 3.35 Hz, *J*_{2"-3"} = 9.40 Hz, H-2''), 3.45 (t, 1H, *J*_{4"-3"-4"-5"} = 9.16 Hz,
19 H-4''). ¹³C NMR (MeOD) δ (ppm) 166.9 (C=O), 156.4 (C-4), 147.2 (C-1), 134.9 (C-4'), 131.0 (C-2', C-6'), 130.8 (C-
20 1'), 129.8 (C-3', H-5'), 123.6 (C-2, C-6), 119.0 (C-3, C-5), 99.8 (C-1''), 74.9 (C-3''), 74.5 (C-5''), 73.3 (C-2''), 71.5 (C-
21 4''), 62.4 (C-6''). HRMS-ESI (*m/z*): [M+H]⁺ calcd for C₁₉H₂₁O₈ 377.1231, found 377.1220; [M+Na]⁺ calcd for
22 C₁₉H₂₀NaO₈ 399.1050, found 399.1040.

23 **4-(β-D-Glucopyranosyloxy)benzen-1-yl benzoate (30)** Minor product of the reaction that gave compound **29**.
24 Colourless crystals obtained in 10% yield; R_f (dichloromethane/MeOH 9:1) = 0.35; m.p. = 192.0 – 193.3 °C; ¹H NMR
25 (MeOD) δ (ppm) 8.16 (d, 2H, *J*_{ortho} = 8.06 Hz, H-2', H-6'), 7.69 (t, 1H, *J*_{ortho} = 7.45 Hz, H-4'), 7.56 (t, 1H, *J*_{ortho} = 7.65
26 Hz, H-3', H-5'), 7.20-7.14 (m, 4H, H-2, H-3, H-5, H-6), 4.91 (H-1'', superimposed with H₂O solvent peak), 3.91 (d, 1H,
27 *J*_{6''_a-6''_b} = 12.06 Hz, H-6''_a), 3.72 (dd, 1H, *J*_{6''_b-6''_a} = 12.00 Hz, *J*_{6''_b-5''} = 5.36 Hz, H-6''_b), 3.50-3.38 (m, 4H, H-2'', H-3'', H-
28 4'', H-5''). ¹³C NMR (MeOD) δ (ppm) 166.9 (C=O), 156.9 (C-4), 147.2 (C-2), 134.9 (C-4'), 131.0 (C-2', C-6'), 130.7
29 (C-1'), 129.8 (C-3', C-5'), 123.6 (C-2, C-6), 118.7 (C-3, C-5), 102.7 (C-1''), 78.2 (C-3''), 77.9 (C-5''), 74.9 (C-2''), 71.3
30 (C-4''), 62.5 (C-6''). HRMS-ESI (*m/z*): [M+Na]⁺ calcd for C₁₉H₂₀NaO₈ 399.1050, found 399.1052.

31 **2-(2,3,4,6-Tetra-O-benzyl-α-D-glucopyranosyloxy)benzen-1-yl benzoate (32)**. Compound **31** (0.360 g, 0.57 mmol)
32 was dissolved in dry dichloromethane (15 mL) together with imidazole (0.086 g, 1.26 mmol, 2.2 eq.) and DMAP (cat).
33 After stirring for 10 min at 0 °C, benzoyl chloride (0.143 mL, 1.18 mmol, 2.2 eq.) was added dropwise. The reaction

1 mixture was stirred at room temperature for 72 h, after which it was washed with brine and extracted with
2 dichloromethane (2 x 20 mL). The organic layers were combined, dried over MgSO₄ and concentrated under reduced
3 pressure. The residue was purified by column chromatography (P. Ether/EtOAc 15:1 → 3:1), affording compound **32**
4 as a colourless oil in 82 % yield. R_f (P. Ether/EtOAc 4:1) = 0.52; $[\alpha]_D^{20} = +50^\circ$ (*c* 0.1, CHCl₃); **¹H NMR** (CDCl₃) δ
5 (ppm) 8.17 (d, 2H, *J*_{ortho} = 7.90 Hz, H-2', H-6'), 7.33 (t, 1H, *J*_{ortho} = 7.34 Hz, H-4'), 7.35-7.06 (m, 24H, benzyl aromatics,
6 H-3, H-4, H-5, H-6, H-3', H-5'), 5.49 (d, 1H, *J*_{1''-2''} = 2.81 Hz, H-1''), 4.77, 4.73 (part A₁ of A₁B₁ system, 1H, *J*_{A₁-B₁} =
7 10.95 Hz, Ph-CH₂), 4.58-4.56 (m, 3H, part A₂ of A₂B₂ system, Ph-CH₂), 4.43-4.37 (m, 2H, part B₁ of A₁B₁ system, part
8 B₂ of A₂B₂ system), 4.34, 4.30 (part A₃ of A₃B₃ system, 1H, *J*_{A₃-B₃} = 10.77 Hz, Ph-CH₂), 4.25, 4.21 (part B₃ of A₃B₃
9 system, 1H, *J*_{A₃-B₃} = 10.95 Hz, Ph-CH₂), 3.88 (br d, 1H, *J*_{2''-3''} = 9.46 Hz, H-2''), 3.79-3.46 (m, 3H, H-3'', H-4'', H-6''a),
10 3.60-3.54 (m, 2H, H-5'', H-6''b). **¹³C NMR** (CDCl₃) δ (ppm) 164.9 (C=O), 148.4 (C-2), 141.1 (C-1), 138.7, 138.5, 138.3,
11 137.9 (benzyl C_q-aromatics), 133.2 (C-4'), 130.5 (C-2', C-6'), 129.6 (C-1'), 128.3-127.5 (benzyl CH-aromatics, C-3', C-
12 5'), 126.8 (C-4), 123.0 (C-5)*, 122.5 (C-6)*, 116.0 (C-3), 96.2 (C-1''), 81.7 (C-3''), 77.2 (C-5''), 76.9 (C-4''), 75.3, 74.7,
13 73.4, 72.6 (Ph-CH₂), 71.2 (C-2''), 68.2 (C-6''). HRMS-ESI (*m/z*): [M+H]⁺ calcd for C₄₇H₄₅O₈ 737.3109, found 737.3109;
14 [M+Na]⁺ calcd for C₄₇H₄₄NaO₈ 759.2928, found 759.2934.

15 **2-(α-D-Glucopyranosyloxy)benzen-1-yl benzoate (33)**. To a solution of compound **32** (0.275 mg, 0.37 mmol) in ethyl
16 acetate (6 mL), Pd/C (10%, 32 mg) was added. The mixture stirred under H₂ atmosphere for 20 hours at room
17 temperature. After reaching completion, the reaction was stopped by filtering Pd/C through a pad of celite and the
18 solvent evaporated under reduced pressure. The residue was purified by column chromatography (1:0 → 30:1
19 AcOEt/MeOH) to afford compound **33** as colourless crystals in 83% yield. R_f (dichloromethane/MeOH 7:1) = 0.35;
20 m.p. = 54.5 – 55.0 °C; $[\alpha]_D^{20} = +123^\circ$ (*c* 0.1, MeOH); **¹H NMR** [CO(CD₃)₂] δ (ppm) 8.20 (d, 2H, *J*_{ortho} = 7.88 Hz, H-2',
21 H-6'), 7.70 (t, 1H, *J*_{ortho} = 7.56 Hz, H-4'), 7.58 (t, 2H, *J*_{ortho} = 7.59 Hz, H-3', H-5'), 7.42 (d, 1H, *J*_{ortho} = 8.56 Hz, H-3),
22 7.28-7.24 (m, 2H, H-4, H-6), 7.10 (t, 1H, *J*_{ortho} = 7.73 Hz, H-5), 5.56 (d, 1H, *J*_{1''-2''} = 3.19 Hz, H-1''), 3.74-3.59 (m, 4H,
23 H-3'', H-4'', H-6''a and H-6''b), 3.53-3.43 (m, 2H, H-2'', H-5''). **¹³C NMR** [CO(CD₃)₂] δ (ppm) 165.0 (C=O), 149.6 (C-
24 2), 141.3 (C-1), 134.1 (C-4'), 130.6 (C-2', C-6'), 130.1 (C-1'), 129.3 (C-3', C-5'), 127.4 (C-4), 123.7 (C-6), 122.9 (C-5),
25 117.9 (C-3), 99.1 (C-1''), 74.4 (C-4''), 74.0 (C-3''), 72.7 (C-2''), 70.8 (C-5''), 62.0 (C-6''). HRMS-ESI (*m/z*): [M+Na]⁺
26 calcd for C₁₉H₂₁O₈ 399.1050, found 399.1064.

27
28
29
30
31
32
33
34
35
36
37
38
39
40
41
42
43
44
45
46
47
48
49
50
51
52
53
54
55
56
57
58
59
60

General procedure for debenzoylation leading to C-glucosyl polyphenols 23 and 24. To a solution of 0.016 mmol of
benzylated C-glucosyl polyphenol (**14**, **16**) in ethyl acetate (6 mL), Pd/C (10%, 32 mg) was added. The mixture stirred
under H₂ atmosphere for 15-26 hours at room temperature. After reaching completion, the reaction was stopped by

1 filtering Pd/C through a pad of celite and the solvent evaporated under reduced pressure. The residue was purified by
2 column chromatography.
3

4
5 **1-[5-(β-D-Glucopyranosyl)-2,4,6-trihydroxyphenyl]ethan-1-one (23)**. Compound synthesized by debenzoylation of
6 compound **14**. The reaction crude was purified by column chromatography (10:1 → 5:1 dichloromethane/MeOH) to
7 give **23** as a yellowish powder in 93% yield. R_f (dichloromethane/MeOH 5:1) = 0.23; m.p. = 150.8 – 153.0 °C; $[\alpha]_D^{20} =$
8 $+ 57^\circ$ (*c* 0.6, MeOH); $^1\text{H NMR}$ (MeOD) δ (ppm) 5.88 (s, 1H, H-5), 4.79 (s, 1H, $J_{1'-2'} = 9.94$ Hz, H-1'), 3.93 (t, 1H, $J_{2'-$
9 $1'-2'-3' = 9.26$ Hz, H-2'), 3.82 (d, 1H, $J_{6'a-6'b} = 11.91$ Hz, H-6'a), 3.71 (dd, 1H, $J_{6'b-6'a} = 12.11$ Hz, $J_{6'b-5'} = 4.87$ Hz, H-6'b),
10 3.46-3.31 (m, 3H, H-3', H-4', H-5'). $^{13}\text{C NMR}$ (MeOD) δ (ppm) 204.9 (C=O), 165.7 (C-2), 165.1 (C-4), 164.2 (C-6),
11 105.6 (C-1), 104.1 (C-3), 96.7 (C-5), 82.5 (C-5'), 79.9 (C-3'), 75.6 (C-1'), 73.1 (C-2'), 71.5 (C-4'), 62.5 (C-6'), 33.0 (CH₃-
12 Ac). HRMS-ESI (*m/z*): $[\text{M}+\text{H}]^+$ calcd for C₁₄H₁₉O₉ 331.1024, found 331.1020; $[\text{M}+\text{Na}]^+$ calcd for C₁₄H₁₈NaO₉
13 353.0843, found 353.0843.
14
15
16
17
18
19
20
21
22
23

24
25 **1-(β-D-Glucopyranosyl)-2-hydroxynaphthalene (24)**. Compound synthesized by debenzoylation of compound **16**. The
26 reaction crude was purified by column chromatography (20:1 → 10:1 dichloromethane/MeOH) to give **24** as a yellowish
27 oil in 91% yield. R_f (dichloromethane/MeOH 10:1) = 0.26; $[\alpha]_D^{20} = + 45^\circ$ (*c* 0.5, MeOH); $^1\text{H NMR}$ [CO(CD₃)₂] δ (ppm)
28 8.16 (br s, 1H, H-8), 7.75 (m, 2H, H-4, H-5), 7.39 (t, 1H, $J_{ortho} = 7.58$ Hz, H-6), 7.27 (t, 1H, $J_{ortho} = 7.36$ Hz, H-7), 7.07
29 (t, 1H, $J_{ortho} = 8.31$ Hz, H-3), 5.43 (d, 1H, $J_{1'-2'} = 9.64$ Hz, H-1'), 3.93-3.83 (m, 3H, H-2', H-6'a and H-6'b), 3.78-3.68 (m,
30 2H, H-3', H-4'), 3.64-3.60 (m, 1H, H-5'). $^{13}\text{C NMR}$ [CO(CD₃)₂] δ (ppm) 155.2 (C-2), 134.3 (C-8a), 130.5 (C-4), 129.7
31 (C-5), 129.0 (C-4a), 126.6 (C-7), 124.8 (C-8), 123.4 (C-6), 120.2 (C-3), 116.7 (C-1), 82.0 (C-5'), 79.4 (C-3'), 78.2 (C-
32 1'), 74.4 (C-2'), 70.7 (C-4'), 61.8 (C-6'). HRMS-ESI (*m/z*): $[\text{M}+\text{Na}]^+$ calcd for C₁₆H₁₉NaO₆ 329.0996, found 329.1001.
33
34
35
36
37
38
39
40
41
42

43 **2-Phenyl-1-(2,4,6-trihydroxyphenyl)ethan-1-one (34)** and **3,5-dihydroxyphenyl 2-phenylacetate (35)**. 1,3,5-
44 Trihydroxybenzene (1.0 g, 7.93 mmol) was dissolved in 2% TfOH/CH₃CN (10 mL) and cooled to 0 °C. Phenylacetyl
45 chloride (1.0 mL, 7.93 mmol) was added at 0 °C and the reaction stirred overnight at room temperature. Then, the crude
46 was poured into ice and extracted with EtOAc. The organic phase was washed with HCl 2M, NaHCO₃ and brine, dried
47 over MgSO₄ and the solvent eliminated under reduced pressure. After column chromatography (5:1 → 3:1
48 Hexane/Acetone) compounds **34** and **35** were obtained in 7% and 25% yield, respectively.
49
50
51
52
53
54
55

56 **3,5-Dihydroxyphenyl 2-phenylacetate (35)**. $R_f = 0.36$ (Hexane/Acetone 3:1); m.p. = 77.9 – 79.6 °C; $^1\text{H NMR}$ (CDCl₃)
57 δ (ppm) 11.70 (s, 2H, OH), 9.30 (s, 1H, OH), 7.30-7.20 (m, 5H, ArCH), 5.94 (s, 2H, ArH), 4.41 (s, 2H, CH₂). $^{13}\text{C NMR}$
58 (CDCl₃) δ (ppm) 200.5 (C=O), 165.6 (ArC, C-4), 165.4 (ArCx2, C-2, C-6), 137.1 (ArC, C-1'), 130.6 (ArCHx2, C-2', C-
59 6'), 128.5 (ArCHx2, C-3', C-5'), 127.0 (ArCH, C-4'), 104.8 (ArC, C-1), 96.2 (ArCHx2, C-3, C-5), 50.0 (CH₂). HRMS-
60 ACS Paragon Plus Environment

ESI (m/z): $[M+H]^+$ calcd for $C_{14}H_{13}O_4$ 245.0808, found 245.0806; $[M+Na]^+$ calcd for $C_{14}H_{12}NaO_4$ 267.0628, found 267.0627.

2-Phenyl-1-(2,4,6-trihydroxyphenyl)ethan-1-one (34). Compound **35** (0.56, 2.49 mmol) was treated with trifluoromethanesulfonic acid (2.2 mL, 25 mmol) at 0 °C. The reaction mixture was warmed up at room temperature for 1 h then, heated for 1 h at 40 °C and then at 100 °C. After one hour more the crude was poured into ice and extracted with EtOAc. The organic phase was washed with HCl 2M, $NaHCO_3$ and brine, dried over $MgSO_4$ and the solvent eliminated under reduced pressure. After column chromatography (5:1 → 3:1 Hexane/Acetone) compound **34** was isolated in 39% yield. $R_f = 0.4$ (Hexane/Acetone 3:1); 1H NMR ($CDCl_3$) δ (ppm) 7.30-7.27 (m, 5H, ArCH), 6.03 – 6.00 (m, 3H, ArH, C-2, C-4, C-6), 3.82 (s, 2H, CH_2). ^{13}C NMR ($CDCl_3$) δ (ppm) 171.9 (C=O), 157.2 (C-2, C-3, C-5), 157.1 (C-1), 129.3 (C-2', C-6'), 128.8 (C-3', C-5'), 127.5 (C-4'), 101.7 (C-2, C-6), 101.2 (C-4), 41.3 (CH_2). HRMS-ESI (m/z): $[M+H]^+$ calcd for $C_{14}H_{13}O_4$ 245.0808, found 245.0805; $[M+Na]^+$ calcd for $C_{14}H_{12}NaO_4$ 267.0628, found 267.0729.

2,4,6-Trihydroxy-3-(2,3,4,6-tetra-O-benzyl- β -D-glucopyranosyl)phenyl]-2-phenylethan-1-one (36). A solution of compound **34** (0.22 g, 0.89 mmol), 2,3,4,6-tetra-O-benzyl-D-glucopyranose (0.34, 0.64 mmol) and drierite (0.3 g) in a mixture of dichloromethane/ CH_3CN (1:1) was stirred for 10 minutes at room temperature. To this solution lowered at -40 °C, TMSOTf (0.16 mL, 0.89 mmol) was added dropwise. The mixture was left at room temperature under stirring overnight. Then, the reaction was stopped by adding trimethylamine and the reaction mixture filtered through a celite pad. The solvent was evaporated under reduced pressure and the residue purified by column chromatography (Hexane/Acetone 7:1) to render compound **36** in 33% yield. $R_f = 0,24$ (Hexane/Acetone 3:1); m.p. = 113.0 – 114.9 °C; $[\alpha]_D^{20} = +25$ ° (c 1, $CHCl_3$); 1H NMR ($CDCl_3$) δ (ppm) 7.38-7.19 (m, 23H, benzyl aromatics), 7.03 – 7.01 (m, benzyl aromatics), 6.02 (br s, 1H, Ph-H5), 4.98 (br s, 2H, Ph- CH_2), 4.89 - 4.85 (m, 2H, H-1'''; part A_1 of A_1B_1 system, Ph- CH_2), 4.74 (d, $J = 10.5$ Hz, 1H, part A_2 of A_2B_2 system, Ph- CH_2), 4.60 - 4.56 (m, 2H, part A_3 of A_3B_3 system; part B_1 of system A_1B_1 , Ph- CH_2), 4.48 (d, $J = 11.9$ Hz, 1H, part B_3 of A_3B_3 system, Ph- CH_2), 4.35 – 4.31 (m, 2H, part A_4 of A_4B_4 system, part B_2 of A_2B_2 system, Ph- CH_2), 4.22 (d, $J = 16.8$ Hz, part B_4 of A_4B_4 system, Ph- CH_2), 3.94 (t, $J = 9.2$ Hz, 1H, H-3'''), 3.85 – 3.70 (m, H-5''', H-2''', H-6'''a, H-6'''b), 3.63 – 3.60 (m, 1H, H-4'''). ^{13}C NMR ($CDCl_3$) δ (ppm) 203.4 (C-1), 164.4 (C-6), 161.3 (C-4), 160.5 (C-2), 138.3, 137.6, 137.4, 135.9, 135.4 (benzyl C_q -aromatics), 129.8-126.6 (benzyl CH-aromatics), 105.9 (C-1), 102.8 (C-3), 98.2 (C-5), 86.2 (C-5'), 82.1 (C-2'), 78.6 (C-4'), 76.8 (C-3'), 76.3, 75.7, 75.3 (CH_2 -Ph), 74.8 (C-1'), 73.3 (CH_2 -Ph), 67.4 (C-6'), 50.3 (CH_2 -Ph). HRMS-ESI (m/z): $[M+H]^+$ calcd for $C_{48}H_{47}O_9$ 767.3215, found 767.3223; $[M+Na]^+$ calcd for $C_{48}H_{46}NaO_9$ 789.3034, found 789.3049.

1 **3-[(β-D-Glucopyranosyl)-2,4,6-trihydroxyphenyl]-2-phenylethan-1-one (37)**. Compound **36** (0.13 g, 0.17 mmol)
2 was dissolved in ethyl acetate (4.0 mL) and methanol (4.0 mL). Then a suspension of Pd/C (10%) (130 mg) in ethyl
3 acetate-methanol was added and the mixture stirred under H₂ atmosphere for 3 hours at room temperature. Pd/C was
4 filtered through a pad of celite and the solvent evaporated under reduced pressure. The residue was purified by column
5 chromatography (dichloromethane/MeOH 7:1) to afford compound **37** in 68% yield. m.p. = 128.5 – 129.3 °C; $[\alpha]_D^{20} = +$
6 47 ° (*c* 0.4, MeOH); ¹H NMR [CO(CD₃)₂] δ (ppm) 7.28 – 7.15 (m, 5H, ArCH), 5.93 (s, 1H, H-5), 4.86 (d, *J* = 9.8 Hz,
7 1H, H-1"), 4.38 (s, 2H, CH₂), 3.80 – 3.70 (m, 3H, H6"a, H6"b, H-2), 3.59 – 3.47 (m, 2H, H-4", H-3"), 3.42 (dt, *J* = 9.5,
8 3.2 Hz, 1H, H-5"). ¹³C NMR [CO(CD₃)₂] δ (ppm) 203.0 (C-1), 163.5 (C-4), 163.4 (C-2), 162.6 (C-6), 135.9 (C-1'),
9 129.7 (C-4'), 127.9 (C-3', C-5'), 126.1 (C-2', C-6'), 104.1 (C-1), 103.3 (C-3), 95.1 (C-5), 80.9 (C-5"), 78.3 (C-3"), 74.9
10 (C-1"), 72.6 (C-2"), 69.6 (C-4"), 60.7 (C-6"), 49.4 (CH₂). HRMS-ESI (*m/z*): [M+H]⁺ calcd for C₂₀H₂₃O₉ 407.1337, found
11 407.1341.
12
13
14
15
16
17
18
19
20
21
22
23
24
25
26

27 Biological Activity Assays

28 **STD-NMR binding studies with IAPP**. NMR experiments were recorded on a Bruker Avance 600 MHz spectrometer
29 equipped with a triple channel cryoprobe head. Immediately before use, lyophilized IAPP was dissolved in 10 mM
30 NaOD in D₂O at a concentration of 160 μM, then diluted 1:1 with 10 mM phosphate buffer saline, pH 7.4 containing
31 100 mM NaCl. To these samples were added the compounds in study, **21** and **37**, to a final concentration of 2 mM. The
32 pH of each sample was verified with a Microelectrode (Mettler Toledo) for 5 mm NMR tubes and adjusted with NaOD
33 and/or DCl. Selective saturation of the protein resonances (on resonance spectrum) was performed by irradiating at –0.5
34 ppm using a series of Eburp2.1000-shaped pulses (50 ms) for a total saturation time of 2.0 s. For the reference spectrum
35 (off resonance), the samples were irradiated at 100 ppm. STD experiments were recorded at two temperatures 298 K
36 and 310 K with a ligand/amyloid oligomers molar ratio of 12:1. Control STD experiments with IAPP without any ligand,
37 and only with ligands **21** and **37** without IAPP were also recorded and taken in account in the STD epitope determination.
38 To determine the epitope mapping of each ligand shown in Figure 3 the STD intensities of each proton were normalized
39 with respect to that with the highest response. Proton resonances from which it was not possible to have an accurate
40 STD information are identified with * in Figure 3.
41
42
43
44
45
46
47
48
49
50
51
52
53
54
55
56

57 **Glucosidase and Cholinesterase inhibition assays**. Measurement of the glucosidase inhibition was carried out using
58 the methodology previously reported by Bols and coworkers.⁸⁰ Inhibition assays were conducted in a double-beam
59 Hitachi U-2900 spectrophotometer, with PS cuvettes at the wavelength indicated in each case. α-Glucosidase
60

(*Saccharomyces cerevisiae*) and β -glucosidase (almonds) were used as model enzymes, and the corresponding *p*-nitrophenyl glycosides as substrates. Initial screening for determining the percentage of inhibition was conducted at a 100 μ M inhibitor concentration. Inhibitor mother solutions were prepared in DMSO and the ratio of DMSO in the cuvette was maintained at 5%. Two 1.2-mL samples in PS cuvettes containing 0.1 M phosphate buffer (pH 6.8) were prepared using the corresponding nitrophenyl glucopyranoside as substrate at a concentration equal to the expected value of K_M . Water (control) or inhibitor solution plus water (100 μ M final concentration) were added to a constant value of 1.14 mL. Finally, reaction was initiated by the addition of a solution of properly diluted enzyme (60 μ L) at 25 $^{\circ}$ C, and was monitored by registering the increase in absorbance at 400 nm for 125 s.

Initial rates were obtained from the slopes of the plots (Abs. vs. t) and used for calculating the percentage of inhibition, using the following equation:

$$\%Inhibition = \frac{v_o - v}{v_o} \times 100$$

where v_o refers to the rate in the control experiment (enzyme), and v refers to the rate in the experiment containing the inhibitor solution. For determining the percentage of inhibition, the substrate concentration was fixed at the K_M value for each enzyme ($[S] = 0.25$ mM for α -glucosidase, and $[S] = 4.0$ mM for β -glucosidase). For compounds showing a significant percentage of inhibition, the mode of inhibition was obtained using the Lineweaver-Burk plot and Cornish-Bowden ($1/v$ vs. $[I]$, $[S]/v$ vs. $[I]$) plots.⁸¹ The procedure followed was the same as above, but using 5 different substrate concentrations, ranging from 0.25 to 4.0 of the expected K_M , while keeping constant the inhibitor concentration (3 different inhibitor concentrations). The reaction rate for the cuvette containing the highest substrate concentration was allowed to be within 0.12-0.15 Abs/min. Kinetic parameters (K_M , V_{max}) were obtained using nonlinear regression analysis (least squares fit) using the Michaelis-Menten equation tool implemented in GraphPad Prism 8.01 software, which in turn were used to calculate the inhibition constants, according to the equations indicated below.

For cholinesterase inhibition tests (acetylcholinesterase (AChE, *electrophorus electricus*) and butyrylcholinesterase (BuChE, equine serum), the Ellman's colorimetric assay⁸² was followed, with minor modifications. DMSO was kept within 1.25% cuvette concentration. The chromogenic agent DTNB [5,5'-dithiobis(2-nitrobenzoic acid)] was fixed at 0.975 mM concentration; 0.1 M phosphate buffer (pH 8.0) was employed, $T = 25$ $^{\circ}$ C, and the reaction was monitored for 125 s at 405 nm. For determining the percentage of inhibition, the substrate concentration (acetylthiocholine iodide for AChE; *S*-butyrylthiocholine iodide for BuChE) was fixed at 29 μ M for AChE and at 18.2 μ M concentration for BuChE.

The mode of inhibition and inhibition constants were obtained as described above for glycosidases.

Competitive inhibition (inhibitor only binds the free enzyme):

$$K_{ia} = \frac{[I]}{\frac{K_{M app}}{K_M} - 1}$$

Mixed inhibition (inhibitor binds both, the free and the complexed enzyme):

$$K_{M app} = K_M \frac{1 + \frac{[I]}{K_{ia}}}{1 + \frac{[I]}{K_{ib}}}$$

$$V_{max app} = \frac{V_{max}}{1 + \frac{[I]}{K_{ib}}}$$

Uncompetitive (the inhibitors only bind the complexed enzyme):

$$K_{M app} = \frac{K_M}{1 + \frac{[I]}{K_{ib}}}$$

$$V_{max app} = \frac{V_{max}}{1 + \frac{[I]}{K_{ib}}}$$

Non-competitive (inhibitor binds both the free enzyme and the complexed enzyme with equal affinity):

$$K_{M app} = K_M$$

$$V_{max app} = \frac{V_{max}}{1 + \frac{[I]}{K_{ib}}}$$

The following inhibitor concentrations were used for the calculation of the inhibition constants:

Genistein

- α -Glucosidase: 0, 10, 20, 30 μ M
- β -Glucosidase: 0, 50, 83.3 μ M

Compound 33

- α -Glucosidase: 0, 33.3, 50 μ M

Experiments were carried out in duplicate, and the data are expressed as the mean \pm SD.

Cell culture. The human induced pluripotent stem cells (hiPSCs) line derived from a health control individual used in this study. The hiPS (control MIFF1)⁷⁰ was kindly provided by Professor Peter Andrews and Dr. Ivana Barbaric (Centre for Stem Cell Biology, The University of Sheffield). hiPSCs were maintained in Vitronectin-coated plates (0.5 μ g/cm²; ThermoFisher Scientific) according to the manufacturer's recommendations in complete TeSR™-E8™ Medium (StemCell Technologies). Culture medium was changed every day. Cells were passaged every 5-7 days as clumps using ReLeSR™ an enzyme-free reagent for cell dissociation (StemCell Technologies) according to the manufacturer's recommendations. For all the experiments in this study, hiPSCs were used between passage 18 and 26, all hiPSCs were cultured in 5% O₂, 5% CO₂ at 37°C.

Natural A β oligomer and control solutions. A solution containing natural amyloid-beta (A β) oligomers (a kind gift of Dr. Claire Garwood) was derived from the conditioned medium of 7PA2 cells,⁴⁶ a Chinese Hamster Ovary cells stably transfected with cDNA encoding APP751, an amyloid precursor protein that contains the Val717Phe familial Alzheimer's disease mutation.^{83,84} In order to obtain natural A β oligomers 5x10⁶ cells were seeded in a T175 flask and cultured in Dulbecco's modified Eagle's medium (DMEM, sigma) supplemented with 10% fetal bovine serum (ThermoFisher), 2 mM L-glutamine (Sigma-Aldrich) 50 mg/mL penicillin/streptomycin. Cells were incubated for 24 hours in 5% CO₂ at 37°C. After 24 h of incubation the cells were washed with serum-free medium and conditioned in 5 mL of plain DMEM without phenol red (ThermoFisher) and lacking any additives, overnight. The oligomer-containing conditioned medium (CM) was collected and cleared of cells and debris by centrifugation at 200 g for 10 min at 4°C. The CM was used as the natural A β oligomer solution in the fear conditioning experiments for HCS. The concentrated CM contained between 1000-2000 pg/mL of A β (1-42) as measured by ELISA (ThermoFisher).

Knockdown experiment. The knockdown is an experimental technique by which the expression of a gene is transiently reduced, for this reason it is necessary to find out the optimal condition in which we have the maximum effect preserving the cell viability. In HEK cells we observed that the detection should not be carried out prior to 24 hours post-transfection and in terms of gene silencing 24 hours siRNA transfection at a non-toxic concentration of 200 nM and 0.2 μ L of DharmaFECT reagent were found to yield good knockdown results. It was interesting to observe also how the gene

1 expression started to recover after 24 hours, even if still under treatment, and also when the transfection medium was
2 replaced with complete medium and incubated for further 24 hours.
3

4
5 Like other GPI-anchored proteins, PrP^C can be released from the cell surface in vitro by the action of exogenous bacterial
6 phosphatidylinositol-specific phospholipase C (PI-PLC). PLC acute cleavage was therefore used to enhance the effect
7
8 of the transient knockdown.
9

10
11
12 All reagents for the knockdown experiment, such as ON-TARGETplus Human PRNP (5621) siRNA – SMARTpool,
13 ON-TARGETplus Non-targeting Pool, ON-TARGETplus GAPD Control Pool, 5X siRNA Buffer, DharmaFECT 1
14 Transfection Reagent and Molecular Grade RNase-free water, were purchased from GE Healthcare Dharmacon. TrypLE
15 Express Enzyme (1X) Phenol Red was from Gibco™ via Thermo Fischer. Opti-MEM® Reduced Serum Medium and
16 Phospholipase C were obtained from Thermo Fisher.
17
18
19
20
21
22

23
24 **HEK cell dosing.** Cells from the routine cell culture were seeded in the 96 well plates (15,000 cells/well), previously
25 coated with polyornithin hydrobromide. After 24 hours the cells were checked to ensure they had attached and were
26 ready for dosing. The complete medium was replaced with Conditioning Medium containing natural A β 1-42 1 x 10³
27 pg/mL for 2 hours and washed with PBS Mg²⁺/Ca²⁺ before being dosed with the compounds, dissolved in phenol red
28 medium, for 1 hour. After that, cells were dosed for 2 hours with compounds at 10 μ M final concentration. The screen
29 of each compound was carried out in triplicate and repeated at least 2 times. Negative control cells were treated with
30 0.5 % DMSO, vehicle of dilution of the drug, and positive controls cells with only A β os. Once dosing was completed,
31 cells were rinsed with PBS (Sigma) and fixed with 100 μ L/well of 4% PFA and incubate 15 min at room temperature.
32 PFA was removed and cells washed with 100 μ L PBS one time or twice if the plates have to be stored in the fridge in
33 PBS. The cells were blocked in 100 μ L PBS-T 5% Donkey serum for 1 hour at RT and incubate with anti- β Amyloid
34 1-16 clone 6E10 anti-mouse (BioLegend) overnight at 4 °C. The antibody was made up in 50 μ L PBS-T 5% Donkey
35 serum with a dilution factor of 1:250. The primary antibody was removed, and the cells washed 3 times with 50 μ L
36 PBS-T 5 min each at RT before adding the secondary antibody Alexa fluor 594 to each well and incubate for 1h at RT.
37 The antibody was made up in PBS-T with a dilution factor of 1:500. Cells were washed 2 times with PBS-T and 1 time
38 with PBS (50 μ L) and nuclei stained with DAPI 100 ng/mL in PBS prepared from 5 mg/mL stock. After the last 2
39 washes cells were left in 100 μ L PBS to be analyzed. Image acquisition was performed by ImageXpress Micro Widefield
40 High Content Screening System and analysis of data with MetaXpress Software Multi-Wavelength Translocation
41 Application Module.
42
43
44
45
46
47
48
49
50
51
52
53
54
55
56
57
58
59
60

Neural differentiation. Neural induction of hiPSCs (Figure 11) was performed using the modified version of dual SMAD inhibition protocol.⁸⁵ hiPSCs were detached by 3 minutes of incubation with Versene Solution (Gibco®), after incubation the solution was removed and 1mL of complete TeSR™-E8™ Medium (StemCell Technologies) was added per well of 6 well plate and detached with a cell lifter (Corning) and then the cell suspension was transferred for Matrigel-coated plate (Corning® Matrigel® Growth Factor Reduced). On the day after plating (day 1), after the cells have reached ~100% confluence, the cells were washed once with PBS and then the medium was replaced for neural medium (50% of DMEM/F-12, 50 % of Neurobasal, 0.5× N₂ supplement, 1x Gibco® GlutaMAX™ Supplement, 0.5x B-27, 50 U mL⁻¹ penicillin and 50 mg mL⁻¹ streptomycin, supplemented with SMAD inhibitors (SMAD-i, DMH-1 2 μM SB431542-10 μM TOCRIS). The medium was changed every day for 7 days, on day 8, when is possible to see a uniform neuroepithelial sheet, the cells were split 1:1 with Accutase (StemPro® Accutase® Cell Dissociation Reagent, Gibco™ A1110501), onto matrigel substrate in the presence of 10 μM of Rock inhibitor (Rock-i, Y-27632 dihydrochloride, Tocris), giving rise to a sheet of neural progenitor cells (NPC). After 24 hours of incubation the medium was removed and replaced for neural medium without Rock-i. Culture medium was changed every second day and once confluent they were split.

Neuronal induction from neural progenitor cells was obtained from previously described methods with modifications.⁸⁴ NPCs were transferred to Poly-L-ornithine/laminin-coated plates (10 μg /mL) and the medium was replaced for neuronal medium (Neurobasal medium, 1x Gibco® GlutaMAX™ Supplement, 1x B-27), supplemented with DAPT 10 μM. The medium was changed every day for 6 days, immature neurons emerged around day 26. On day 40 the young neurons were split with accutase onto to Poly-L-ornithine/laminin-coated plates (10 μg /mL) and the medium was replaced for neuronal medium without DAPT and supplemented with 10nM of BDNF. The cells were then fed at alternate days with neuronal medium until day 75.

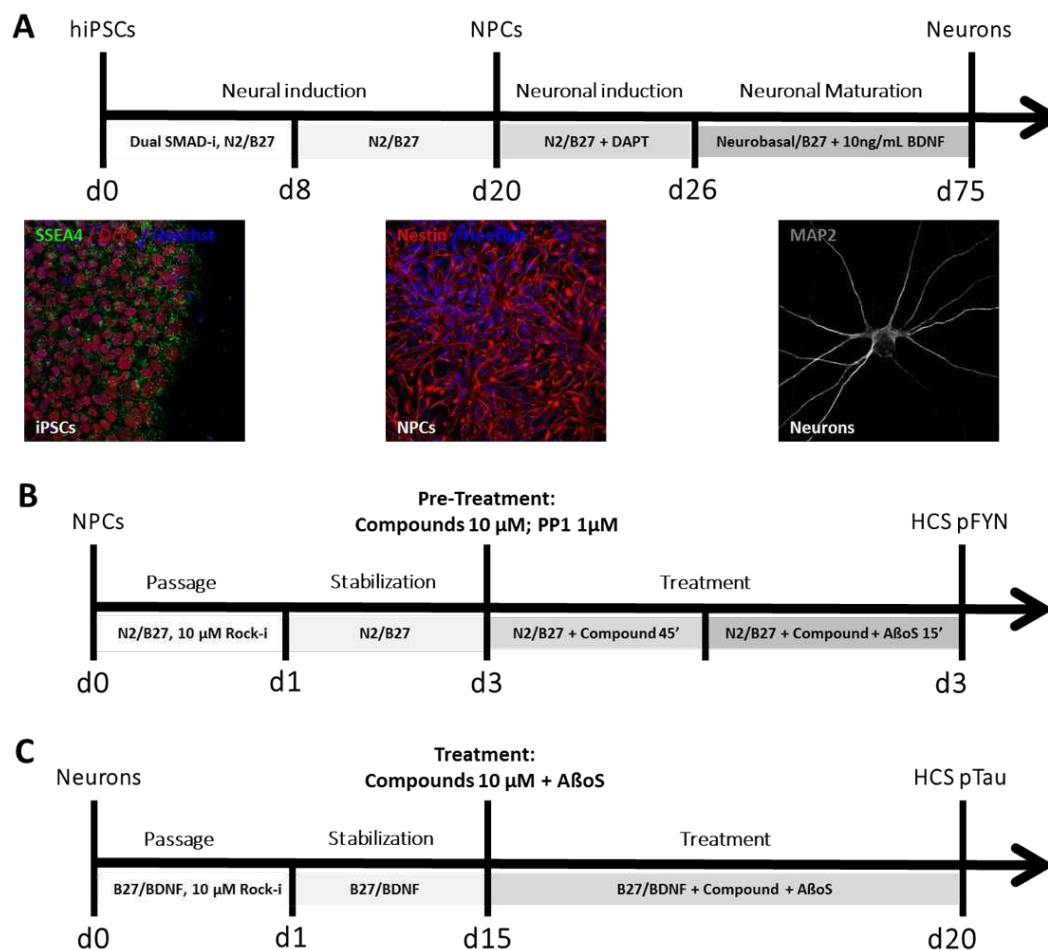


Figure 11. Differentiation of cortical neurons from iPSCs. (A) Outline of cortical differentiation protocol. (B) Outline of the treatment and High-content screening for pFyn kinase. (C) Outline of the treatment and High-content screening for pTau.

Fluorescence-Activated Cell Sorting (FACS) analysis. After treatment with 100 nM siRNA (48 hours) samples were washed with PBS Ca⁺⁺/Mg⁺⁺ and treated for one hour with PLC 0.4 U/mL before to be harvested by TrypLE Express Enzyme (1X) Phenol Red. Cells were resuspended in fresh medium, counted with a haemocytometer, transferred into an eppendorf tube (1-1.5 x 10⁶ cells) and spun down at 1000 rpm for 5 minutes. The supernatant was decanted, and the pellets were resuspended with cold PBS Ca⁺⁺/Mg⁺⁺ to wash the cells 1 times at 2000 rpm for 5 minutes at 4 °C. During the experiment was always useful to check the viability of the cells as in which should be around 95% and not less than 90%. The cells were than resuspend in ice cold FACS buffer (PBS Ca⁺⁺/Mg⁺⁺, 10% FBS, 1% sodium azide) 1 mL for 5-10 mins. Sodium azide prevent the modulation and internalization of surface antigens which can produce a loss of fluorescence intensity. The primary anti-AβoS 8H4 (conc. 0.01 M) was diluted 1:200 in 100 μL PBS 5% BSA and then the cells were resuspended in this solution and incubated for 1 hours on ice and protected from light. The same was done for the Isotype (conc. 2.5 mg/mL) 0.8:200. The cells were washed two times with cold PBS Ca⁺⁺/Mg⁺⁺ by centrifugation at 2000 rpm for 5 min and incubate with the secondary antibody

1 in dark for 1 hour under gentle agitation. The fluorochrome-labeled secondary antibody Alexa Fluor 488 was diluted
2 1:500 in 100 μ L PBS 5% BSA. Before the analysis the cells were washed and resuspend in 300 μ L cold PBS
3
4 $\text{Ca}^{++}/\text{Mg}^{++}$ and 2 μ L of propidium iodide (PI) added to each sample to exclude dead cells. For best results, all
5
6 reagents/solutions used were cold and cells kept on ice and analyzed immediately on the flow cytometer.
7

8
9 **Immunocytochemistry (ICC) analysis.** After the transfection with 100 nM siRNA (48 hours) the same samples were
10
11 treated for 1 hour with PLC 0.4 U/mL. The cells were rinsed with PBS and Conditioning Medium containing natural
12
13 $\text{A}\beta$ 1-42 (1 x 10³ pg/mL) was added. After 2 hours cells were washed with PBS $\text{Mg}^{2+}/\text{Ca}^{2+}$, fixed with 100 μ L/well of
14
15 4% PFA and incubated 15 min at room temperature. PFA was removed and cells washed with 100 μ L PBS one time or
16
17 twice if the plates had to be stored in the fridge in PBS. The cells were blocked in 100 μ L PBS-T 5% Donkey serum for
18
19 1 hour at RT and incubate with anti- β Amyloid 1-16 clone 6E10 anti-mouse overnight at 4 °C. The antibody was made
20
21 up in 50 μ L PBS-T 5% Donkey serum with a dilution factor of 1:250. The primary antibody was removed, and the cells
22
23 washed 3 times with 50 μ L PBS-T 5 min each at RT before adding the secondary antibody Alexa fluor 488 to each well
24
25 and incubated for 1h at RT. The antibody was made up in PBS-T with a dilution factor of 1:500. Cells were washed 2
26
27 times with PBS-T and 1 time with PBS (50 μ L) and nuclei stained with 4,6-diamidino-2-phenylindole (DAPI) 100
28
29 ng/mL in PBS prepared from 5 mg/mL stock. After the last 2 washes cells were left in 100 μ L PBS to be analyzed.
30
31 Image acquisition was performed by ImageXpress Micro Widefield High Content Screening System and analysis of
32
33 data with MetaXpress Software Multi-Wavelength Translocation Application Module.
34
35

36
37 **Treatments.** The cells were exposed to the solution containing natural $\text{A}\beta$ oligomers obtained from 7PA2 cells [1000
38
39 pg/mL of $\text{A}\beta$ (1-42)]. The compounds were diluted at 10 mM in DMSO (Sigma Chemical Co), and kept out of light at -
40
41 20°C until use. PP1 (Potent, selective Src family kinase inhibitor) was obtained from Tocris (1397) stored at 1 mM in
42
43 DMSO (Sigma Chemical Co), and kept out of light at -20°C until use. To determine the effects of the compounds on
44
45 inhibit activation of Fyn Kinase, NPC-cultures were pre-treated for 45 minutes with 10 μ M of the compounds or 1 μ M
46
47 of PP diluted in neurobasal medium without phenol red. After pre-treatment the cells were exposed to 1000 pg/mL of
48
49 $\text{A}\beta$ oligomers in association with the compounds for 15 minutes; control cultures were treated with DMSO, the vehicle
50
51 of dilution of the drugs. PP1 was used as a control of inhibition of Fyn activation. In order to evaluate the potential of
52
53 the compounds to inhibit the hyperphosphorylation of Tau, cortical neurons were exposed to 1000 pg/mL of $\text{A}\beta$
54
55 oligomers in association with 10 μ M of the compounds for 5 days.
56
57

58
59 **Immunofluorescence.** For immunostaining, hiPSCs, NPC and neurons were washed with phosphate-buffered saline
60
(PBS) and fixed by immersion in 4% *p*-formaldehyde for 15 minutes at room temperature. Following fixation, samples

1 were washed three times with PBS and permeabilized with 0.3% Triton X-100 in PBS (Sigma) for 5 min in order to
2 detect intracellular antigens. After permeabilization, cells were blocked by incubation with PBS containing 5% Donkey
3 serum (DS) (Millipore) for 1 h. After blocking, cell cultures were incubated overnight at 4°C with primary antibodies
4 diluted in PBS containing 1% of DS. After 3 washes with PBS, cells were incubated with secondary antibodies diluted
5 in PBS containing 1% of DS for 1h at room temperature in the dark. The samples were washed with PBS three more
6 times and incubated with 1.0 mg/mL DAPI for nuclear staining. The following primary antibodies were used at the
7 indicated dilutions: anti-SSEA4 (MC813-70) (mouse, 1:200; ThermoFisher, 41-4000), anti-Oct4 [EPR17929] (Rabbit,
8 1:250; Abcam, ab181557), anti-Nestin [EPR17929] (Rabbit, 1:500; BioLegend, 841901), anti-Tubulin β 3 (TUJ1)
9 (mouse, 1:1000; BioLegend, 801201), anti-MAP2 (Guinea pig, 1:1000; Synaptic systems, 188004), anti-phospho-Tau
10 PHF-Tau (Thr181) (mouse, 1:500; ThermoFisher, MN1050), Phospho-Fyn (Tyr530) (rabbit, 1:500; ThermoFisher,
11 PA5-36644). The following secondary antibodies were used at the indicated dilutions: Alexa Fluor 488-conjugated
12 Donkey anti-Mouse IgG IgG conjugated (1:400; ThermoFisher A-21202), Alexa Fluor 594-conjugated Donkey anti-
13 rabbit IgG (1:400; ThermoFisher, A-31572), Alexa Fluor 594-conjugated Donkey anti-mouse IgG (1:400;
14 ThermoFisher, A-21203), Alexa Fluor 647-conjugated Goat anti-Guinea Pig IgG (1:400; ThermoFisher, A-21450). All
15 experiments included cultures where the primary antibodies were not added, and unspecific stained was not observed in
16 such negative controls. Images were taken from the 63 \times objective on a Leica TCS SP5 Confocal Laser Scanning
17 Microscope coupled with the LAS AF lite software (Wetzlar, Germany). We used 386, 488 and 594 nm lasers, along
18 with the appropriate excitation and emission filters. These settings were kept consistent while taking images from
19 all cultures.

20
21
22
23
24
25
26
27
28
29
30
31
32
33
34
35
36
37
38
39
40
41 **High-content image screening (HCS).** NPC cells were plated at 1×10^4 cells per well on Poly-L-ornithine/laminin-
42 coated 96-well plates, after 3 days the cells were treated. After the treatment the cells were fixed and stained for
43 pFyn kinase and Alexa Fluor™ 594 Phalloidin was used as a marker that define the boundary of cells and DAPI
44 for nuclear staining. A quantitative imaging analysis of the NPC cells was conducted through the The Opera
45 Phenix™ High Content Screening System at $\times 40$ magnification using the The Columbus™ Image analysis system. The
46 morphological features number of cells and number of spots per cell were assessed for both treated and control cells.
47 At least 15 fields were randomly selected and scanned per well of a 96-well plate in triplicate. To identify and
48 remove any false readings generated by the system, three random A β and control wells were selected and counted
49 manually (blind to group). For the pTau experiment, the treatment with compounds was done concomitantly with
50 A β medium being changed after 3 days of treatment and cells were allowed to differentiate for 2 more days. On day
51
52
53
54
55
56
57
58
59
60

5 cells were fixed for immunocytochemistry. The morphological features assessed for both treated and control were number of cells and Intensity Cell Alexa 568 per cell.

MTT assay. Cortical neural cells were plated on 96 wells plate at a density of 1×10^4 cells/well and kept in a controlled environment (37°C and $5\% \text{CO}_2$). After 3 days, cells were exposed for 24 h to the medium containing the compounds at concentration of 1-50 μM . The effect of treatment on cell viability was assessed by measuring mitochondrial enzymatic activity by the 3-(4,5-dimethylthiazol-2-yl)-2,5-diphenyltetrazolium bromide assay (MTT Formazan; Sigma Aldrich Co). Two hours before the end of the treatment, the MTT solution was added to each well (10 μL / well) at a final concentration of 1 $\mu\text{g}/\text{mL}$, diluted in neural medium. After 2 hours, the cells were lysed with a volume of 60 $\mu\text{L}/\text{well}$ acidified isopropanol solution at room temperature under agitation for 10 minutes to complete dissolution of the formazan crystals. The optical absorbance of each sample was measured using the spectrophotometer at a wavelength of 490 nm (*PHERASTAR FS microplate reader*). The cell cytotoxicity was quantified by measuring the conversion of MTT into MTT formazan by mitochondrial dehydrogenases of viable cells. Each experimental condition was performed in eight replicate wells in at least three independent experiments. The results show the percentage of viability of the cells, and control cells treated with DMSO were considered as 100%.

Aggregation assays. For light scattering and spectrophotometric measurements, each compound was dissolved in 10 mM phosphate buffer saline (PBS) containing 100 mM NaCl, (pH 7.4, filtered through paper with 5 μm pores) and 1.25% DMSO for compounds **8**, **9**, **10**, **23**, **24**, and **33**, 2.5% for compounds **21** and **26**, and 5% for compounds **18** and **25**, to a final concentration of 10, 50 or 100 μM . After mixing with a vortex, samples were incubated for 2 hours at room temperature protected from light. The positive and negative controls were prepared under the same conditions, i.e., in PBS and the same DMSO concentrations used for the compounds: 1.25%, 2.5% or 5%.

Absorbance measurements were performed at room temperature ($24^\circ\text{C} \pm 1$) with a Jasco V-560 UV/Vis double beam spectrophotometer, at room temperature using quartz cuvettes with 1 cm optical path.

Light scattering (Rayleigh) was determined by measuring the intensity of light scattered at 90° and 550 nm with a Fluorolog Model 3.22 spectrofluorimeter in right-angle geometry (Horiba Jobin Yvon) at room temperature using 1 cm x 1 cm quartz Suprasil® cuvettes and setting both excitation and emission wavelengths to 550 nm, with a bandwidth of 1 nm. Three independent replicates were performed for each compound at each concentration, with at least 10 measurements per replicate.

Log $D_{7.4}$ determination. The *in-silico* prediction tool ALOGPS⁸⁶ was used to estimate the octanol-water partition coefficients ($\log P$) of the compounds. Depending on these values, the compounds were classified either as hydrophilic

(log P below zero), moderately lipophilic (log P between zero and one) or lipophilic (log P above one) compounds. For each category, two different ratios (volume of octan-1-ol to volume of buffer) were defined as experimental parameters (Table 5).

Table 5. Compound classification based on estimated log P values.

Compound category	log P	Ratios (octan-1-ol: buffer)
Hydrophilic	< 0	30:140, 40:130
moderately lipophilic	0 - 1	70:110, 110:70
Lipophilic	> 1	3:180, 4:180

Equal amounts of phosphate buffer (0.1 M, pH 7.4) and octan-1-ol were mixed and shaken vigorously for 5 min to saturate the phases. The mixture was left until separation of the two phases, and the buffer was retrieved. Stock solutions of the test compounds were diluted with buffer to a concentration of 1 μ M. For each compound, three determinations per octan-1-ol:buffer ratio were performed in different wells of a 96-well plate. The respective volumes of buffer containing analyte (1 μ M) were pipetted to the wells and covered by saturated octan-1-ol according to the chosen volume ratio. The plate was sealed with aluminum foil, shaken (1350 rpm, 25 $^{\circ}$ C, 2 h) on a Heidolph Titramax 1000 plate-shaker (Heidolph Instruments GmbH & Co. KG, Schwabach, Germany) and centrifuged (2000 rpm, 25 $^{\circ}$ C, 5 min, 5804 R Eppendorf centrifuge, Hamburg, Germany). The aqueous phase was transferred to a 96-well plate for analysis by liquid chromatography-mass spectrometry (LCMS, see below). Log P coefficients were calculated from the octan-1-ol:buffer ratio (o:b), the initial concentration of the analyte in buffer (1 μ M), and the concentration of the analyte in buffer (c_B) according to the following equation:

$$\log P = \log\left(\frac{1 \mu\text{M} - c_B}{c_B} \times \frac{1}{o:b}\right)$$

Results are presented as the mean \pm SD of three independent experiments. If the mean of two independent experiments obtained for a given compound did not differ by more than 0.1 units, the results were accepted.

Parallel artificial membrane permeability assay (PAMPA). Effective permeability (log P_e) was determined in a 96-well format with PAMPA.⁸⁷ For each compound, measurements were performed at pH 7.4 in quadruplicates. Four wells of a deep well plate were filled with 650 μ L of PRISMA HT universal buffer, adjusted to pH 7.4 by adding the requested

1 amount of NaOH (0.5 M). Samples (150 μ L) were withdrawn from each well to determine the blank spectra by UV/Vis-
2 spectroscopy (190 to 500 nm, SpectraMax 190, Molecular Devices, Silicon Valley, CA, USA). Then, analyte dissolved
3 in DMSO (10 mM) was added to the remaining buffer to yield 50 μ M solutions. To exclude precipitation, the optical
4 density (OD) was measured at 650 nm, and solutions exceeding OD 0.01 were filtrated. Afterwards, samples (150 μ L)
5 were withdrawn to determine the reference spectra. Further 200 μ L were transferred to each well of the donor plate of
6 the PAMPA sandwich (pIon, P/N 110 163). The filter membranes at the bottom of the acceptor plate were infused with
7 5 μ L of GIT-0 Lipid Solution and 200 μ L of Acceptor Sink Buffer were filled into each acceptor well. The sandwich
8 was assembled, placed in the GutBoxTM, and left undisturbed for 16 h. Then, it was disassembled and samples (150
9 μ L) were transferred from each donor and acceptor well to UV-plates for determination of the UV/Vis spectra. Effective
10 permeability ($\log P_e$) was calculated from the compound flux deduced from the spectra, the filter area, and the initial
11 sample concentration in the donor well with the aid of the PAMPA Explorer Software (pIon, version 3.5).
12
13
14
15
16
17
18
19
20
21
22
23
24

25 **LC-MS measurements.** Analyses were performed using a 1100/1200 Series HPLC System coupled to a 6410 Triple
26 Quadrupole mass detector (Agilent Technologies, Inc., Santa Clara, CA, USA) equipped with electrospray ionization.
27 The system was controlled with the Agilent MassHunter Workstation Data Acquisition software (version B.01.04). The
28 column used was an AtlantisR T3 C18 column (2.1 x 50 mm) with a 3 μ m-particle size (Waters Corp., Milford, MA,
29 USA). The mobile phase consisted of eluent A: 10 mM ammonium acetate, pH 5.0 in 95:5, H₂O:MeCN; and eluent B:
30 MeCN containing 0.1% formic acid. The flow rate was maintained at 0.6 mL/min. The gradient was ramped from 95%
31 A/5% B to 5% A/95% B over 1 min, and then hold at 5% A/95% B for 0.1 min. The system was then brought back to
32 95% A/5% B, resulting in a total duration of 4 min. MS parameters such as fragmentor voltage, collision energy and
33 polarity were optimized individually for each drug, and the molecular ion was followed for each compound in the
34 multiple reaction monitoring mode. The concentrations of the analytes were quantified by the Agilent Mass Hunter
35 Quantitative Analysis software (version B.01.04).
36
37
38
39
40
41
42
43
44
45
46
47
48
49
50

51 ASSOCIATED CONTENT

52 **Supporting Information Availability**

53 Supporting information is available free of charge via the Internet at <http://pubs.acs.org>:
54
55

56 **SI items**

57 DFT calculations
58
59
60

1 STD-NMR experiments

2
3 ThT fluorescence assays

4
5 Membrane PAINS calculations

6
7
8 Aggregation studies

9
10
11 ¹H NMR and ¹³C NMR spectra of novel final compounds and key intermediates

12
13
14 Analysis of the purity of tested compounds by HPLC-DAD-ESI(-)MS

15
16
17 Analysis of the purity of tested compounds by HPLC-DAD

18
19
20 Molecular Formula Strings

21
22 AUTHOR INFORMATION

23
24
25 *Corresponding Authors:* Amélia Pilar Rauter, e-mail: aprauter@fc.ul.pt; Tel: +351968810971

26
27
28 Beining Chen, e-mail: b.chen@sheffield.ac.uk, Tel: +447710075082

29
30
31 *Author contributions:* § A. M. de Matos and M. Teresa Blázquez-Sanchez contributed equally.

32
33 ACKNOWLEDGEMENTS

34
35
36 The European Union is gratefully acknowledged for the support of the project entitled “Diagnostic and Drug Discovery
37 Initiative for Alzheimer's Disease” (D3i4AD), FP7-PEOPLE-2013-IAPP, GA 612347. The authors also thank the
38 Portuguese Foundation for Science and Technology (FCT) for the PhD scholarships attributed to AMM
39 (SFRH/BD/93170/2013), RN (SFRH/BD/116614/2016), AD (PD/BD/142847/2018), and A. B.-O.
40 (SFRH/BD/145600/2019), for the research grant CEECIND/03414/2018 given to R.F.M.A, for the support of both the
41 Centro de Química Estrutural (project UIDB/00100/2020) and the Applied Molecular Biosciences Unit
42 (UCIBIO project UID/Multi/04378/2019), and FM also thanks FCT for the IF investigator project (IF/00780/2015).
43 The NMR spectrometers are part of the National NMR Network (PTNMR) and are partially supported by Infrastructure
44 Project No 22161 (co-financed by FEDER through COMPETE 2020, POCI and PORL and FCT through
45 PIDDAC). MM also acknowledges FCT for the individual grant CEECIND/02300/2017 and the Research Unit grant
46 UID/MULTI/04046/2019. Diogo Vila-Viçosa is also acknowledged for fruitful discussions on performed DFT
47 calculations. The Dirección General de Investigación of Spain (CTQ2016-78703-P), the Junta de Andalucía (FQM134),
48 and FEDER (501100008530) are also acknowledged for financial support.

ABBREVIATIONS USED

1
2 AChE, Acetylcholinesterase; AD, Alzheimer's disease; A β , Amyloid beta; A β os, A β oligomers; AFM, Atomic force
3 microscopy; BBB, Blood-brain barrier; BuChE, Butyrylcholinesterase; cDNA, Complementary DNA; CHO, Chinese
4 Hamster Ovary cells; *clogP*, Calculated partition coefficient; CM, Conditioned medium; DAPI, 4,6-Diamidino-2-
5 phenylindole; DFT, Density functional theory; DID, Diabetes-induced dementia; DMAP, 4-Dimethylaminopyridine;
6 DMEM, Dulbecco's modified Eagle's medium; DMSO, Dimethyl sulfoxide; DTNB, 5,5'-Dithiobis(2-nitrobenzoic
7 acid); ELISA, Enzyme-linked immunosorbent assay; FACS, Fluorescence-activated cell sorting; GLUT, Glucose
8 transporter; GPI, Glycosylphosphatidylinositol; HCS, High-content image screening; HEK, Human embryonic kidney;
9 HPLC, High Performance Liquid Chromatography; IAPP, Islet amyloid polypeptide; ICC, Immunocytochemistry; IDE,
10 Insulin degrading enzyme; hiPSC, Human induced pluripotent stem cell line; Ket, Ketoconazole; LC-MS, Liquid
11 chromatography coupled to mass spectrometry; log D, Distribution coefficient; log *P*, Partition coefficient; log *P_e*,
12 Effective permeability; mA β , Monomeric A β ; MeCN, Acetonitrile; MTT, 3-(4,5-Dimethylthiazol-2-yl)-2,5-diphenyl-
13 2*H*-tetrazolium bromide; NFT, Neurofibrillary tangles; NPC, Neural progenitor cell; PAINS, Pan-assay interference
14 compounds; PAMPA, Parallel artificial membrane permeability assay; PBS, Phosphate-buffered saline; PFA,
15 Paraformaldehyde; pFyn, Src family kinase; PHF, Paired helical filaments; PMF, Potential of mean force; PLC,
16 Phospholipase C; POPC, 1-Palmitoyl-2-oleoyl-*sn*-glycero-3-phosphocholine; PP1, Protein phosphatase 1; PrPC,
17 Cellular prion protein; pTau, Phosphorylated Tau; Quer, Quercetin; SGLT, Sodium glucose linked transporter; siRNA,
18 Small interfering RNA; SFK, Src family kinases; STD, Saturation-transfer difference; T2D, Type 2 diabetes; TfOH,
19 Trifluoromethanesulfonic acid; ThT, Thioflavin-T; TMSOTf, Trimethylsilyl trifluoromethanesulfonate; UV,
20 Ultraviolet; Vis, Visible.

References

1. Williams, R.; Colagiuri, S.; Chan, J.; Gregg, E. W.; Ke, C.; Lim, L. L.; Yang, X. IDF Diabetes Atlas, eds. Karuranga, S.; Malanda, B.; Saeedi, P.; Salpea, P., 9th ed., International Diabetes Federation, United kingdom, 2019, p.35.
2. Matos A. M.; Macedo M. P.; Rauter A. P. Bridging type 2 diabetes and Alzheimer's disease: assembling the puzzle pieces in the quest for the molecules with therapeutic and preventive potential. *Med. Res. Rev.* 2018, 38, 261-324.
3. Nygaard H. B. Targeting Fyn kinase in Alzheimer's disease. *Biol. Psychiatry.* 2018, 83, 369-376.
4. Um J. W.; Strittmatter S. M. Amyloid- β induced signaling by cellular prion protein and Fyn kinase in Alzheimer disease. *Prion.* 2013, 7, 37-41.

- 1
2
3
4
5
6
7
8
9
10
11
12
13
14
15
16
17
18
19
20
21
22
23
24
25
26
27
28
29
30
31
32
33
34
35
36
37
38
39
40
41
42
43
44
45
46
47
48
49
50
51
52
53
54
55
56
57
58
59
60
5. Smith L. M.; Zhu R.; Strittmatter S. M. Disease-modifying benefit of Fyn blockade persists after washout in mouse Alzheimer's model. *Neuropharmacology*. 2018, 130, 54-61.
6. Kaufman A. C.; Salazar S. V.; Haas L. T.; Yang J.; Kostylev M. A.; Jeng A. T.; Robinson S. A.; Gunther E. C.; van Dyck C. H.; Nygaard H. B.; Strittmatter S. M. Fyn inhibition rescues established memory and synapse loss in Alzheimer mice. *Ann. Neurol.* 2015, 77, 953-971.
7. Lambert M. P.; Barlow A. K.; Chromy B. A.; Edwards C.; Freed R.; Liosatos M.; Morgan T. E.; Rozovsky I.; Trommer B.; Viola K. L.; Wals P.; Zhang C.; Finch C. E.; Krafft G. A.; Klein W. L. Diffusible, nonfibrillar ligands derived from A β (1-42) are potent central nervous system neurotoxins. *Proc. Natl. Acad. Sci. U. S. A.* 1998, 95, 6448-6453.
8. Yamada E.; Pessin J. E.; Kurland I. J.; Schwartz G. J.; Bastie C. C. Fyn-dependent regulation of energy expenditure and body weight is mediated by tyrosine phosphorylation of LKB1. *Cell Metab.* 2010, 11, 113-124.
9. Lee T. W.; Kwon H.; Zong H.; Yamada E.; Vatish M.; Pessin J. E.; Bastie C. C. Fyn deficiency promotes a preferential increase in subcutaneous adipose tissue mass and decreased visceral adipose tissue inflammation. *Diabetes*. 2013, 62, 1537-1546.
10. Yang Y.; Tarabra E.; Yang G. S.; Vaitheesvaran B.; Palacios G.; Kurland I. J.; Pessin J. E.; Bastie C. C. Alteration of de novo glucose production contributes to fasting hypoglycaemia in Fyn deficient mice. *PLoS One*. 2013, 8, e81866.
11. Oskarsson M. E.; Paulsson J. F.; Schultz S. W.; Ingelsson M.; Westermark P.; Westermark G. T. In vivo seeding and cross-seeding of localized amyloidosis: a molecular link between type 2 diabetes and Alzheimer's disease. *Am. J. Pathol.* 2015, 185, 834-846.
12. Baram M.; Atsmon-Raz Y.; Ma B.; Nussinov R.; Miller Y. Amylin-A β oligomers at atomic resolution using molecular dynamics simulations: a link between Type 2 diabetes and Alzheimer's disease. *Phys. Chem. Chem. Phys.* 2016, 18, 2330-2338.
13. Nabavi S. F.; Sureda A.; Dehpour A. R.; Shirooie S.; Silva A. S.; Devi K. P.; Ahmed T.; Ishaq N.; Hashim R.; Sobarzo-Sánchez E.; Daglia M.; Braidy N.; Volpicella M.; Vacca R. A.; Nabavi S. M. Regulation of autophagy by polyphenols: Paving the road for treatment of neurodegeneration. *Biotechnol. Adv.* 2017, 36, 1768-1778.
14. Jia J. J.; Zeng X. S.; Song X. Q.; Zhang P. P.; Chen L. Diabetes mellitus and Alzheimer's disease: The protection of epigallocatechin-3-gallate in streptozotocin injection-induced models. *Front. Pharmacol.* 2017, 8, 834.

15. Guo Y.; Zhao Y.; Nan Y.; Wang X.; Chen Y.; Wang S. (-)-Epigallocatechin-3-gallate ameliorates memory impairment and rescues the abnormal synaptic protein levels in the frontal cortex and hippocampus in a mouse model of Alzheimer's disease. *Neuroreport*. 2017, 28, 590-597.
16. Chen S.; Nimick M.; Cridge A. G.; Hawkins B. C.; Rosengren R. J. Anticancer potential of novel curcumin analogs towards castrate-resistant prostate cancer. *Int. J. Oncol.* 2018, 52, 579-588.
17. Rauter, A. P.; Ennis, M.; Hellwich, K. H., Herold, B. J., Horton, D.; Moss, G. P., Schomburg, I. Nomenclature of flavonoids (IUPAC recommendations 2017), *Pure Appl. Chem.* 2018, 90, 1429-1486.
18. Biasutto L.; Marotta E.; Bradaschia A.; Fallica M.; Mattarei A.; Garbisa S.; Zoratti M.; Paradisi C. Soluble polyphenols: synthesis and bioavailability of 3,4',5-tri(alpha-D-glucose-3-O-succinyl) resveratrol. *Bioorg. Med. Chem. Lett.* 2009, 19, 6721-6724.
19. Hollman P. C. H. Absorption, bioavailability, and metabolism of flavonoids. *Pharm. Biol.* 2004, 42S, 74-83.
20. Xiao J. Dietary flavonoid aglycones and their glycosides: Which show better biological significance? *Crit. Rev. Food Sci. Nutr.* 2017, 57, 1874-1905.
21. Ladiwala A.; Mora-Pale M.; Lin J.; Bale S.; Fishman Z.; Dordick J.; Tessier P. Polyphenolic glycosides and aglycones utilize opposing pathways to selectively remodel and inactivate toxic oligomers of amyloid β . *ChemBioChem.* 2011, 12, 1749-1758.
22. Xiao J.; Capanoglu E.; Jassbi A. R.; Miron A. Advance on the flavonoid C-glycosides and health benefits. *Crit. Ver. Food Sci. Nutr.* 2016, 56 Suppl 1, S29-S45.
23. Jesus A. R.; Vila-Viçosa D.; Machuqueiro M.; Marques A. P.; Dore T. M.; Rauter A. P. Targeting type 2 diabetes with C-glucosyl dihydrochalcones as selective sodium glucose co-transporter 2 (SGLT2) inhibitors: Synthesis and biological evaluation. *J. Med. Chem.* 2017, 60, 568-579.
24. de Matos, A. M.; Calado, P.; Rauter, A. P. Recent Advances on SGLT2 Inhibitors: Synthetic Approaches, Therapeutic Benefits and Adverse Events. In *Successful Drug Discovery, Volume 5*, eds J. Fischer, C. Klein and W. E. Childers, Wiley-VCH, Weinheim, in press, 2020. DOI: 10.1002/9783527826872.ch4
25. Jesus A. R.; Dias C.; Matos A. M.; de Almeida R. F.; Viana A. S.; Marcelo F.; Ribeiro R. T.; Macedo M. P.; Airoidi C.; Nicotra F.; Martins A.; Cabrita E. J.; Jiménez-Barbero J.; Rauter A. P. Exploiting the therapeutic potential of 8- β -D-glucopyranosylgenistein: Synthesis, antidiabetic activity, and molecular interaction with islet amyloid polypeptide and amyloid β -peptide (1-42). *J. Med. Chem.* 2014, 57, 9463-9472.

- 1
2
3
4
5
6
7
8
9
10
11
12
13
14
15
16
17
18
19
20
21
22
23
24
25
26
27
28
29
30
31
32
33
34
35
36
37
38
39
40
41
42
43
44
45
46
47
48
49
50
51
52
53
54
55
56
57
58
59
60
26. Rawat P.; Kumar M.; Rahuja N.; Lal Srivastava D. S.; Srivastava A. K.; Maurya R. Synthesis and antihyperglycemic activity of phenolic C-glycosides. *Bioorg. Med. Chem. Lett.* 2011, 21, 228-233.
27. He L.; Zhang Y. Z.; Tanoh M.; Chen G.; Praly J. P.; Chrysin E. D.; Tiraidis C.; Kosmopoulou M.; Leonidas D. D.; Oikonomakos N. G. In the search of glycogen phosphorylase inhibitors: Synthesis of C-D-glycopyranosylbenzo(hydro)quinones – Inhibition of and binding to glycogen phosphorylase in the crystal. *Eur. J. Org. Chem.* 2007, 4, 596-606.
28. Jaramillo C.; Knapp S. Synthesis of C-aryl glycosides. *Synthesis.* 1994, 1994, 1-20.
29. Nomura S.; Sakamaki S.; Hongu M.; Kawanishi E.; Koga Y.; Sakamoto T.; Yamamoto Y.; Ueta K.; Kimata H.; Nakayama K.; Tsuda-Tsukimoto M. Discovery of canagliflozin, a novel C-glucoside with thiophene ring, as sodium-dependent glucose cotransporter 2 inhibitor for the treatment of type 2 diabetes mellitus. *J. Med. Chem.* 2010, 53, 6355-6360.
30. Liao H.; Leng W.-L.; Hoang K. L. M.; Yao H.; He J.; Voo A. Y. H.; Liu X.-W. Asymmetric syntheses of 8-oxabicyclo[3,2,1]octane and 11-oxatricyclo[5.3.1.0]undecane from glycols. *Chem. Sci.* 2017, 8, 6656-6661.
31. Jarreton O.; Skrydstrup T.; Espinosa J.-F.; Jiménez-Barbero J.; Beau J.-M. Samarium diiodide promoted C-glycosylation: An application to the stereospecific synthesis of α -1,2-C-mannobioside and its derivatives. *Chem. Eur. J.* 1999, 5, 430-441.
32. Yuan X.; Linhardt R. J. Recent Advances in the synthesis of C-oligosaccharides. *Curr. Top Med. Chem.* 2005, 5, 1393–1430.
33. Santos R. G.; Jesus A. R.; Caio J. M.; Rauter A. P. Fries-type reactions for the C-glycosylation of phenols. *Curr. Org. Chem.* 2011, 15, 128-148.
34. Matsumoto T.; Katsuki M.; Suzuki K. New approach to C-aryl glycosides starting from phenol and glycosyl fluoride. Lewis acid-catalyzed rearrangement of O-glycoside to C-glycoside. *Tetrahedron Lett.* 1988, 29, 6935-6938.
35. Kometani T.; Kondo H.; Fujimori Y. Boron trifluoride-catalyzed rearrangement of 2-aryloxytetrahydropyrans: a new entry to C-arylglycosidation. *Synthesis-Stuttgart.* 1988, 12, 1005-1007.
36. Furuta T.; Kimura T.; Kondo S.; Mihara H.; Wakimoto T.; Nukaya H.; Tsuji K.; Tanaka K. Concise total synthesis of flavone C-glycoside having potent anti-inflammatory activity. *Tetrahedron.* 2004, 60, 9375–9379.
37. Kumazawa T.; Kimura T.; Matsuba S.; Sato S.; Onodera J. Synthesis of 8-C-glucosylflavones. *Carbohydr. Res.* 2011, 334, 183–193.

- 1 38. Mahling J.-A.; Jung K.-H.; Schmidt R. R. Synthesis of flavone C-glycosides vitexin, isovitexin and isoembigenin.
2 *Leibigs Ann. Chem.* 1995, 1995, 461–466.
3
- 4 39. Haverkamp J.; van Dongen J.P.C.M.; Vliegthart J.F.G. PMR and CMR spectroscopy of methyl 2,3,4,6-tetra-O-
5 methyl- α - and - β -D-glucopyranoside : An application to the identification of partially methylated glucoses. *Tetrahedron*
6
7 1973, 29, 3431-3439.
8
- 9 40. Wegmann B.; Schmidt R. R. The application of the trichloroacetimidate method to the synthesis of α -D-gluco- and
10
11 α -D-galactopyranosides, *J. Carbohydr. Chem.* 1987, 6, 357-375 and references cited therein.
12
13
- 14 41. Cai X.; Ng K.; Panesar H.; Moon S.-J.; Paredes M.; Ishida K.; Hertweck C.; Minehan T. G. Total synthesis of the
15
16 antitumor natural product polycarcin V and evaluation of its DNA binding profile. *Org. Lett.* 2014, 16, 2962–2965.
17
18
- 19 42. Wei X.; Liang D.; Wang Q.; Meng X.; Li Z. Total synthesis of mangiferin, homomangiferin, and neomangiferin. *Org.*
20
21 *Biomol. Chem.* 2016, 14, 8821-8831.
22
23
- 24 43. Wu Z.; Wei G.; Lian G.; Yu B. Synthesis of mangiferin, isomangiferin, and homomangiferin. *J. Org. Chem.* 2010, 75,
25
26 5725–5728.
27
28
- 29 44. Morris G. P.; Clark I. A.; Vissel B. Inconsistencies and controversies surrounding the amyloid hypothesis of
30
31 Alzheimer's disease. *Acta Neuropathol. Commun.* 2014, 2, 135.
32
33
- 34 45. Hardy J.; Selkoe D. J. The amyloid hypothesis of Alzheimer's disease: Progress and problems on the road to
35
36 therapeutics. *Science*, 2002, 297, 353–356.
37
38
- 39 46. Kittelberger, K. A. Piazza, F.; Tesco, G.; Leon G. Reijmers L. G., Natural amyloid-beta oligomers acutely impair
40
41 the formation of a contextual fear memory in mice. *PLoS ONE* 2012, 7, e29940.
42
- 43 47. Matrone, C.; Petrillo, F.; Nasso, R.; Ferreti, G., Fyn tyrosine kinase as harmonizing factor in neuronal functions and
44
45 dysfunctions, *Int. J. Mol. Sci.* 2020, 21, 4444.
46
47
- 48 48. Sato M.; Murakami K.; Uno M.; Nakagawa Y.; Katayama S.; Akagi K.; Masuda Y.; Takegoshi K.; Irie K. Site-
49
50 specific inhibitory mechanism for amyloid β 42 aggregation by catechol-type flavonoids targeting the Lys residues. *J.*
51
52 *Biol. Chem.* 2013, 288, 23212-23224.
53
54
- 55 49. Shoichet, B. K. Screening in a spirit haunted world. *Drug Discov. Today*, 2006, 11, 607-615.
56
57
- 58 50. Seidler, J.; McGovern, S. L.; Doman, T. N.; Shoichet, B. K. Identification and prediction of promiscuous
59
60 aggregating inhibitors among known drugs. *J. Med. Chem.*, 2003, 46,4477-4486.

- 1
2
3
4
5
6
7
8
9
10
11
12
13
14
15
16
17
18
19
20
21
22
23
24
25
26
27
28
29
30
31
32
33
34
35
36
37
38
39
40
41
42
43
44
45
46
47
48
49
50
51
52
53
54
55
56
57
58
59
60
51. Vallverdú-Queralt, A.; Biler, M.; Meudec, E.; Le Guernevé, C.; Vernhet, A.; Jean-Paul Mazauric, J.-P.; Legras, J. L.; Loonis, M.; Trouillas, P.; Cheynier, V.; Dangles, O. *p*-Hydroxyphenyl-pyranoanthocyanins: An experimental and theoretical investigation of their acid-base properties and molecular interactions. *Int. J. Mol. Sci.* 2016, 17, 1842.
52. McGovern, S. L.; Shoichet, B. K. Kinase inhibitors: not just for kinases anymore. *J. Med. Chem.* 2003, 46, 1478-1483.
53. Coan, K. D. E.; Shoichet, B. K. Stoichiometry and physical chemistry of promiscuous aggregate-based inhibitors. *J. Am. Chem. Soc.* 2008, 130, 9606-9612.
54. Bruno, F. F.; Trotta, A.; S Fossey, S.; Nagarajan, S.; Nagarajan, R.; Samuelson, L. A.; Jayant Kumar, J. Enzymatic synthesis and characterization of polyQuercetin. *J. Macromol. Sci. A*, 2010, 47, 1191-1196.
55. Momić, T.; Savić, J.; Černigoj, U.; Polonca Trebše, P.; Vasić, V. Protolytic equilibria and photodegradation of quercetin in aqueous solution. *Collect. Czech. Chem. Commun.*, 2007, 72, 1447-1460.
56. Mezzetti, A.; Lapouge, C.; Cornard, J.-P. Protic equilibria as the key factor of quercetin emission in solution. Relevance to biochemical and analytical studies. *Phys. Chem. Chem. Phys.*, 2011, 13, 6858-6864.
57. de Granada-Flor, A.; Sousa, C.; Filipe, H. A. L.; Santos, M. S. C. S., de Almeida, R. F. M. Quercetin dual interaction at the membrane level, *Chem. Commun.*, 2019, 55, 1750-1753.
58. Eva Zupancic, E.; Carreira, A. C.; de Almeida, R. F. M., Silva, L. C. Biophysical implications of sphingosine accumulation in membrane properties at neutral and acidic pH. *J. Phys. Chem. B*, 2014, 118, 4858-4866.
59. Zhou Y.; Shi J.; Chu D.; Hu, W.; Z. Guan; G. Cheng-Xin; Iqbal, K.; Liu, F. Relevance of phosphorylation and truncation of Tau to the etiopathogenesis of Alzheimer's disease. *Front Aging Neurosci.* 2018, 10, doi:10.3389/fnagi.2018.00027.
60. Iqbal K.; Liu F.; Gong C. X.; Grundke-Iqbal I. Tau in Alzheimer disease and related tauopathies. *Curr. Alzheimer Res.* 2010, 7, 656-664.
61. Liu, F.; Shi, J.; Tanimukai, H.; Gu, J.; Gu, J.; Grundke-Iqbal, I.; Iqbal, K.; Gong C. X. Reduced O-GlcNAcylation links lower brain glucose metabolism and tau pathology in Alzheimer's disease. *Brain* 2009, 132, 1820-1832.
62. Köpke, E.; Tung, Y. C.; Shaikh, S.; Alonso, A. C.; Iqbal, K.; Grundke-Iqbal, I. Microtubule-associated protein tau. Abnormal phosphorylation of a non-paired helical filament pool in Alzheimer disease. *J. Biol. Chem.* 1993, 268, 24374-2384.

63. Desmarais J. A.; Unger C.; Damjanov I.; Meuth M.; Andrews P. Apoptosis and failure of checkpoint kinase 1 activation in human induced pluripotent stem cells under replication stress. *Stem Cell Res. Ther.* 2016, 7, 17.
64. Bischoff H. The mechanism of alpha-glucosidase inhibition in the management of diabetes. *Clin. Invest. Med.* 1995, 18, 303-311.
65. Melo E. B.; Gomes A.S.; Carvalho I. α - and β -Glucosidase inhibitors: chemical structure and biological activity. *Tetrahedron* 2006, 62, 10277-10302.
66. Rauter A. P.; Jesus A.; Martins A.; Dias C.; Ribeiro R.; Macedo M. P.; Justino J.; Mota-Filipe H.; Pinto R.; Sepodes B.; Medeiros M.; Jiménez Barbero J.; Airoidi C.; Nicotra F. New C-Glycosylpolyphenol Antidiabetic Agents, Effect on Glucose Tolerance and Interaction with Beta-Amyloid. Therapeutic Applications of the Synthesized Agent(s) and of *Genista tenera* Ethyl Acetate Extracts Containing Some of Those Agents. US14/384,145, Oct 03, 2017.
67. Jean L.; Thomas B.; Tahiri-Alaoui A.; Shaw M.; Vaux D. J. Heterologous amyloid seeding: Revisiting the role of acetylcholinesterase in Alzheimer's disease. *PLoS One* 2007, 2, e652.
68. Greig N. H.; Utsuki T.; Ingram D. K.; Wang Y.; Pepeu G.; Scali C.; Yu Q. S.; Mamczarz J.; Holloway H. W.; Giordano T.; Chen D.; Furukawa K.; Sambamurti K.; Brossi A.; Lahiri D. K. Selective butyrylcholinesterase inhibition elevates brain acetylcholine, augments learning and lowers Alzheimer β -amyloid peptide in rodent. *Proc. Natl. Acad. Sci. U. S. A.* 2005, 102, 17213–17218.
69. Diamant S.; Podoly E.; Friedler A.; Ligumsky H.; Livnah O.; Soreq H. Butyrylcholinesterase attenuates amyloid fibril formation *in vitro*. *Proc. Natl. Acad. Sci. U. S. A.* 2006, 103, 8628–8633.
70. Araujo J. A.; Greig N. H.; Ingram D. K.; Sandin J.; Rivera C.; Milgram N. W. Cholinesterase inhibitors improve both memory and complex learning in aged beagle dogs. *J. Alzheimers Dis.* 2011, 26, 143–155.
71. Greig N. H.; Lahiri D. K.; Sambamurti K. Butyrylcholinesterase: an important new target in Alzheimer's disease therapy. *Int Psychogeriatr.* 2002, 14 Suppl 1, 77-91.
72. Mushtaq G.; Greig N. H.; Khan J. A.; Kamal M. A. Status of acetylcholinesterase and butyrylcholinesterase in Alzheimer's disease and type 2 diabetes mellitus. *C.N.S. Neurol. Disord. Drug Targets* 2014, 13, 1432–1439.
73. Rao A. A.; Sridhar G. R.; Das U. N. Elevated butyrylcholinesterase and acetylcholinesterase may predict the development of type 2 diabetes mellitus and Alzheimer's disease. *Med. Hypotheses* 2007, 69, 1272-1276.
74. Sato K. K.; Hayashi T.; Maeda I.; Koh H.; Harita N.; Uehara S.; Onishi Y.; Oue K.; Nakamura Y.; Endo G.; Kambe H.; Fukuda K. Serum butyrylcholinesterase and the risk of future type 2 diabetes: the Kansai Healthcare Study. *Clin. Endocrinol. (Oxf)*. 2014, 80, 362-367.

- 1
2
3
4
5
6
7
8
9
10
11
12
13
14
15
16
17
18
19
20
21
22
23
24
25
26
27
28
29
30
31
32
33
34
35
36
37
38
39
40
41
42
43
44
45
46
47
48
49
50
51
52
53
54
55
56
57
58
59
60
75. Iwasaki T.; Yoneda M.; Nakajima A.; Terauchi Y. Serum butyrylcholinesterase is strongly associated with adiposity, the serum lipid profile and insulin resistance. *Intern. Med.* 2007, 46, 1633-1639.
76. Zhang Y.; Zhang T.; Wang F.; Xie J. Brain tissue distribution of spinosin in rats determined by a new high-performance liquid chromatography-electrospray ionization-mass/mass spectrometry method. *J. Chromatogr. Sci.* 2015, 53, 97-103.
77. Di L.; Kerns E. H. Profiling drug-like properties in discovery research. *Curr. Opin. Chem. Biol.* 2003, 7, 402-408.
78. I Yang, J. J.; Ursu, O.; Lipinski, C. A.; Sklar, L. A.; Oprea, T. I.; Bologa, C. G. Badapple: promiscuity patterns from noisy evidence, *J. Cheminformatics* 2016, 8, 29.
79. Ingolfsson, H. I.; Thakur, P.; Herold, K. F.; Hobart, E. A.; Ramsey, N. B.; Periole, X.; de Jong, D. H.; Zwama, M.; Yilmaz, D.; Hall, K.; Maretzky, T.; Hemmings, H. C.; Blobel, C.; Marrink, S. J.; Kocer, A.; Sack, J. T.; Andersen, O. S. Phytochemicals perturb membranes and promiscuously alter protein function. *ACS Chem. Biol.* 2014, 9, 1788-1798.
80. Bols M.; Hazell R. G.; Thomsen I. B. 1-Azafagomine: A hydroxyhexahydropyridazine that potently inhibits enzymatic glycoside cleavage. *Chem. Eur. J.* 1997, 3, 940-947.
81. Cornish-Bowden, A. A simple graphical method for determining the inhibition constants of mixed, uncompetitive and non-competitive inhibitors. *Biochem. J.* 1974, 137, 143-144.
82. Ellman G. L.; Courtney K. D.; Andres Jr V.; Feather-Stone R. M. A new and rapid colorimetric determination of acetylcholinesterase activity. *Biochem. Pharmacol.* 1961, 7, 88-95.
83. Walsh D. M.; Klyubin I.; Fadeeva J. V.; Cullen W. K.; Anwyl R.; Wolfe M. S.; Rowan M. J.; Selkoe D. J. Naturally secreted oligomers of amyloid beta protein potently inhibit hippocampal long-term potentiation in vivo. *Nature* 2002, 416, 535-539.
84. Shankar G. M.; Welzel A.T; McDonald J. M.; Selkoe D. J.; Walsh D. M. Isolation of low-n amyloid β -protein oligomers from cultured cells, CSF, and brain. *Methods Mol. Biol.* 2011, 670, 33-44.
85. Shi Y.; Kirwan P.; Livesey F. J. Directed differentiation of human pluripotent stem cells to cerebral cortex neurons and neural networks. *Nat. Protoc.* 2012, 7, 1836-1846.
86. VCCLAB - Virtual Computational Chemistry Laboratory. <http://www.vcclab.org>, accessed April 23, 2019
87. Kansy M.; Senner F.; Gubernator K. Physicochemical high throughput screening: parallel artificial membrane permeation assay in the description of passive absorption processes. *J. Med. Chem.* 1998, 41, 1007-1010.

Table of Contents graphic

